For Reference

NOT TO BE TAKEN FROM THIS ROOM

PHASE BEHAVIOR IN THE METHANE-CARBON DIOXIDE-HYDROGEN SULFIDE SYSTEM

by

ALFRED P. LORENZO

DEPARTMENT OF CHEMICAL AND PETROLEUM ENGINEERING

UNIVERSITY OF ALBERTA

EDMONTON, ALBERTA

NOVEMBER, 1957

Ex libris
universitatis
albertaensis

UNIVERSITY OF ALBERTA
QUAECUMQUE VERA

Thesis
1958
#17

THE UNIVERSITY OF ALBERTA

PHASE BEHAVIOR IN THE METHANE-CARBON DIOXIDE-HYDROGEN SULFIDE SYSTEM

A Dissertation

Submitted to

The Faculty of Graduate Studies

In Partial Fulfilment

of the Requirements for the Degree

of Master of Science in Chemical Engineering

Department of Chemical and Petroleum Engineering

by

Alfred P. Lorenzo, B. Sc.

Edmonton, Alberta

November, 1957

Digitized by the Internet Archive
in 2017 with funding from
University of Alberta Libraries

https://archive.org/details/phasebehaviorinm00lore

ABSTRACT

The phase behavior of the methane-carbon dioxide-hydrogen sulfide system was investigated at pressures of 400, 1000 and 1600 lbs/in.^{2} abs. at a temperature of 40 degrees F.; and at pressures of 1000 and 1600 lbs/in.^{2} abs. at a temperature of 160 degrees F.

The experimental technique employed involved preparation in the gas phase of mixtures of known composition with subsequent compression of the system to the two phase vapor-liquid region. Published data on each of the three binary systems was employed to facilitate the study of the ternary system. Experimental determinations of the compositions of co-existing vapor and liquid phases were carried out at each pressure; thus defining the isobaric, three component, two phase region. The isobaric ternary diagrams served to outline the ternary liquid and vapor surfaces existing from 169 to 1949 lbs/in.^{2} abs. at 40 degrees F. and from 779 to 1660 lbs/in.^{2} abs. at 160 degrees F.

Correlation of the experimental data was achieved by calculation of experimental equilibrium ratios for each component. The determination of the effect of pressure on the equilibrium ratios enabled the prediction of the compositions of co-existing phases at intermediate pressures of 700 and 1300 lbs/in.^{2} abs. at 40 degrees F. and at 1300 lbs/in.^{2} abs. at 160 degrees F. Calculation of activity coefficients illustrated the deviation of the liquid phase from ideal solution behavior. Non-ideality in the gas phase, resulting from the effect of pressure, was accounted for by the introduction of fugacities in the calculation of the activity coefficients.

The experimental results indicate that at low pressures, where no ternary critical point formation occurs, the dew point and bubble point curves are nearly straight lines and may be roughly approximated by use of the ideal solution law; the approximation being more reliable for the liquid phase than for the vapor phase. At higher pressures, deviation from idealized vapor-liquid behavior is very great.

Equilibrium ratios were found to be functions of pressure, temperature and system composition with the effect of pressure being somewhat greater than that of temperature. The activity coefficients indicate that the deviation of the liquid phase from ideal solution behavior is also a function of pressure, temperature and system composition and that each of these variables has an effect that is of relatively the same magnitude.

ACKNOWLEDGMENTS

The author feels deeply indebted to Dr. D. B. Robinson of the Department of Chemical and Petroleum Engineering, University of Alberta, who directed the research project from its inception and whose efforts contributed greatly to its success.

Many thanks are due to Mr. R. Kirby for his excellent work on the construction of the experimental equipment and to Mr. F. Butz for his assistance in the performance of the experimental tests.

The author is also very grateful for the generous financial support that was provided by the National Research Council of Canada.

TABLE OF CONTENTS

CHAPTER		PAGE
I.	INTRODUCTION	1
II.	THEORY	3
	(1) Three Component Phase Equilibrium	3
	(2) Phase Behavior of CH_4 - CO_2 - H_2S System	4
	(3) Deviations From Ideal Behavior	10
	(a) Ideal Solution Law	10
	(b) Behavior of Real Systems	12
	(c) The Concept of the Activity Coefficient	13
III.	EXPERIMENTAL EQUIPMENT	18
	(1) Experimental Technique Employed	18
	(2) Modification of Existing Experimental Apparatus	19
	(a) Equilibrium Cell	19
	(b) Air Bath	19
	(c) Measuring Cell	21
	(d) Measurement of Experimental Variables	21
	(e) Valves, Tubing and Fittings	22
	(f) Refrigeration System	23
	(g) Heating System	25
	(h) Sampling and Analytical Procedure	26
	(i) Gaseous Components	27

CHAPTER PAGE

IV. EXPERIMENTAL RESULTS 28

(1) Experimental Phase Equilibrium Data 28

(A) Data at 40 Degrees F. 28

(a) CH_4 - H_2S System 28

(b) CO_2 - H_2S System 28

(c) Ternary System 31

(B) Data at 160 Degrees F. 37

(a) CH_4 - H_2S System 37

(b) CO_2 - H_2S System 37

(c) Ternary System 37

(2) Correlation of Experimental Data 43

(a) Use of Composition Parameter 43

(b) Equilibrium Ratios 45

(c) Activity Coefficients 58

(d) Predicted Phase Equilibrium Data 71

(e) General Description of Ternary System at 40 Degrees F. 76

(f) General Description of Ternary System at 160 Degrees F. 80

V. CONCLUSIONS 82

(1) Validity of Experimental Results 82

(2) Discussion of Experimental Data 84

List of References 87

APPENDIX (1) Tabulated Data 89

(2) Sample Calculations 107

LIST OF TABLES

TABLE		PAGE
I.	Phase Composition Data at 40 Degrees F. and 400 lbs/in.^{2} abs.	89
II.	Phase Composition Data at 40 Degrees F. and 1000 lbs/in^2 abs.	90
III.	Phase Composition Data at 40 Degrees F. and 1600 lbs/in.^{2} abs.	91
IV.	Phase Composition Data at 160 Degrees F. and 1000 lbs/in.^{2} abs.	92
V.	Phase Composition Data at 160 Degrees F. and 1600 lbs/in.^{2} abs.	93
VI.	Equilibrium Ratios at 40 Degrees F. and 400 lbs/in.^{2} abs.	94
VII.	Equilibrium Ratios at 40 Degrees F. and 1000 lbs/in.^{2} abs.	95
VIII.	Equilibrium Ratios at 40 Degrees F. and 1600 lbs/in.^{2} abs.	96
IX.	Equilibrium Ratios at 160 Degrees F. and 1000 lbs/in.^{2} abs.	97
X.	Equilibrium Ratios at 160 Degrees F. and 1600 lbs/in.^{2} abs.	98
XI.	Activity Coefficients at 40 Degrees F. and 400 lbs/in.^{2} abs.	99
XII.	Activity Coefficients at 40 Degrees F. and 1000 lbs/in.^{2} abs.	100
XIII.	Activity Coefficients at 40 Degrees F. and 1600 lbs/in.^{2} abs.	101
XIV.	Activity Coefficients at 160 Degrees F. and 1000 lbs/in.^{2} abs.	102
XV.	Activity Coefficients at 160 Degrees F. and 1600 lbs/in.^{2} abs.	103

TABLE PAGE

XVI. Predicted Phase Composition Data at 40 Degrees F. and 700 lbs/in.^{2} abs. 104

XVII. Predicted Phase Composition Data at 40 Degrees F. and 1300 lbs/in.^{2} abs. 105

XVIII. Predicted Phase Composition Data at 160 Degrees F. and 1300 lbs/in.^{2} abs. 106

LIST OF FIGURES

FIGURE		PAGE
1.	Ternary Isobaric Diagrams at 40 Degrees F.	
	Part (a)	7
	Part (b)	8
	Part (c)	9
2.	Ternary Isobaric Diagrams at 160 Degrees F.	11
3.	Schematic Apparatus Assembly	20
4.	Pressure-Composition Diagram for CH_4 - H_2S System at 40 Degrees F.	29
5.	Pressure-Composition Diagram for CO_2 - H_2S System at 40 Degrees F.	30
6.	Molar Composition Diagram at 400 lbs/in.^{2} abs. and 40 Degrees F.	32
7.	Molar Composition Diagram at 1000 lbs/in.^{2} abs. and 40 Degrees F.	33
8.	Molar Composition Diagram at 1600 lbs/in.^{2} abs. and 40 Degrees F.	34
9.	Pressure-Composition Diagram for CH_4 - H_2S System at 160 Degrees F.	38
10.	Pressure-Composition Diagram for CO_2 - H_2S System at 160 Degrees F.	39
11.	Molar Composition Diagram at 1000 lbs/in.^{2} abs. and 160 Degrees F.	41
12.	Molar Composition Diagram at 1600 lbs/in.^{2} abs. and 160 Degrees F.	42
13.	Equilibrium Ratios for CH_4 at 40 Degrees F.	47
14.	Equilibrium Ratios for CO_2 at 40 Degrees F.	48
15.	Equilibrium Ratios for H_2S at 40 Degrees F.	49

FIGURE PAGE

16. Critical C Values at 40 Degrees F. 50

17. Equilibrium Ratios for CH_4 at 160 Degrees F. 53

18. Equilibrium Ratios for CO_2 at 160 Degrees F. 54

19. Equilibrium Ratios for H_2S at 160 Degrees F. 55

20. Critical C Values at 160 Degrees F. 56

21. Theoretical Equilibrium Ratios 59

22. Activity Coefficients for CH_4 at 40 Degrees F. 62

23. Activity Coefficients for CO_2 at 40 Degrees F. 63

24. Activity Coefficients for H_2S at 40 Degrees F. 64

25. Activity Coefficients for CH_4 at 160 Degrees F. 67

26. Activity Coefficients for CO_2 at 160 Degrees F. 68

27. Activity Coefficients for H_2S at 160 Degrees F. 69

28. Predicted Molar Composition Diagram at 700 lbs/in.^{2} abs. and 40 Degrees F. 73

29. Predicted Molar Composition Diagram at 1300 lbs/in.^{2} abs. and 40 Degrees F. 74

30. Predicted Molar Composition Diagram at 1300 lbs/in.^{2} abs. and 160 Degrees F. 75

31. Phase Diagram for the Ternary System at 40 Degrees F. .. 77

32. Phase Diagram for the Ternary System at 160 Degrees F. . 80

LIST OF SYMBOLS

c - component in a system

C - composition parameter defined as the ratio of the mole fraction of carbon dioxide in the vapor phase to the sum of the mole fractions of methane and carbon dioxide in the vapor phase

F - number of variables or degrees of freedom in a system

f - fugacity of a pure component

$\bar{f}$ - fugacity of a component in a solution

f_p - fugacity of a pure component at a pressure equal to the system pressure

f^* - fugacity of a pure component at a pressure equal to its own vapor pressure at the system temperature

γ - activity coefficient

i - subscript referring to any component

K - equilibrium ratio

μ - chemical potential

n - number of moles of a component in the gas phase

p - partial pressure in vapor phase

P^* - vapor pressure

π, P - absolute system pressure

ϕ - number of phases

R - universal gas constant

T - absolute temperature in degrees Rankine

V - volume of gas phase

x - mole fraction of a component in the liquid phase

y - mole fraction of a component in the vapor phase

Z - compressibility factor

Superscripts

L - referring to liquid phase

o - referring to standard state of pressure and concentration

v - referring to vapor phase

I. INTRODUCTION

The investigation into the phase behavior of the methane-carbon dioxide-hydrogen sulfide system begun by Bailey (1) was continued in this study. Phase equilibrium determinations at temperatures above and below that previously investigated were conducted. Necessary modifications of the existing experimental equipment, required to extend the temperature range of the study, and improvements in the mechanical design of the equipment were made. The general experimental technique and analytical procedure employed by Bailey were not significantly altered and hence the estimated accuracy of the results is comparable to that which he reported.

The theoretical treatment of the data was modified extensively. No attempt was made to calculate compressibility factors for the saturated vapor phase, as was done by Bailey, since it was decided that the accuracy of the volumetric measurement of the vapor phase at test conditions was insufficient to yield meaningful results. The technique employed in calculating activity coefficients was altered so as to result in a coefficient which gave a better indication of the deviation of the liquid phase from ideal solution behavior. Deviations from ideality in the gas phase, resulting from the effects of pressure were accounted for by the introduction of fugacities rather than included in an overall activity coefficient.

The determination of activity coefficients over a considerable temperature range has enabled prediction of the effect of temperature

change, as well as the effects of changes in pressure and system composition, on the ideality of the liquid phase.

II. THEORY

(1) Three Component Phase Equilibrium

Consideration of the phase rule

$$\phi + F = c + 2 \quad --- (1)$$

indicates that a single phase three component system has four degrees of freedom and, hence, in order to represent such a system in three space coordinates it is necessary to specify one variable as constant for the whole diagram. Phase equilibrium studies usually are carried out under isothermal conditions and therefore temperature is selected as the invariant quantity. Three dimensional representation of the phase equilibrium may then be achieved by selecting pressure as the ordinate and two independent concentrations as abscissae.

The difficulties involved in representing phase equilibria by means of three dimensional models are partially overcome by the use of isobaric sections which represent vapor-liquid equilibrium at a particular pressure and temperature. The phase compositions for a three component system are conveniently represented in two dimensions by the use of equilateral triangles which permit direct plotting of the two independent concentrations and the dependent concentration.

A three dimensional model may be constructed from the isobaric sections by representing pressure on a perpendicular to the plane of the triangular diagram. Thus, the complete isothermal phase equilibrium model consists of a prism in which each side represents the pressure-composition diagram for one of the three binary systems. Liquid

compositions are represented by one surface within the prism and vapor compositions by a second surface. The compositions of any two co-existing phases may be indicated by straight tie lines connecting these two surfaces. Any specific point within the prism represents a three component system at a particular pressure. The single phase liquid or vapor regions are represented by solid portions within the prism and hence possess three degrees of freedom. The two dimensional surfaces represent the boundaries between the single phase regions and the two phase region. Any system within the region enclosed by the boundary surfaces will separate into two co-existing phases.

In the two dimensional isobaric section the single phase regions and the two phase region appear as areas possessing two degrees of freedom as specified by the phase rule, while the boundary surfaces appear as lines. Such sections may be conveniently used for the direct plotting of the experimental data and then a three dimensional model may be constructed to give a clearer idea of the nature of the overall phase equilibrium at the particular temperature selected.

(2) Phase Behavior of the Methane-Carbon Dioxide-Hydrogen Sulfide System

The general form of the isobaric phase equilibrium diagrams for the ternary system may be predicted from a consideration of the pressure-composition diagrams for the binary systems which are available in the literature for this particular ternary system. The methane-hydrogen sulfide system was reported in 1951 by Reamer, Sage and Lacey (12). The carbon dioxide-hydrogen sulfide system was reported in 1953 by Bierlein

and Kay (2). The methane-carbon dioxide system was reported in 1954 by Donnelly and Katz (4). This latter work extended to a maximum temperature of only 29 degrees F. and so could not be used in this study in which data were obtained at temperatures of 40 degrees F. and 160 degrees F. The critical temperature of hydrogen sulfide is 212.7 degrees F. (11), of carbon dioxide is 88.0 degrees F. (2), and of methane is minus 115.8 degrees F. (10).

At 40 degrees F. both hydrogen sulfide and carbon dioxide may exist as liquids under their own vapor pressures. Accordingly, all three binary systems - methane and hydrogen sulfide, carbon dioxide and hydrogen sulfide, methane and carbon dioxide - exist as liquids. In the carbon dioxide-hydrogen sulfide phase diagram at 40 degrees F. the bubble point and dew point curves extend across the entire composition range since the system temperature is below the critical temperature of both components. However, in the methane-hydrogen sulfide phase diagram at 40 degrees F. the bubble point and dew point curves terminate at the binary critical point, which represents the maximum pressure at which the two phase region can exist at this temperature. The critical pressure for the methane-hydrogen sulfide pair is 1949 lbs/in.^{2} abs. and occurs at a composition of 0.55 mole fraction methane.

Fig. 1 represents typical ternary isobaric composition diagrams which may be predicted from the two component data without any experimental investigation of the ternary system. The binary pressure-composition diagrams and the triangular composition diagram are represented in the same plane in order to clearly illustrate the

relationships between them.

Part (a) illustrates the phase equilibrium at a pressure, P_a, between the vapor pressure of hydrogen sulfide (169 lbs/in.^{2} abs.) and the vapor pressure of carbon dioxide (570 lbs/in.^{2} abs.). At this pressure both the methane-hydrogen sulfide and carbon dioxide-hydrogen sulfide systems form two phases and hence the ternary two phase region extends from the methane-hydrogen sulfide axis to the carbon dioxide-hydrogen sulfide axis. The methane-carbon dioxide system does not exist as a liquid at this pressure.

Part (b) illustrates the phase equilibrium at a pressure, P_b, between the vapor pressure of carbon dioxide (570 lbs/in.^{2} abs.) and the critical pressure of the methane-carbon dioxide system (estimated as 1240 lbs/in.^{2} abs. from consideration of the data obtained by Donnelly and Katz at 29 degrees F.). At such a pressure the binary systems methane-hydrogen sulfide and methane-carbon dioxide form two phases but the carbon dioxide-hydrogen sulfide does not since the system pressure is greater than the vapor pressure of either component.

Part (c) illustrates the phase equilibrium at a pressure, P_c, between the critical pressure of the methane-carbon dioxide system (approx. 1240 lbs/in.^{2} abs.) and the critical pressure of the methane-hydrogen sulfide system (1949 lbs/in.^{2} abs.). At such a pressure only the methane-hydrogen sulfide system forms two phases. Hence, the ternary two phase region no longer extends to the methane-carbon dioxide axis and, furthermore, as the pressure is increased this region diminishes until it meets the methane-hydrogen sulfide axis at the critical pressure

FIG. 1 - PART (A).

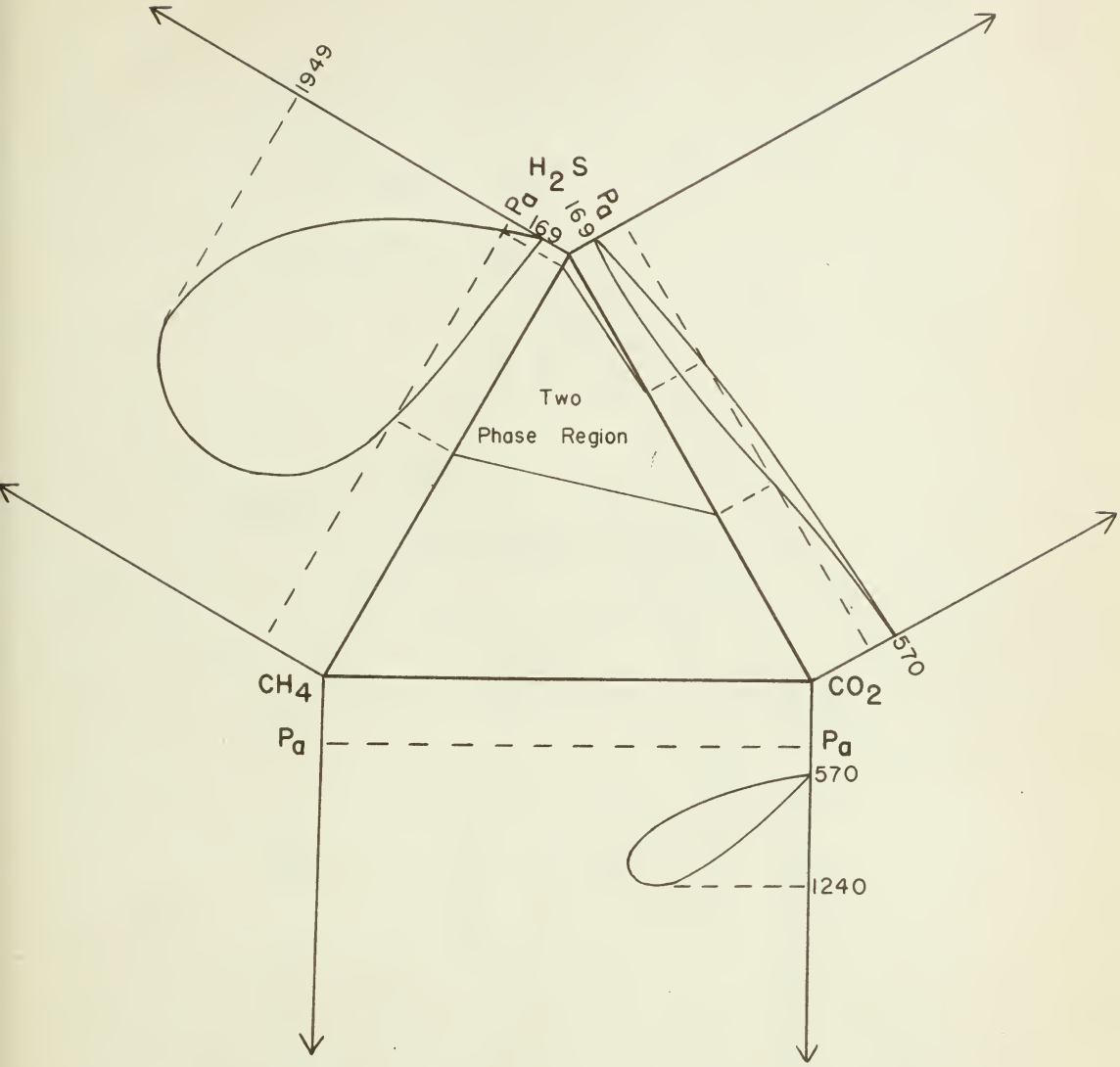

Isobaric Section At P_a Where $169 < P_a < 570$ lbs./in.^{2} abs.

TERNARY ISOBARIC DIAGRAM AT 40°F.

FIG. I - PART (B).

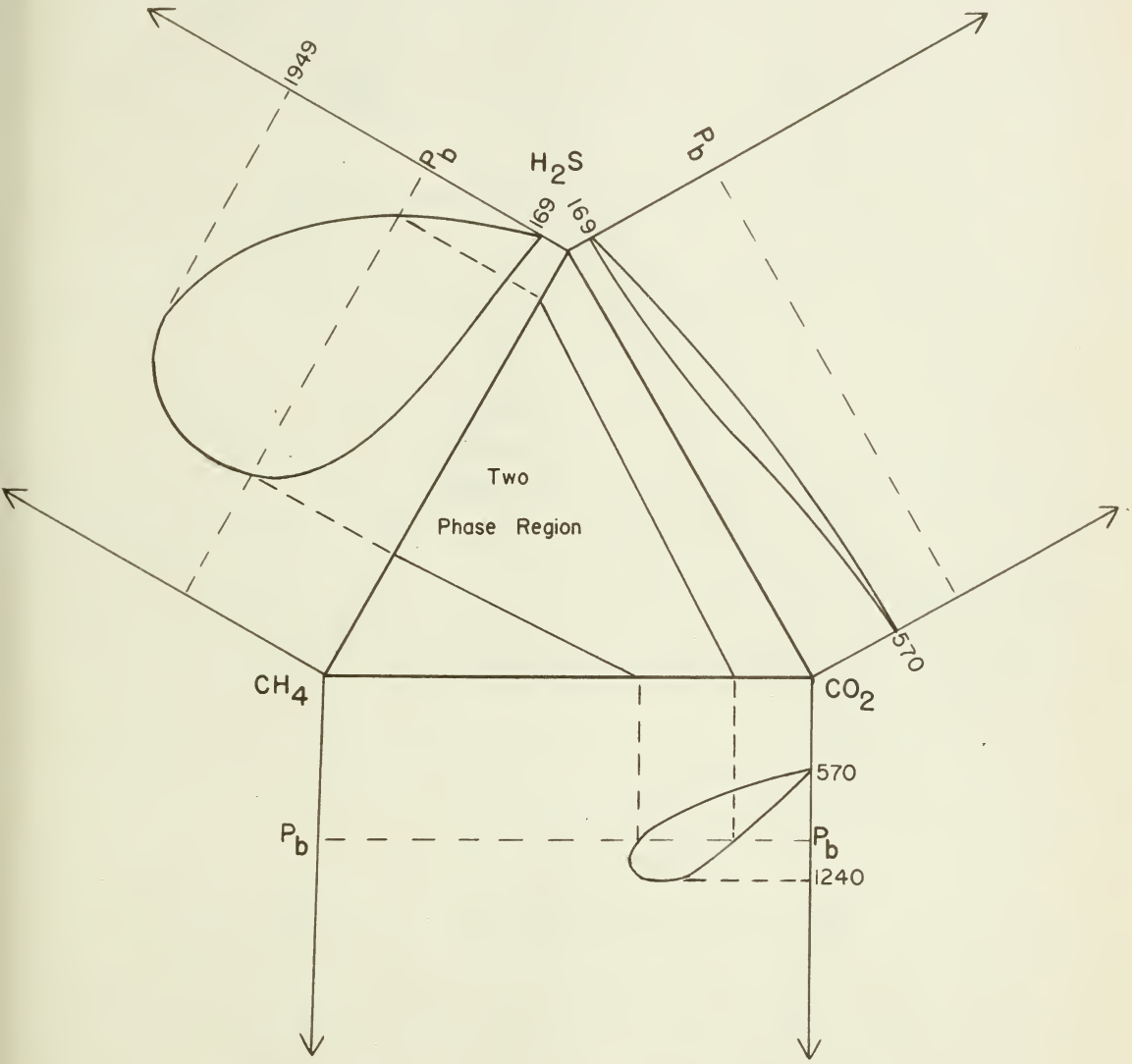

Isobaric Section At P_b Where $570 < P_b < 1240$ lbs/in.^{2} abs.

TERNARY ISOBARIC DIAGRAM AT 40°F.

FIG. I - PART (C).

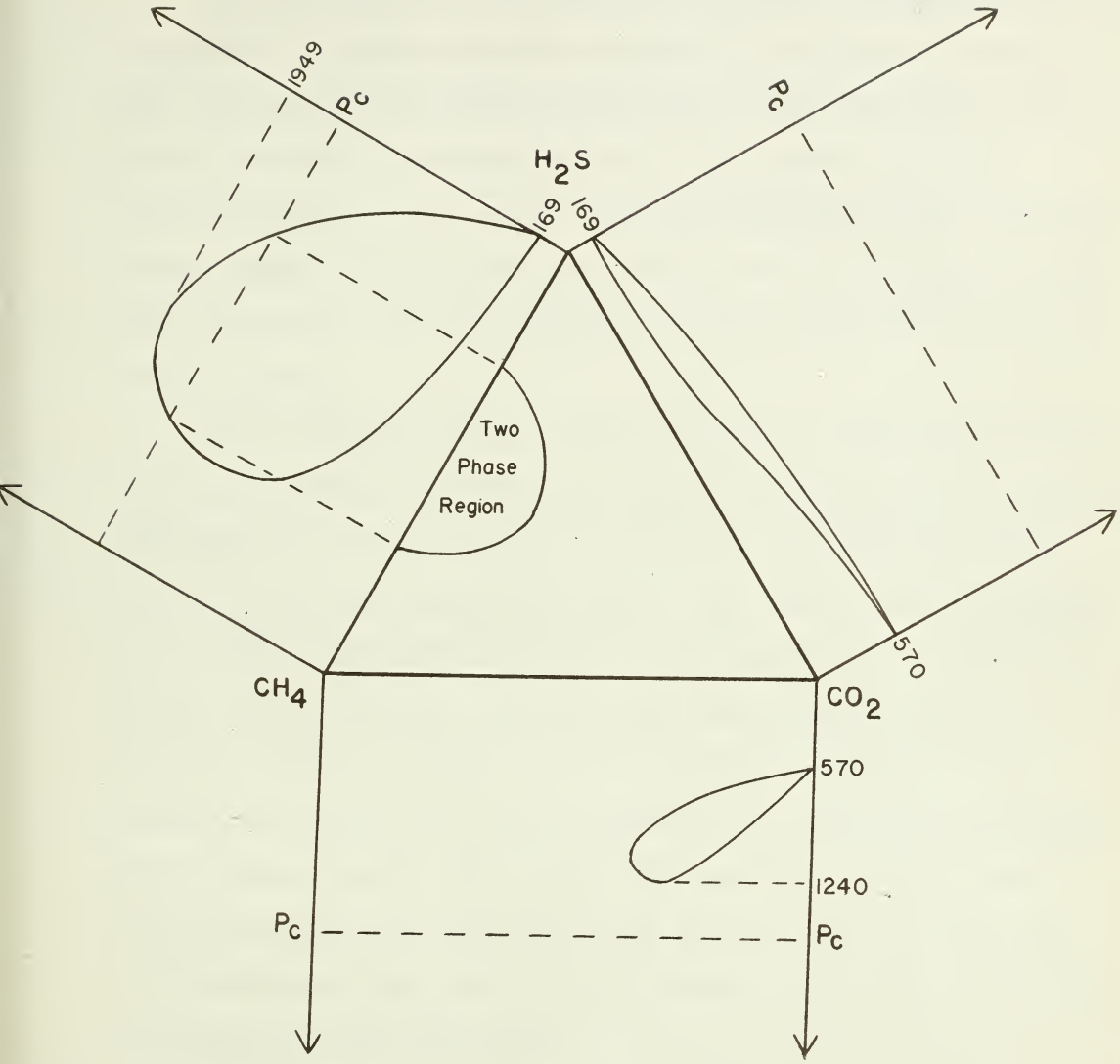

Isobaric Section At P_c Where $1240 < P_c < 1949$ lbs/in.^{2} abs.

TERNARY ISOBARIC DIAGRAM AT 40°F.

of the methane-hydrogen sulfide system.

At a temperature of 160 degrees F. the critical temperatures of both methane and carbon dioxide are exceeded by a considerable amount. Thus, the methane-carbon dioxide system does not form two phases at any pressure and hence no pressure-composition loop exists. Also, the pressure-composition loops of both the methane-hydrogen sulfide and carbon dioxide-hydrogen sulfide systems are located near to the hydrogen sulfide axis. Accordingly, the three component two phase region must be rich in hydrogen sulfide.

Fig. 2 represents ternary isobaric diagrams at 160 degrees F. which may be predicted from the binary data reported in the literature. Part (a) illustrates the phase equilibrium at a pressure, P_a, between the vapor pressure of hydrogen sulfide (779 lbs/in.^{2} abs.) and the critical pressure of the carbon dioxide-hydrogen sulfide system (approx. 1220 lbs/in.^{2} abs.). In this case the two phase three component region extends across the triangular diagram. Part (b) illustrates the phase equilibrium at a pressure, P_b, between the critical pressure of the carbon dioxide-hydrogen sulfide system (approx. 1220 lbs/in.^{2} abs.) and the critical pressure of the methane-hydrogen sulfide system (1660 lbs/in.^{2} abs.). In this case the three component two phase region has diminished to a small area along the methane-hydrogen sulfide axis.

(3) Deviations From Ideal Behavior

(a) Ideal Solution Law

According to Dalton's Law the partial pressure of a component present in an ideal vapor phase in equilibrium with liquid containing the

FIG. 2

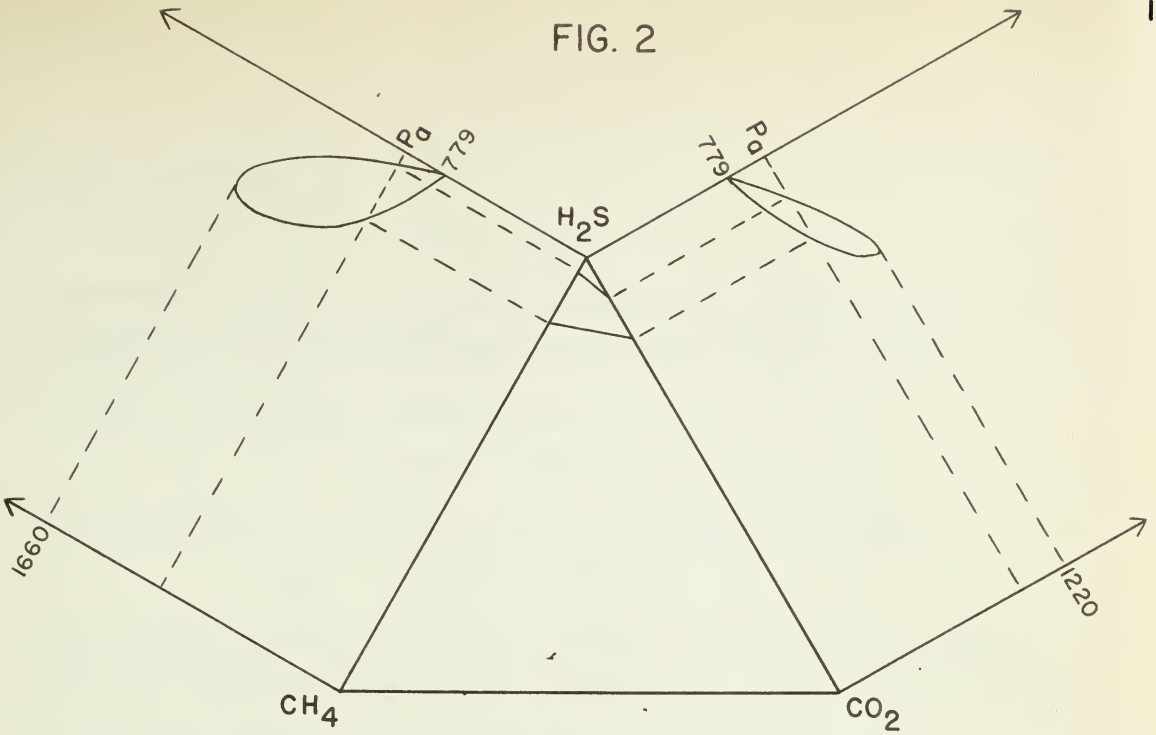

Part (a). Isobaric Section At P_a Where $779 < P_a < 1220$ lbs / in.^{2} abs.

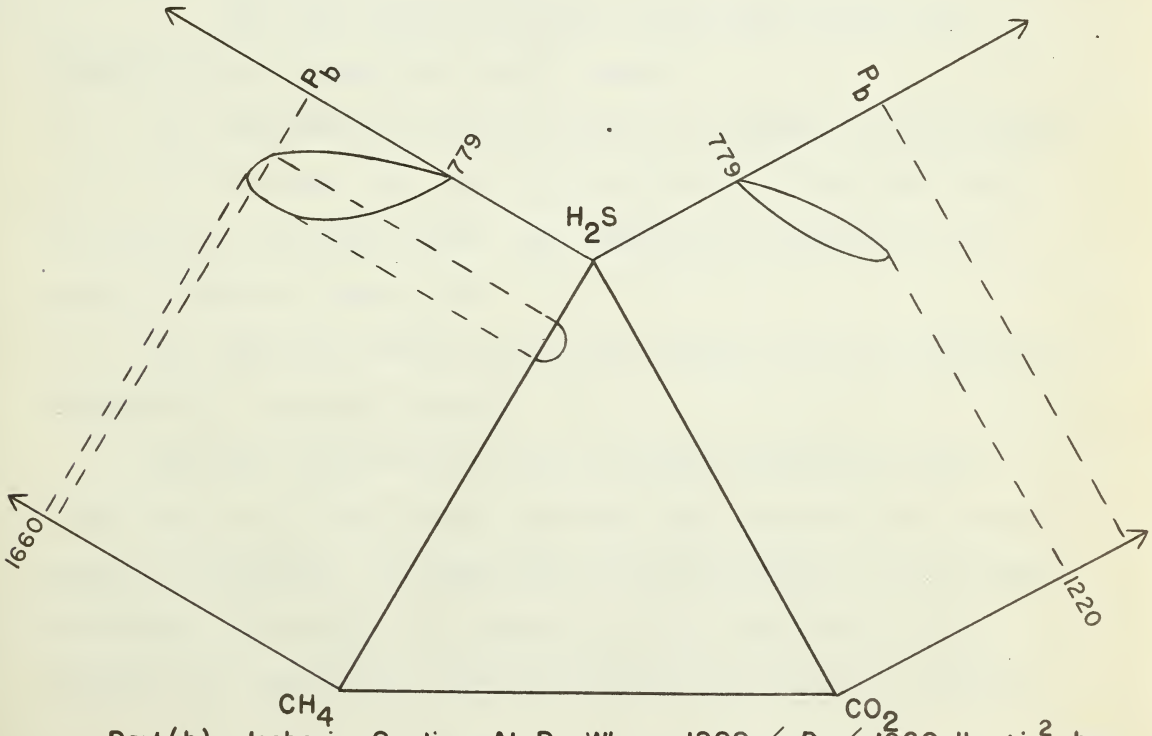

Part (b). Isobaric Section At P_b Where $1220 < P_b < 1660$ lbs / in.^{2} abs.

TERNARY ISOBARIC DIAGRAMS AT 160°F.

component is given as:

$$P_i = y_i \pi \quad \text{--- (2)}$$

According to Raoult's Law the partial pressure of a component present in a vapor phase in equilibrium with a liquid which contains the component and behaves as an ideal solution is given as:

$$P_i = x_i P_i^* \quad \text{--- (3)}$$

Combining these two expressions leads to the ideal solution law.

$$y_i \pi = x_i P_i^* \quad \text{--- (4)}$$

which relates the distribution of a component between liquid and vapor phases, in equilibrium at the system pressure, to the vapor pressure of the pure component at the system temperature.

(b) Behavior of Real Systems

The ideal solution law does not correctly describe the behavior of real systems for several reasons:

(1) Non-ideality in the gas phase, i.e. Dalton's Law inapplicable.

(2) Deviation from ideal solution behavior in the liquid phase, i.e. Raoult's Law inapplicable. This deviation is considered to be a result of molecular association.

(3) The vapor pressure of the pure component does not necessarily represent its "escaping tendency."

The ideal solution law is never strictly applicable to vapor-liquid phase equilibrium because conditions must always be such that the solution is non-ideal. An ideal solution may be defined as one in which the partial molal volumes are independent of the composition of the solution, i.e. one in which the volumes of the components are additive.

This is the case for a gaseous mixture at any pressure, provided the system temperature is above the critical temperatures of all the components, but, at such a temperature two phase equilibrium cannot exist. In order for the liquid phase to possess the property of additive volumes, the temperature of the system must be such that the vapor pressure of the most volatile component in the pure state is less than the system pressure. However, at such conditions of temperature and pressure two phases cannot exist. In vapor-liquid equilibria, each component is stable in only one of the phases when it exists in the pure state at the system temperature and pressure; and hence the requirements for an ideal solution can never be met.

(c) <u>The Concept of the Activity Coefficient</u>

The activity coefficient has been introduced as a means of allowing for deviations from the ideal solution law. If it is considered to be a factor which corrects for all deviations from ideality in both gas and liquid phases, then the modified ideal solution law is written as:

$$y_i \pi = \gamma_i \; x_i \; P_i^* \quad \text{--- (5)}$$

A better procedure is to correct for deviations from ideality in the gas phase, resulting from the effect of pressure, by introducing fugacities and to account for deviations from ideal solution behavior in the liquid phase and for the effect of molecular interactions in the gas phase by the use of the activity coefficient.

The fugacity of any component in a solution may be defined by the equation:

$$d\mu_i = RT \, d \ln \bar{f}_i \quad \text{--- (6)}$$

Considering the vapor phase and integrating between two isothermal states, i.e. between an arbitrary standard state at system temperature and the system conditions:

$$\mu_i^{v} - \mu_i^{ov} = RT \ln \frac{\bar{f}_i^{v}}{\bar{f}_i^{ov}} \quad \text{--- (7)}$$

Also, the fugacity of a component in a solution is given by:

$$\bar{f}_i^{v} = \gamma_i^{v} y_i f_{p_i} \quad \text{--- (8)}$$

Hence:

$$\mu_i^{v} - \mu_i^{ov} = RT \ln \frac{\gamma_i^{v} y_i f_{p_i}}{\bar{f}_i^{ov}} \quad \text{--- (9)}$$

Considering the liquid phase and integrating between the same two isothermal states:

$$\mu_i^{L} - \mu_i^{oL} = RT \ln \frac{\bar{f}_i^{L}}{\bar{f}_i^{oL}} \quad \text{--- (10)}$$

Also,

$$\bar{f}_i^{L} = \gamma_i^{L} x_i f_i^{*} \quad \text{--- (11)}$$

Hence:

$$\mu_i^{L} - \mu_i^{oL} = RT \ln \frac{\gamma_i^{L} x_i f_i^{*}}{\bar{f}_i^{oL}} \quad \text{--- (12)}$$

Since the vapor and liquid are in equilibrium the change in the chemical potential in going from the conditions of the standard state to those of the actual system must be the same for both phases.

The fugacity of a component existing in vapor and liquid phases in equilibrium must be the same in each phase. Hence, equating equations

(9) and (12) and cancelling terms gives:

$$\gamma_i^{v} \; y_i \; f_{P_i} = \gamma_i^{L} x_i \; f_i^* \quad \text{--- (13)}$$

Thus:

$$y_i \; f_{P_i} = \frac{\gamma_i^{L}}{\gamma_i^{v}} \; x_i \; f_i^* \quad \text{--- (14)}$$

Letting:

$$\frac{\gamma_i^{L}}{\gamma_i^{v}} = \gamma_i \quad \text{--- (15)}$$

Then:

$$y_i \; f_{P_i} = \gamma_i \; x_i \; f_i^* \quad \text{--- (16)}$$

$$\frac{y_i}{x_i} = \gamma_i \; \frac{f_i^*}{f_{P_i}} \quad \text{--- (17)}$$

In terms of equilibrium ratios:

$$K_{i_{Exp}} = \gamma_i \; K_{i_{\text{Theor.}}} \quad \text{--- (18)}$$

The equilibrium ratio, $K_{i_{Exp}}$, is the experimental ratio of the mole fraction of component i in the vapor phase to the mole fraction of component i in the liquid phase. The theoretical equilibrium ratio is equal to the experimental equilibrium ratio if there is ideal vapor-liquid behavior, since in this case the activity coefficient is unity.

Since this procedure requires the use of fugacities rather than pressures it is necessary to evaluate these from consideration of the

properties of the pure components. By the definition of fugacity:

$$v\,d\,P = R\,T\;d\;\ln\;f \quad \text{--- (19)}$$

Hence:

$$\ln\;\frac{f_P}{f^*} = \frac{1}{R\,T}\int_{P^*}^{P} v\,d\,P \quad \text{--- (20)}$$

Thus, the value of $\frac{f_P}{f^*}$ at any pressure may be found by graphically evaluating $\int_{P^*}^{P} v\,d\,P$, at constant temperature. This graphical integration requires pressure-volume data for the pure component over a range from the vapor pressure of the component, at the system temperature, to the pressure of the system.

At a temperature of 40 degrees F. the system is above the critical temperature of methane and hence the vapor pressure of pure methane at the system temperature is an imaginary value which may be obtained only by extrapolation of a plot of the natural logarithm of the vapor pressure versus the inverse of the absolute temperature. With both hydrogen sulfide and carbon dioxide the system temperature is below the critical temperature and hence the vapor pressures of these components at the system temperature are real. However, pressure-volume data can be used only for pressures below the respective vapor pressures, i.e. for pressures at which the pure component can exist as a vapor at the system temperature. The $\frac{f^*}{f_P}$ values at pressures above the vapor pressure may be obtained by plotting $\frac{f^*}{f_P}$ versus pressure and extrapolating using the curve for an arbitrary temperature above the critical temperature as a guide.

At a temperature of 160 degrees F., the system is above the critical temperature of both methane and carbon dioxide and hence the vapor pressures of these components at the system temperature are imaginary. In this case pressure-volume data at pressures up to the system pressure can be obtained for both methane and carbon dioxide. However, for hydrogen sulfide the $\frac{f^*}{f_P}$ values at system pressures above its vapor pressure must be obtained in a manner analogous to that used at 40 degrees F.

This technique of evaluating activity coefficients places the interpretation of vapor-liquid equilibrium data on a more quantitative basis and enables prediction of the deviation from ideality of the liquid with change in pressure or temperature. The experimental determination of the relative proportion of each component in gas and liquid phases in equilibrium is required since theoretical methods based on the thermodynamics of equilibrium are severely limited in utility due to their complexity and to the necessity of obtaining some experimental data to evaluate constants.

III. EXPERIMENTAL EQUIPMENT

(1) Experimental Technique Employed for the Study of the Methane-Carbon Dioxide-Hydrogen Sulfide System.

This study involved the use of a variable-volume, visual type equilibrium cell adapted from a liquid level gauge. Changes of pressure within the system were brought about by addition of mercury to the cell by means of a hand operated mercury pump. Work at a temperature above that of the room was carried out by heating the constant temperature air bath surrounding the equilibrium cell by means of an electrical coil; while work at a temperature below room temperature was carried out by cooling the air bath with a standard compression type refrigerating system.

Phase equilibrium was achieved by rocking the entire cell with resultant intermingling of the gas and liquid phases due to the mixing action of the mercury within the cell. Pressure was measured by means of a Bourdon gauge and temperature by means of copper-constantan thermocouples embedded in the wall of the equilibrium cell. Sampling of the gas phase was carried out under constant pressure conditions by addition of mercury to the cell at a rate just equal to that at which the gas was removed. The remainder of the gas phase was removed under constant pressure conditions prior to the sampling of the liquid phase.

Fig. 3 is a schematic drawing of the experimental apparatus illustrating the general assembly of the basic equipment.

(2) Modification of Existing Experimental Apparatus

Extensive modifications of the equipment used by Bailey were carried out. These were required both to improve upon the mechanical performance of the apparatus and to enable study of the system at temperatures below room temperature.

(a) Equilibrium Cell

No changes were made in the actual variable-volume type equilibrium cell used by Bailey. However, the bolts holding the equilibrium cell in position were discarded and the cell was supported by two specially machined stainless steel end fittings, held by set screws passing through collars welded to the end plates of the air bath. This gave a rigid mounting and also allowed for increased free space around the cell to facilitate installation of other apparatus in the air bath. The end fittings were tapped to take Aminco Union-type Superpressure connections. Lighting of the equilibrium cell was achieved by means of a Jerguson Level Gauge Illuminator consisting of a single light connected to a strip of lucite which was held flush against the sight ports of the equilibrium cell by stainless steel strapping.

(b) Air Bath

The overall length of the air bath was reduced by several inches as such a reduction was made possible by the new method used to position the equilibrium cell. This brought about a decrease in weight and also made rocking of the air bath and attachment of pressure fittings more convenient. The interior of the bath was lined with 1 inch thick insulation giving inside dimensions of about 10 inches by 12 inches by 34 inches.

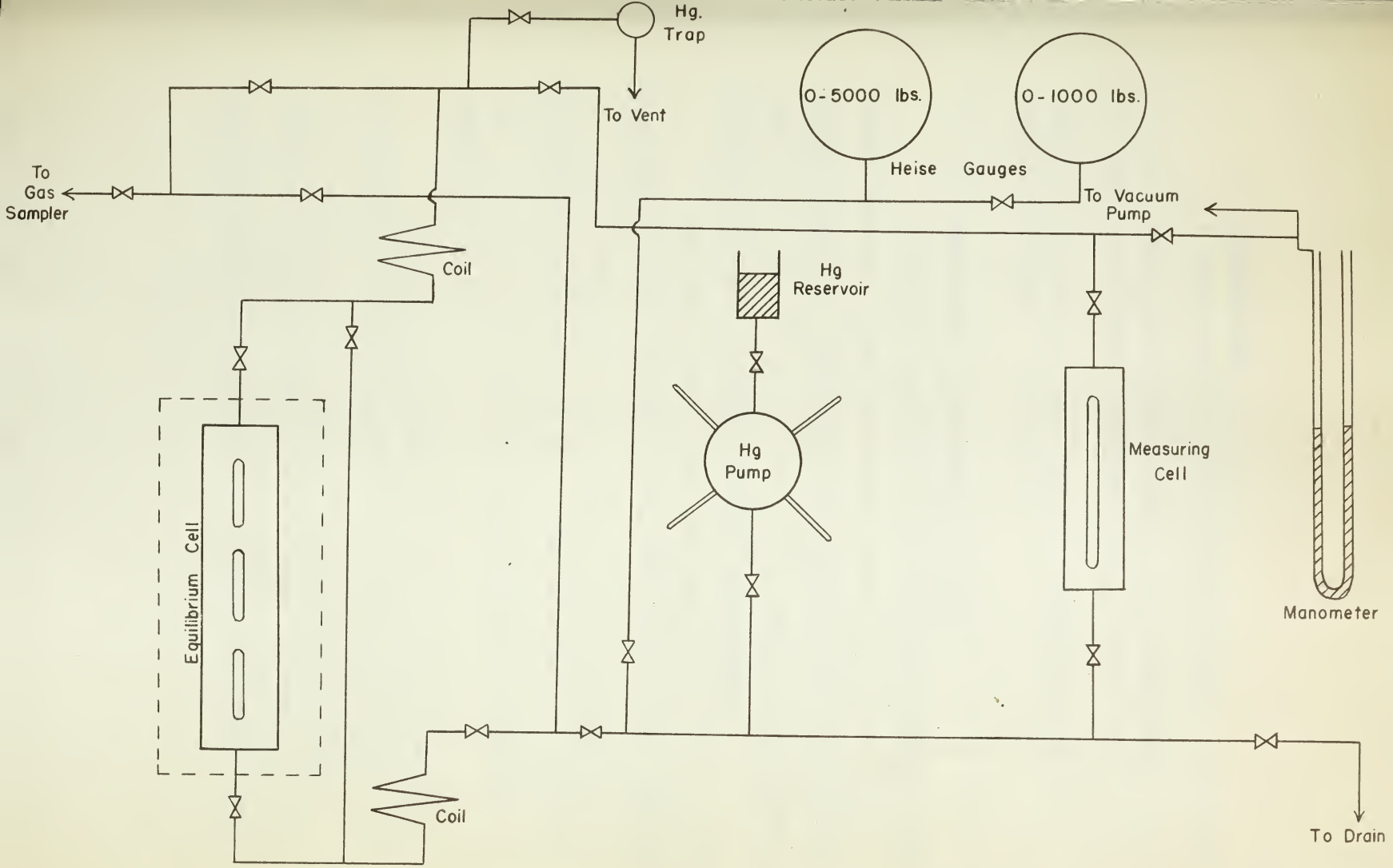

FIG. 3 SCHEMATIC APPARATUS ASSEMBLY

(c) Measuring Cell

A single Jerguson cell, approximately 120 c. c. in volume, was used to facilitate make-up of required system compositions. The cell was attached to the Dexion framework by means of two U - bolts. It was exposed to the room air and its temperature measured by means of a thermocouple embedded in the cell wall.

(d) Measurement of Experimental Variables

Temperature measurements were carried out by means of three copper-constantan thermocouples embedded one half inch in the wall of the equilibrium cell. Thermocouple cold junctions were held at the ice point and the leads were joined to a multiple position switch connecting to a Leeds and Northrup Portable Precision Potentiometer.

Pressure measurements were obtained by the use of two Bourdon-tube pressure gauges manufactured by the Heise Gauge Company. One gauge had a pressure range of 0 - 1000 lbs/in.^{2}, with 2 lb subdivisions and an estimated accuracy of $\pm$ 1 lb/in.^{2}. The second gauge had a pressure range of 0 - 5000 lb/in.^{2} with 10 lb subdivisions and an estimated accuracy of $\pm$ 5 lb/in.^{2}.

Volumetric measurements were made by direct determination of the elevation of the fluid interfaces by means of a cathetometer which could be read to 0.1 m. m. Volumes were obtained by determining differences in elevation relative to a permanent datum and then using these measurements in conjunction with volumetric calibration curves.

(e) Valves, Tubing and Fittings

All valves, tubing and fittings manufactured by the Ruska Company were removed since difficulty had been encountered by Bailey in regard to valve failures. These were replaced by Superpressure equipment manufactured by the American Instrument Co., Inc.

Valves used were of the 30,000 p. s. i. series; having stainless steel bodies and heat-treated stainless steel stems. Two-way through type and two-way angle type valves, both having port openings of 1/8 inch., were employed. Fittings were of the union type, made of 18 - 8 stainless steel and machined from solid bar stock. The tubing was made of 304 stainless steel and had $\frac{1}{4}$ inch outside diameter and 3/32 inch inside diameter with a pressure rating of 30,000 p. s. i. at 100 degrees F.

The union type connections consisted of a male tube having a 59 degree conical seating surface that was fitted into a corresponding 60 degree female conical seat in the body. An inner sleeve having a left hand thread was placed over the male tube and a gland nut having a right hand thread slipped over the sleeve and screwed into the opening in the body. In order to connect the tubing and fittings, the ends of the tubing were prepared, using special hand tools, by first turning the end to a cone and then threading it to take the inner sleeve of the coupling. The tubing was bent as required by clamping it in a vise and then slipping a piece of pipe over the free end and using it as a lever. To permit the rocking of the air bath, two coils of high pressure tubing were specially prepared by Aminco. The valves were supported by bolting them to the Dexion framework by means of the mounting holes in the valve body.

(f) Refrigeration System

A refrigeration unit was installed to maintain the equilibrium cell at 40 degrees F. The motor-compressor and air-cooled condenser, which were manufactured by Frigidaire Division of General Motors, were mounted, together with the starting box, as a single unit. The motor was rated at $\frac{1}{2}$ H. P. and the unit drew line amperage of 8.2 amps. The system employed Freon 12 as refrigerant and the evaporator coil was constructed of twenty-five feet of $\frac{1}{2}$ inch copper tubing. The expansion valve was a Frigidaire Modulux Refrigerant Control valve; which made use of a gas-charged modulating bulb, clamped to the suction line near the evaporator outlet. The valve used was an MX - 6 AC model, having a temperature range of -30 to +40 degrees F. A silica gel drier was installed between the condenser and the evaporator to remove moisture from the refrigerant, and a sight glass was installed just before the expansion valve to ensure that the line was filled with liquid.

The evaporator coil was set in a small cork-insulated tank filled with ethylene glycol which was used as the coolant. A Minneapolis Honeywell Refrigeration Temperature Controller was used to maintain the ethylene glycol at the desired temperature by switching the compressor on and off. Pressure changes in a vapor filled capsule, which was submerged in the glycol, were transmitted through capillary tubing to a bellows which operated a mercury switch and thus cycled the compressor. A minimum temperature differential of approximately $2\frac{1}{2}$ degrees could be set on the controller so that the compressor would be switched on at a temperature $2\frac{1}{2}$ degrees above the cut-out temperature.

The glycol was pumped by means of a 1/15 H. P. centrifugal pump, manufactured by Eastern Engineering Co., through a series of $\frac{1}{2}$ inch finned copper tubes arranged in a wooden duct mounted on the air bath. Flexible connections of Tygon tubing were used between the pump and the finned tubes to permit rocking of the air bath. After passing through the finned tubes, the glycol was returned to the storage tank and thus continual circulation was achieved.

Openings were cut into the air bath, near the top and the bottom of the wooden duct, to permit a small blower, mounted on the air bath, to circulate air over the finned tubes and around through the air bath. The temperature of the air was controlled by an American Instrument Co. bimetallic thermostat mounted on the top of the air bath. The thermostat operated in conjunction with an electronic relay which actuated a solenoid valve located in a by-pass line from the discharge of the centrifugal pump.

The solenoid valve was fastened to a bar of angle iron mounted on the storage tank. A flexible connection between the solenoid valve and the centrifugal pump was provided so that the shock resulting from the functioning of the solenoid valve was not transmitted to the pump. When the solenoid valve opened it permitted flow through the by-pass line and so reduced the flow of glycol through the finned tubes; thus lessening the cooling effect in the air bath. When the solenoid valve closed, all the glycol passed through the finned tubes and so maximum cooling was achieved. A manually operated valve was installed in series with the solenoid valve to regulate the amount of flow which the opening of the

solenoid would allow through the by-pass.

Control of the temperature in the air bath was thus dependent upon a balance between the range over which the glycol temperature fluctuated, the setting of the thermostat to control the solenoid valve, and the position of the manually operated valve.

(g) Heating System

For work at temperatures above room temperature the leads to the solenoid valve used in the refrigerating system were connected to a coil of nichrome wire mounted in the wooden duct in the space previously occupied by the finned copper tubing. Voltage to the heating coil was controlled by means of a Variac variable potential unit and approximately 60 volts were required to maintain the cell temperature at 160 degrees F. Sufficient air circulation was provided by the blower used in the refrigerating system and temperature regulation was achieved by the on-off action of the bimetallic thermostat.

For the phase equilibrium study at 160 degrees F. it was found to be necessary to maintain the temperature of the throttling valve above that of the equilibrium cell. This was due to the fact that the cooling effect resulting from throttling the gas phase from system pressure to atmospheric pressure caused the temperature of the valve body and connections on the upstream side of the valve stem to drop. Accordingly, the less volatile component in the vapor phase, i.e. the hydrogen sulfide, was preferentially condensed out and drops of condensate running down into the liquid phase could be observed. This condensation destroyed the equilibrium; making the vapor phase too rich in methane and in carbon

dioxide and the liquid phase too rich in hydrogen sulfide.

To overcome this difficulty, the temperature of the throttling valve and the connecting tubing above the air bath was maintained at a level approximately 100 degrees greater than the temperature of the equilibrium cell. This was accomplished by mounting a piece of transite pipe, approximately 6 inches high and 7 inches in diameter, on the air bath so that it completely enclosed the throttling valve. An electrical heating coil was mounted inside the section of transite pipe and approximately 60 volts were supplied through a Variac. By this means the temperature of the valve could be maintained at the desired level. Since the heating unit was mounted on the top of the air bath the insulation inside the bath prevented it from affecting the temperature of the equilibrium cell. This heating system was found to be very effective in completely preventing any condensation during the sampling operation.

(h) Sampling and Analytical Procedure

Sampling was carried out in exactly the same manner used by Bailey. No difficulties were encountered due to failure of the Aminco Super-pressure valves. However, extreme care was required in throttling from cell pressure to atmospheric pressure across the valve mounted at the top of the equilibrium cell.

No change was made in the analytical technique as an attempt to use a gas chromotography method proved unsuccessful. Hydrogen sulfide was determined by Tutweiler titration, methane by Orsat and carbon dioxide by difference. The Orsat analysis equipment used by Bailey was

replaced by a new build-up model manufactured by the Burrell Corporation.

(1) Gaseous Components

The gas cylinders were connected into a manifold system using 1/8 inch O. D. Ruska tubing rated to withstand 15,000 lbs/in^2 abs. A pressure regulator was connected to the methane cylinder as its pressure was too high to admit methane to the system at cylinder pressure. Throttling valves were connected to the carbon dioxide and hydrogen sulfide cylinders and these gases were admitted at cylinder pressure.

The carbon dioxide used was supplied by Liquid Carbonic Co. and rated at 99 mole % purity. The methane had a purity of 99.8 mole % and was supplied by Phillips Petroleum Co. The hydrogen sulfide was supplied by the Matheson Co. A typical analysis provided by the manufacturer was as follows:

Hydrogen sulfide	-	98.8 mole %
Methylene chloride	-	0.4 mole %
Methyl mercaptan	-	0.3 mole %
Nitrogen	-	0.2 mole %
Carbon dioxide	-	0.3 mole %

IV. EXPERIMENTAL RESULTS

(1) Experimental Phase Equilibrium Data

(A) Data at 40 Degrees F.

The preliminary stage of the experimental investigation involved a check on the data for the binary systems reported in the literature. Data at 40 degrees F. were directly available for the methane-hydrogen sulfide system and could be interpolated from values reported at temperatures near 40 degrees F. for the carbon dioxide-hydrogen sulfide system. Although two phase equilibrium occurs in the methane-carbon dioxide system at 40 degrees F., the maximum temperature reported in the literature was 29 degrees F. and hence no check for this system could be carried out.

(a) Methane-Hydrogen Sulfide System

The pressure-composition loop for the methane-hydrogen sulfide pair is illustrated by Fig. 4. Experimental determinations of the compositions of co-existing vapor and liquid phases were carried out at five different pressures ranging from 400 to 1600 lbs/in^2 abs. The values obtained show a maximum deviation from the literature data of about 2 % with most points agreeing within 1 % or better.

(b) Carbon Dioxide-Hydrogen Sulfide System

The pressure-composition loop for the carbon dioxide-hydrogen sulfide system is illustrated by Fig. 5. Experimental checks of the interpolated literature data were carried out at three different

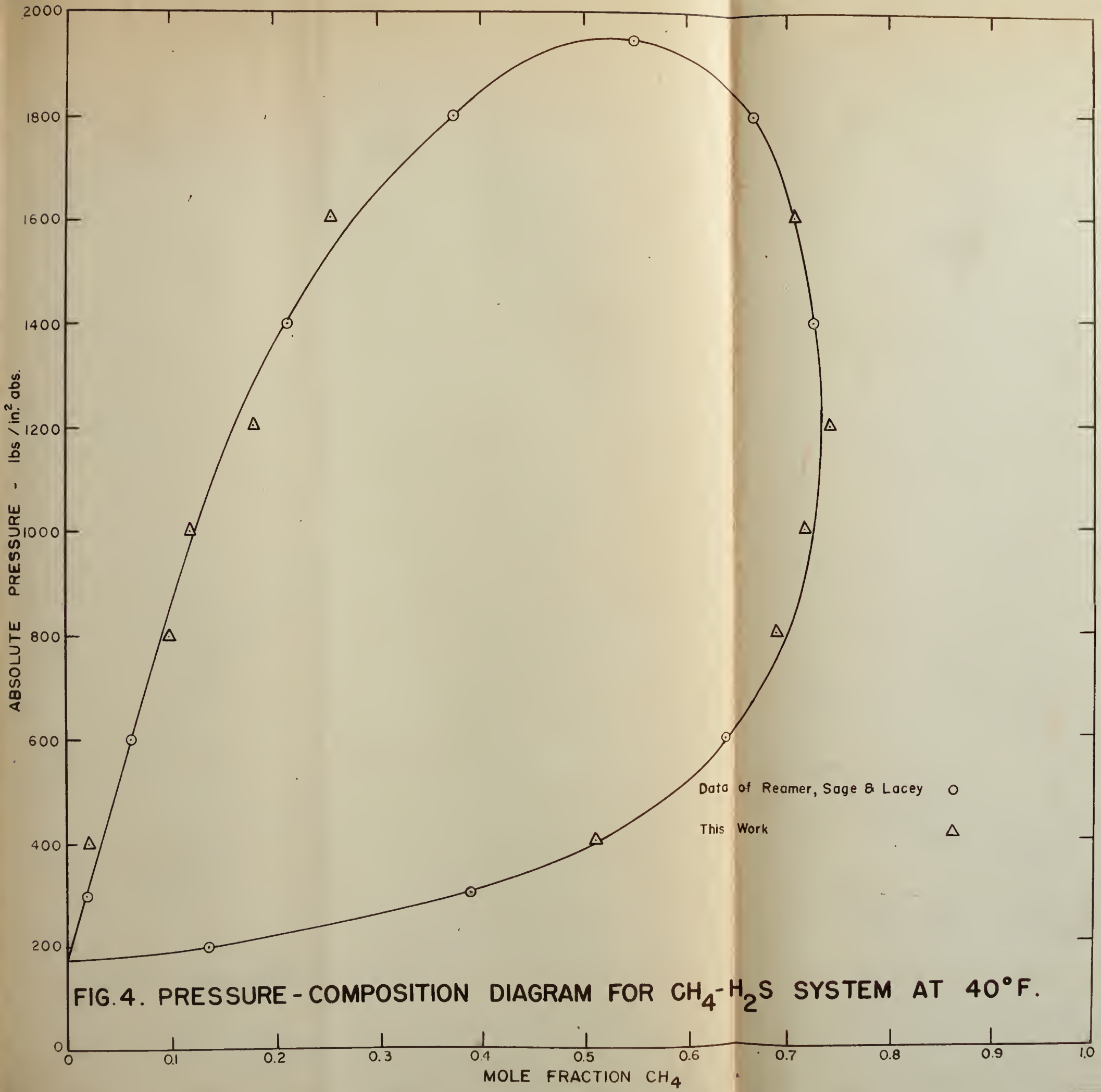

FIG. 4. PRESSURE - COMPOSITION DIAGRAM FOR CH_4-H_2S SYSTEM AT 40°F.

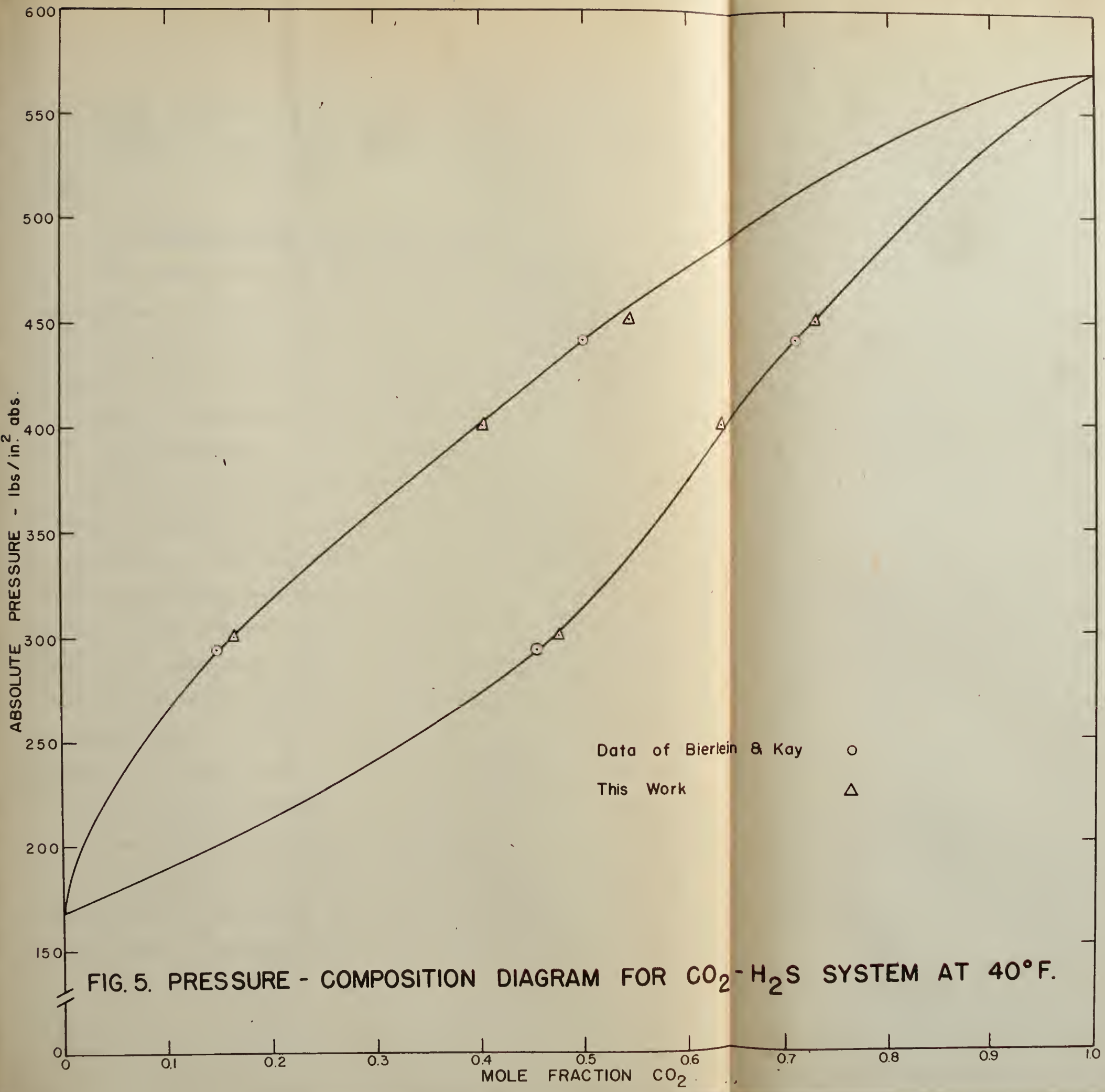

FIG. 5. PRESSURE - COMPOSITION DIAGRAM FOR CO_2-H_2S SYSTEM AT 40°F.

pressures and agreement was better than 1 % except in the case of the liquid composition at 450 lbs/in.^{2} abs. where the deviation was about 2 %.

(c) Phase Equilibrium in the Ternary System

The ternary phase equilibrium at 40 degrees F. was described by the experimental determination of the dew point and bubble point loci at pressures of 400, 1000 and 1600 lbs/in.^{2} abs. The experimental data are reported in Tables 1, 2 and 3 in the appendix and the isobaric phase equilibrium is graphically illustrated by Figs. 6, 7 and 8.

The intersections of the dew point and bubble point loci with the axes of the equilateral triangle represent respectively the vapor and liquid phase compositions of the binary systems. Hence, the comparison of the binary data with the literature data gave a check on the terminal points of the ternary dew point and bubble point loci. In ternary systems, material balance considerations show that the overall composition, the vapor phase composition and the liquid phase composition must lie on a straight line and thus a check on the reliability of the experimental work is provided. Consideration of the phase equilibrium diagram for the ternary system indicates that the overall system composition reported was high in carbon dioxide and in methane in almost every case. It is very probable that the reason for this error lies in the fact that carbon dioxide and methane were transferred from the measuring cell to the equilibrium cell and that in this operation a small fraction of the gas was trapped in the mercury lines; and, hence,

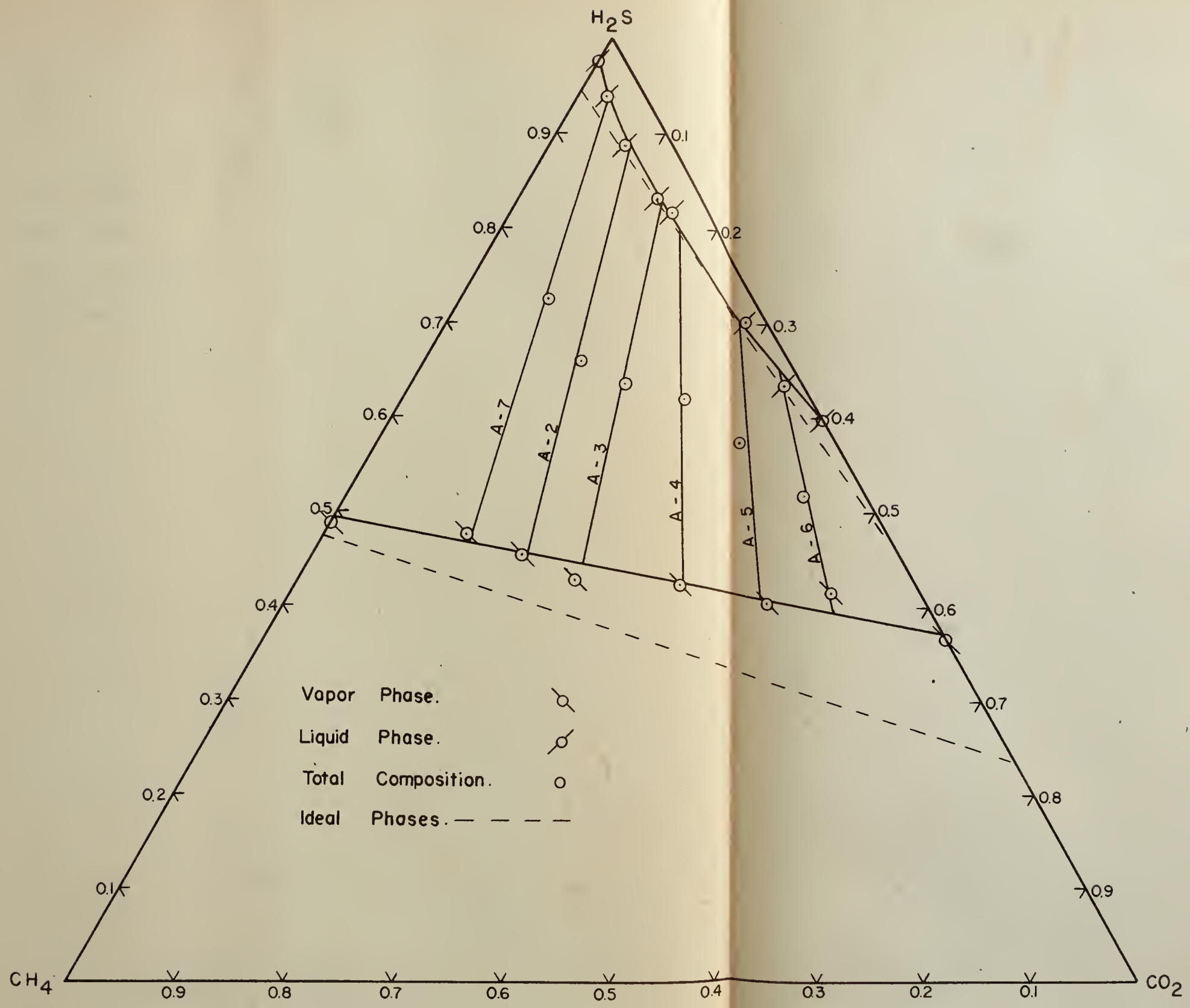

FIG. 6. MOLAR COMPOSITION DIAGRAM

T = 40° F. P = 400 lbs. / in.^{2} abs.

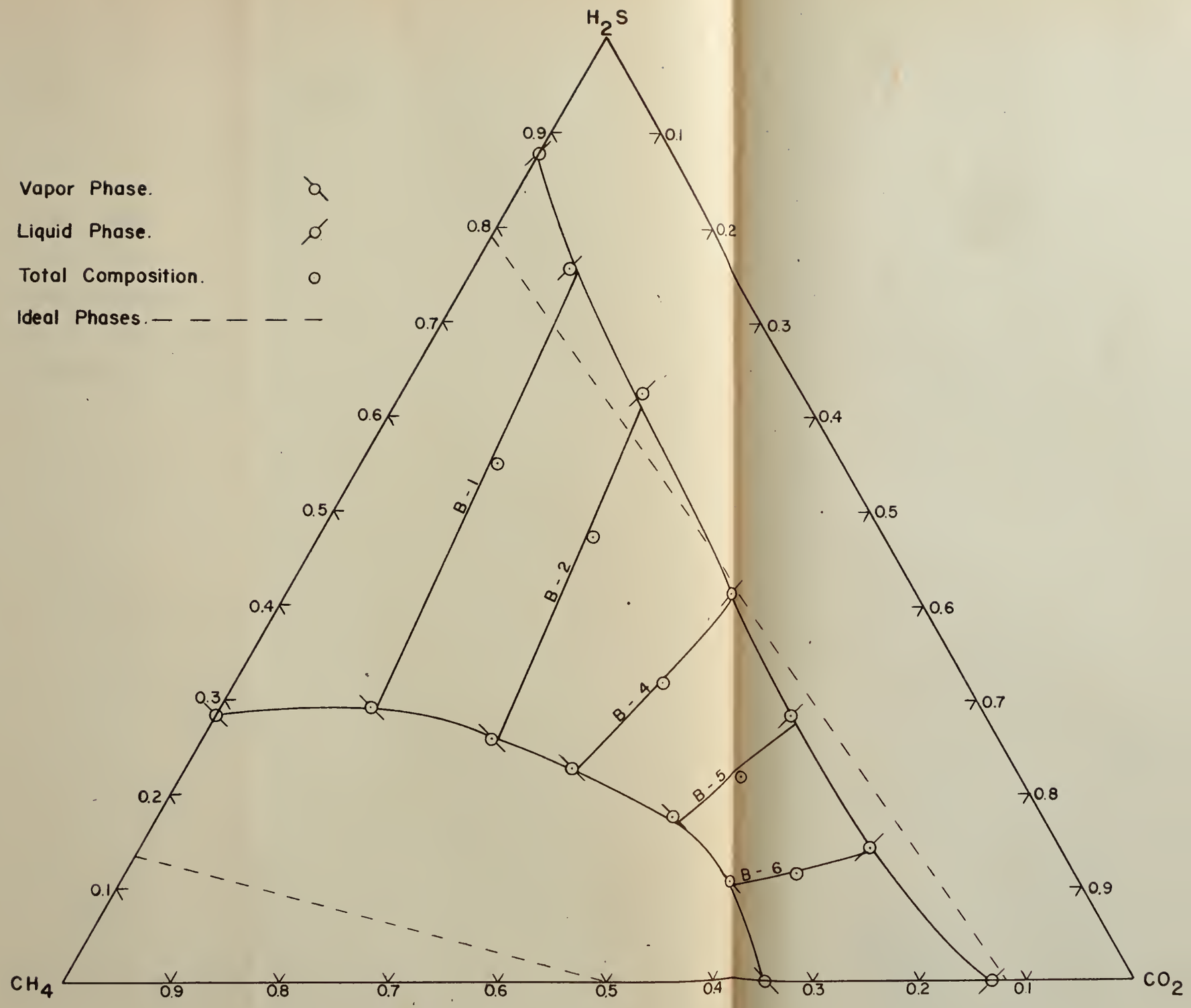

FIG. 7. MOLAR COMPOSITION DIAGRAM

T = 40° F. P = 1000 lbs./in.^{2} abs.

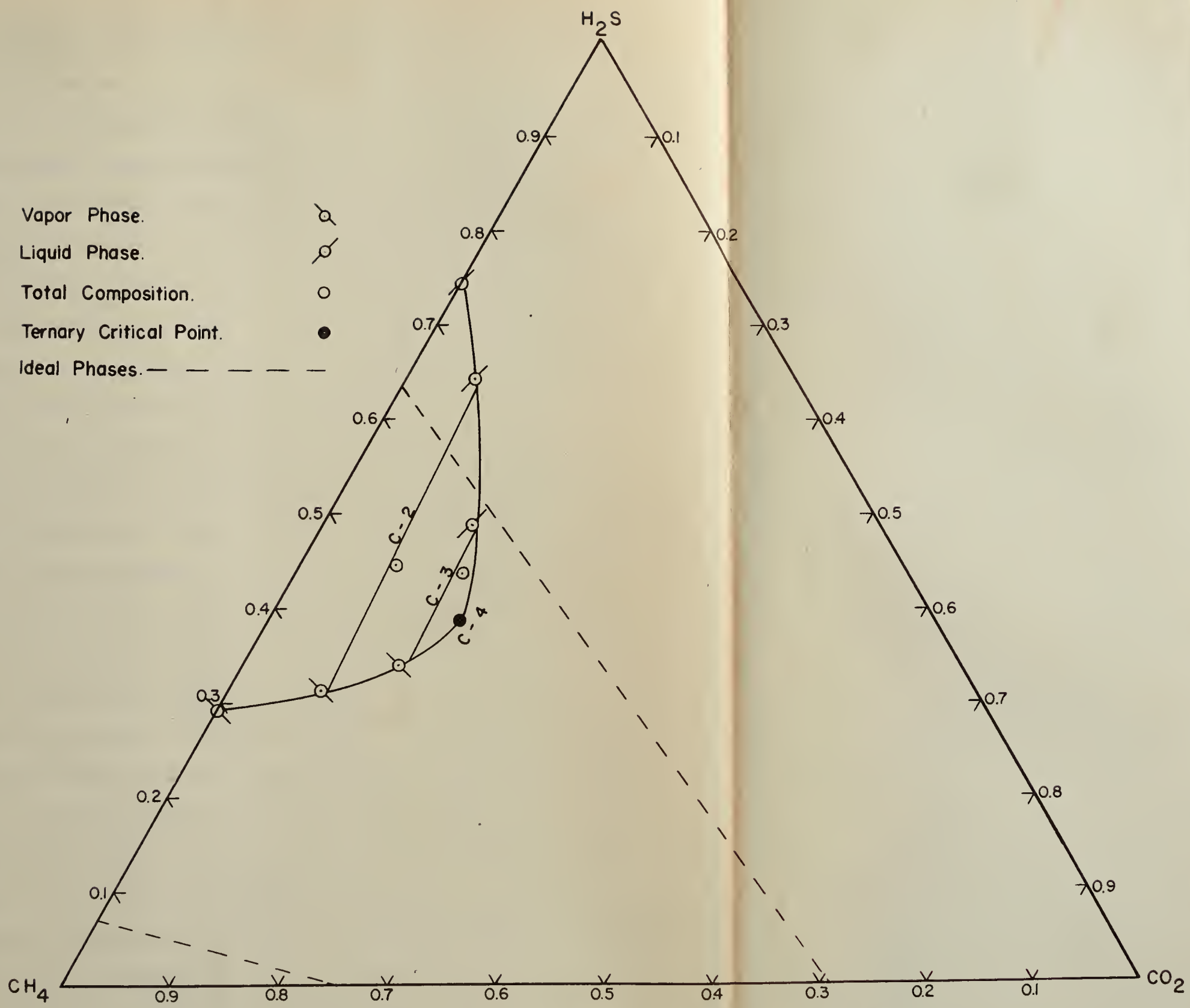

FIG. 8. MOLAR COMPOSITION DIAGRAM

T = 40° F. P = 1600 lbs. / in.^{2} abs.

the reported overall composition was higher in these components than the actual system.

Fig. 6 illustrates the phase equilibrium at a pressure between the vapor pressure of hydrogen sulfide and the vapor pressure of carbon dioxide; and, hence, the two phase region extends from the methane-hydrogen sulfide axis to the carbon dioxide-hydrogen sulfide axis. The dew point locus, i.e. the locus of vapor phase compositions, was drawn as a best fit straight line. The bubble point locus, i.e. the locus of liquid phase compositions, was almost a straight line having only a very slight curvature towards the two phase region.

Phase equilibrium at a pressure between the vapor pressure of carbon dioxide and the critical pressure of the methane-carbon dioxide pair is illustrated by Fig. 7. In this case the two phase region extends from the methane-hydrogen sulfide axis to the methane-carbon dioxide axis. The dew point locus exhibits considerable curvature towards the two phase region and a similar curvature is exhibited by the bubble point locus, but to a much lesser extent. This tendency for the dew point and bubble point loci to merge is probably a result of the development of intermolecular forces of the type that lead to the formation of azeotropes. None of the binary systems form azeotropes but the existence of such intermolecular forces is discussed by Bierlein and Kay (2) in their study of the carbon dioxide-hydrogen sulfide system. Evidence for the existence of these forces in the binary system is found in the inflection of the pressure-composition curves near the carbon dioxide axis; and in the fact that the dew point and bubble point loci tend to merge with

one another, giving a flat terminal slope to the loop. A similar region, in which the pressure-composition curves tend to become horizontal, occurs as the composition of a minimum-boiling azeotrope is approached in a system where such an azeotrope is found.

Fig. 7 also shows a change in the slope of the tie lines, from one yielding more carbon dioxide in the vapor phase than in the liquid phase to the opposite case as the percentage of carbon dioxide in the overall system is increased. This indicates that there must be one particular system - containing about 33% carbon dioxide - which would separate into vapor and liquid phases containing identical amounts of carbon dioxide.

Fig. 8 illustrates the phase equilibrium at a pressure above the critical pressure of the methane-carbon dioxide system but below the critical pressure of the methane-hydrogen sulfide system. In this case, the two phase region has diminished to a small line along the methane-hydrogen sulfide axis; and the boundary surfaces curve sharply in towards the critical point. Certain of the effects described by Bailey as occuring at the critical point in his work at 100 degrees F. were noted at the critical point for a pressure of 1600 lbs/in.^{2} abs. and a temperature of 40 degrees F. However, no indications of the color phenomena described were present at the lower temperature. A nearly indistinguishable flat hairline meniscus was noted and pronounced ebullition of the system occurred upon an abrupt pressure reduction of only a few pounds. Momentary darkening of the system also occurred with subsequent slow reforming of the two phases.

(B) Data at 160 Degrees F.

A check on the data reported in the literature for the binary system at 160 degrees F. was carried out. Data were directly available for the methane-hydrogen sulfide system at this temperature and could be interpolated for the carbon dioxide-hydrogen sulfide system. A temperature of 160 degrees F. is above the critical temperatures of both methane and carbon dioxide and, hence, two phase equilibrium does not occur in the methane-carbon dioxide pair at this temperature.

(a) Methane-Hydrogen Sulfide System

Fig. 9 represents the pressure-composition diagram for the methane-hydrogen sulfide system at 160 degrees F. Experimental checks of the published data were carried out at pressures of 1000 and 1600 lbs/in.^{2} abs. and agreement was better than 1% in both cases.

(b) Carbon Dioxide-Hydrogen Sulfide System

The pressure-composition loop for the carbon dioxide-hydrogen sulfide system at 160 degrees F. is illustrated by Fig. 10. An experimental check of the interpolated literature data was carried out at a pressure of 1000 lbs/in.^{2} abs. and agreement was again better than 1%.

(c) Phase Equilibrium in the Ternary System

The ternary phase equilibrium at 160 degrees F. was described by the experimental determination of the dew point and bubble point loci at pressures of 1000 and 1600 lbs/in.^{2} abs. The experimental data are reported in Tables 4 and 5 in the Appendix and the isobaric phase

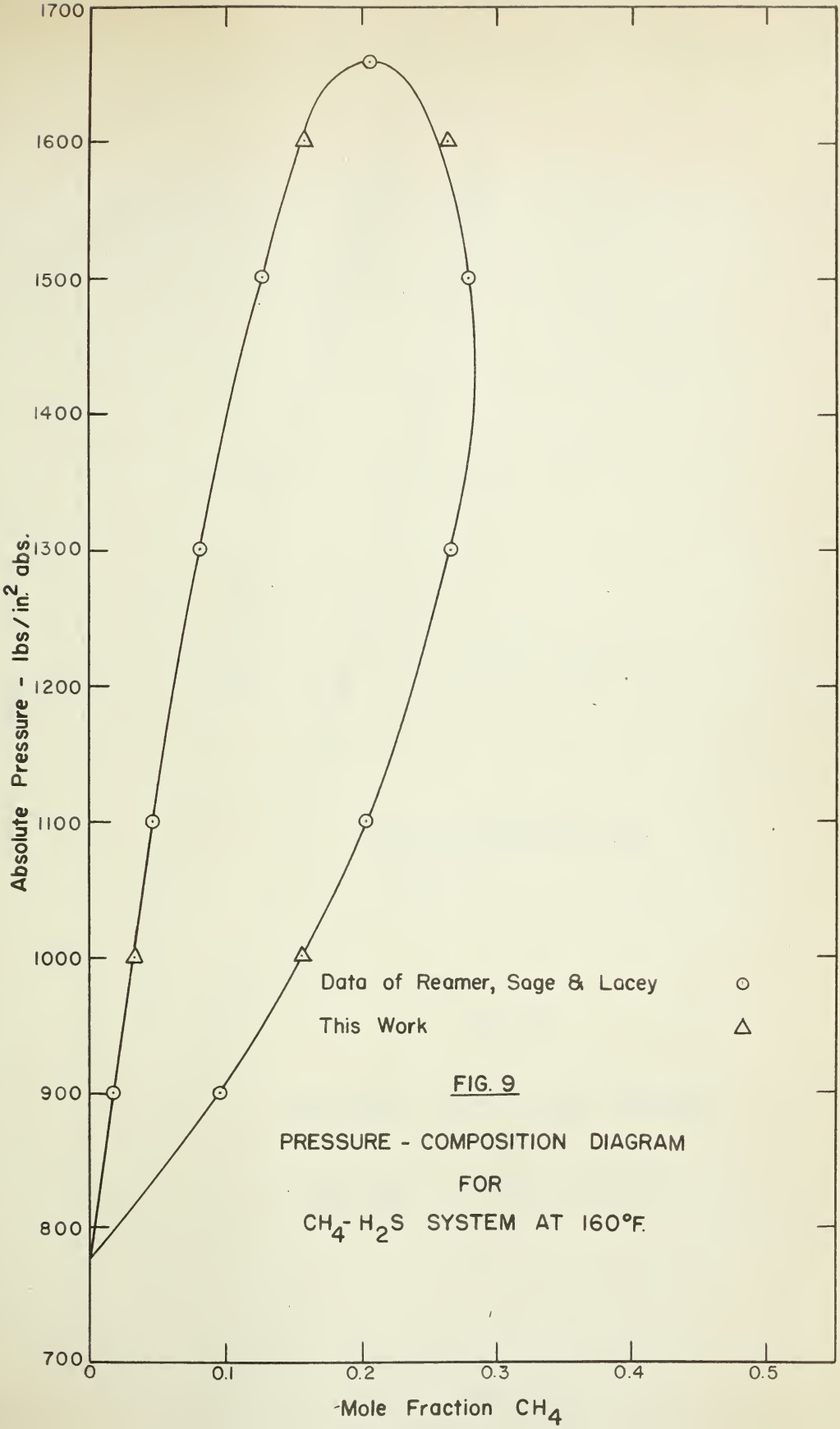

FIG. 9

PRESSURE - COMPOSITION DIAGRAM

FOR

CH_4 - H_2S SYSTEM AT 160°F.

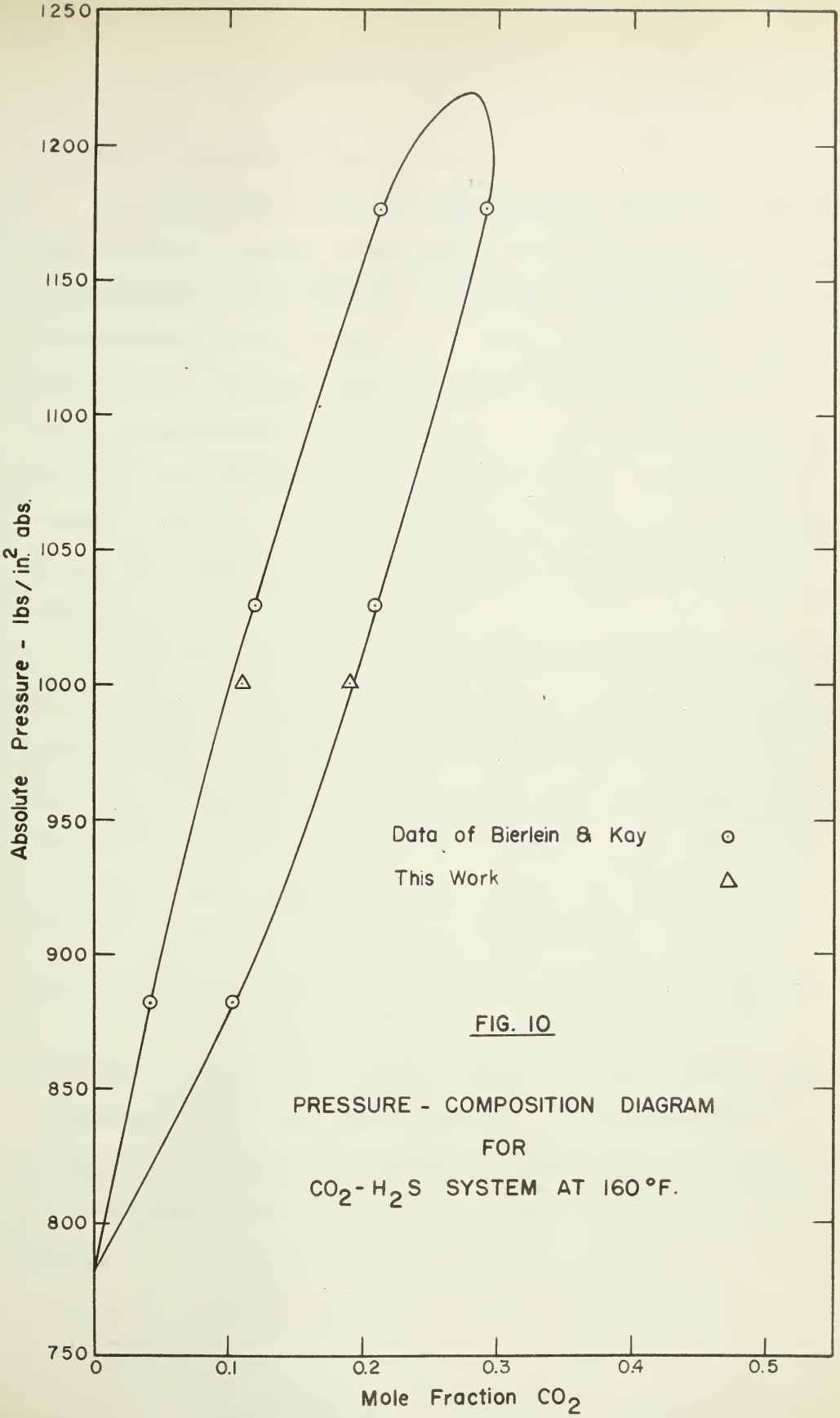

FIG. 10

PRESSURE - COMPOSITION DIAGRAM FOR CO_2 - H_2S SYSTEM AT 160 °F.

equilibrium illustrated by Figs. 11 and 12.

Fig. 11 describes the phase equilibrium at a pressure between the vapor pressure of hydrogen sulfide and the critical pressure of the carbon dioxide-hydrogen sulfide system . The two phase region extends from the methane-hydrogen sulfide boundary to the carbon dioxide-hydrogen sulfide boundary. Since two phase equilibrium occurs only in systems that are rich in hydrogen sulfide, only the portion of the triangular diagram above the 75 per cent hydrogen sulfide boundary was shown. In this case the dew point locus was a straight line joining the vapor phase compositions of the binary systems; while the bubble point locus exhibited slight curvature towards the two phase region.

Fig. 12 describes the phase equilibrium at a pressure between the critical pressure of the carbon-dioxide-hydrogen sulfide system and the critical pressure of the methane-hydrogen sulfide system. Only the portion of the triangular diagram above the 65 per cent hydrogen sulfide boundary is shown. The two phase region has diminished to a very small loop along the methane-hydrogen sulfide boundary and, hence, is adequately portrayed by a single three component system in the two phase region along with the ternary critical point. The composition for run E - 2 is shown as being just within the two phase region since this composition appeared to be the critical one for a system pressure about 25 pounds greater than the required pressure. It was not possible to determine the exact critical composition for a pressure of 1600 lbs/in^2 abs. due to the experimental errors arising in the preparation of the overall system.

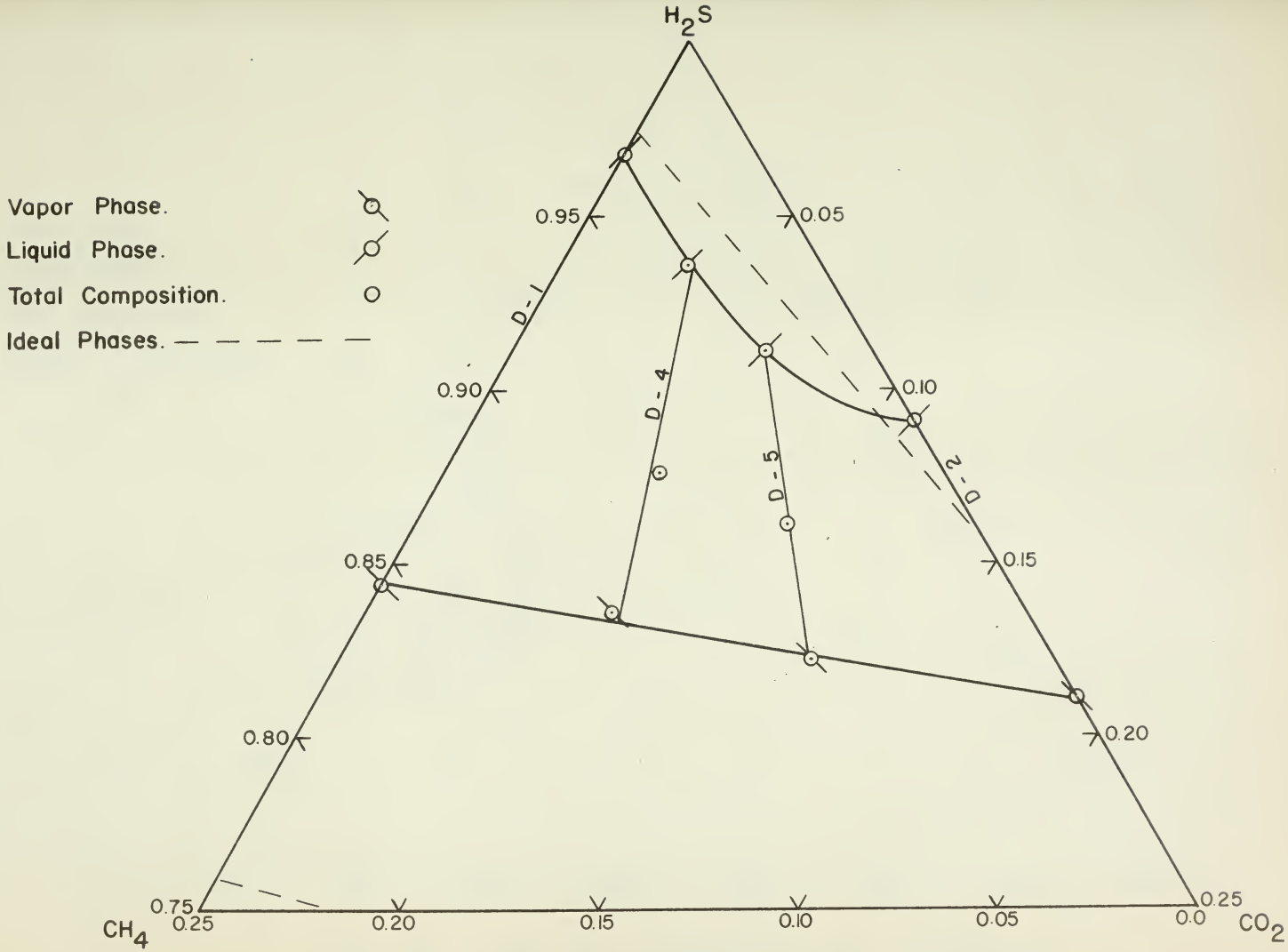

FIG. 11. MOLAR COMPOSITION DIAGRAM

T = 160°F. P = 1000 lbs./in.^{2} abs.

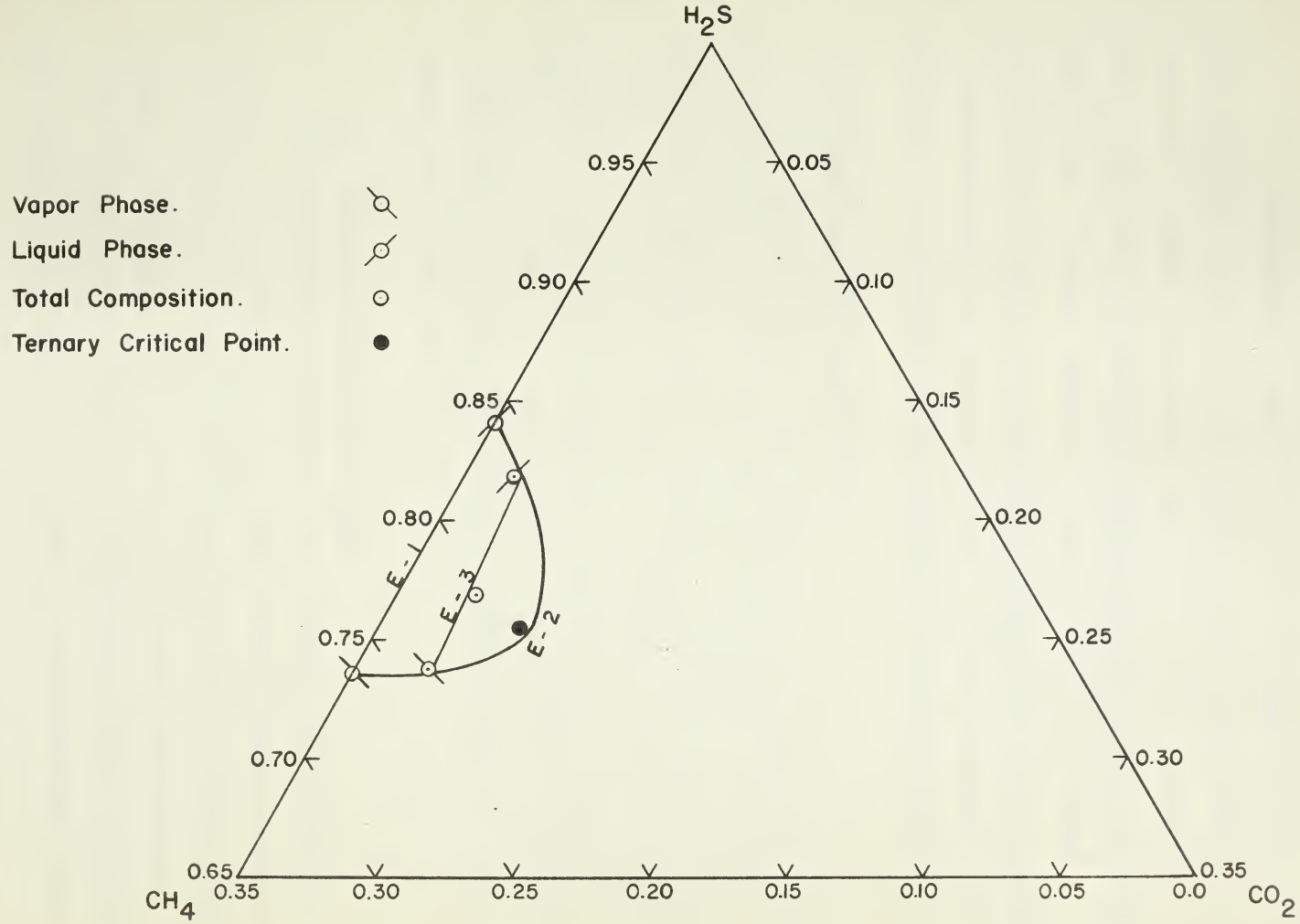

FIG. 12. MOLAR COMPOSITION DIAGRAM

T = 160°F. P = 1600 lbs./in.^{2} abs.

The phenomena at the ternary critical point were similar to those described for the work at 40 degrees F.; but, at the higher temperature, definite color effects were noted. At the equilibrium pressure the system consisted of a single phase with a uniform reddish-orange color. An abrupt decrease in pressure of only a few pounds caused a violent eruption and momentary darkening of the entire system. This was followed by a return to the normal colorless appearance of the system with an accompanying rapid formation of a more dense phase.

(2) Correlation of Experimental Data

The correlation of the experimental data was accomplished by means of determination of equilibrium ratios and determination of activity coefficients. The experimental equilibrium ratios were calculated from the test data and then the variation of equilibrium ratio with pressure for definite composition parameters was illustrated for each component. Activity coefficients were computed by means of the technique described in the theory and the effect of variation in composition at a fixed system pressure was graphically illustrated.

(a) Use of a Composition Parameter

The experimental determination of the ternary phase equilibrium resulted in the establishment of tie lines located at random intervals on the triangular diagrams. The tie lines were randomly spaced for two reasons. In the first place, it was not possible to prepare an exact overall composition as required with the experimental technique employed; and, secondly, even if the desired composition could have been prepared

the overall system compositions required to yield definite vapor phase or liquid phase compositions could not be determined beforehand. Hence, in order to be able to compare data taken at different pressures it was necessary to establish tie lines at regular values of a composition parameter.

The composition parameter chosen was the ratio of the mole fraction of carbon dioxide in the gas phase to the sum of the mole fractions of methane and carbon dioxide in the gas phase. The parameter could equally well have been based on the liquid phase. Methane and carbon dioxide were selected to establish the parameter since in most cases the overall system was rich in hydrogen sulfide and, hence, use of the mole fraction hydrogen sulfide would have resulted in a smaller range of possible parameter values at each pressure.

A graphical technique was employed in establishing tie lines at even values of the composition parameter. On the methane-carbon dioxide axis of a triangular diagram the mole fraction of hydrogen sulfide is zero and, hence, along this axis:

$$y_{CH_4} + y_{CO_2} = 1 \quad \text{---} \quad (21)$$

therefore:

$$C = \frac{y_{CO_2}}{y_{CH_4} + y_{CO_2}} = y_{CO_2} \quad \text{---} \quad (22)$$

The properties of the equilateral triangle are such that any line passing from one axis of the triangle through the opposite apex represents a locus of points having a constant ratio of the compositions of the two

components represented by the other apices. Hence, a line drawn from a particular value of C on the methane-carbon dioxide axis through the hydrogen sulfide apex must cut the dew point locus at a composition corresponding to that value of the composition parameter C. Thus, the points where the tie lines corresponding to even values of the composition parameter terminate on the dew point locus may be obtained.

To locate the points where the tie lines terminate on the bubble point locus, a graphical method of interpolating between the existing randomly placed experimental tie lines was employed. A line was drawn parallel to the methane-carbon dioxide axis from the intersection of each experimental tie line with the dew point locus and a second line was drawn parallel to the methane-hydrogen sulfide axis from the intersection with the bubble point locus. Thus, a series of triangles, each having the apex opposite the hypotenuse located on the dew point locus, was formed. A line was then drawn through the apex of each triangle which lies opposite the corresponding tie line. This line represents a locus of points which are located at the apices of similar triangles for each and every tie line. A triangle can be drawn for each tie line corresponding to a regular value of the composition parameter and, hence, the required intersections of these tie lines with the bubble point locus may be obtained.

(b) Equilibrium Ratios

By plotting tie lines at even values of the parameter C on each triangular phase equilibrium diagram, the corresponding values of the

experimental equilibrium ratio for each component were calculated. In this manner, equilibrium ratios were obtained from data which had been smoothed in regard to tie line location. These data for the phase equilibrium study at 40 degrees F. are presented in Tables 6, 7 and 8 for pressures of 400, 1000 and 1600 lbs/in.^{2} abs. respectively.

The variation of the equilibrium ratio with pressure at even values of the composition parameter C was illustrated for methane in Fig. 13. The values at a parameter of zero are for the methane-hydrogen sulfide system and, hence, a comparison between the results published in the literature and the results obtained in this study was made. Curves representing higher values of the composition parameter were drawn in using the first curve as a guide and thus a graphical smoothing of the equilibrium ratio data was achieved. No curves for values of C greater than 0.6 were shown since such values represent systems which form two phases only at the lowest pressure studied. No curve exists for a value of the parameter C equal to unity since this represents the carbon dioxide-hydrogen sulfide system.

The curves become asymptotic to the vapor pressure of hydrogen sulfide at a temperature of 40 degrees F. This is due to the fact that at pressures near the lowest pressure at which two phases may exist the more volatile components would be distributed almost entirely in the gas phase and hence their equilibrium ratios would be very high. The pressures at which the curves terminate at an equilibrium ratio of unity correspond to the critical pressures for each particular system. These pressures were obtained from a plot of pressure versus critical C value which is

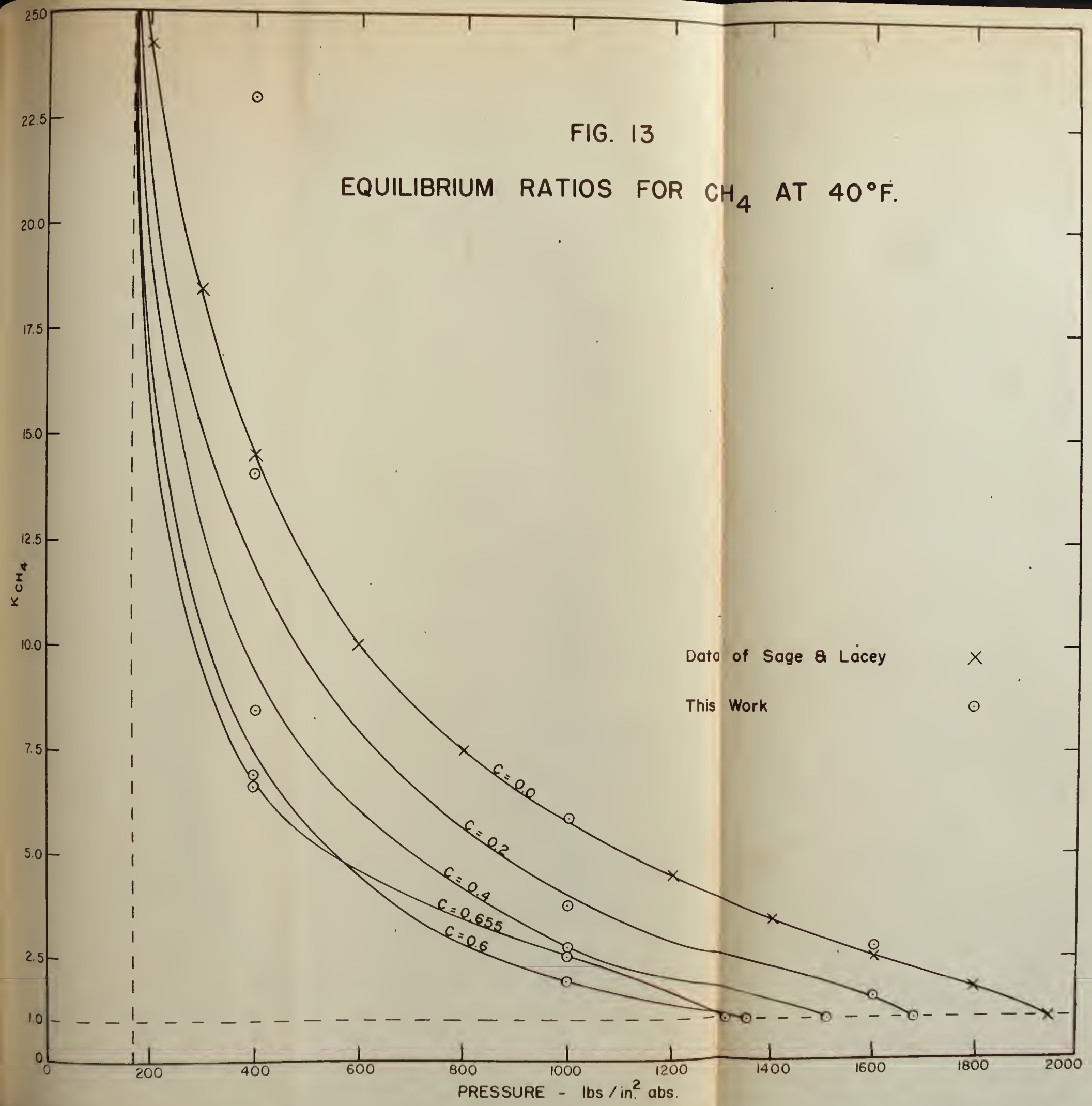
FIG. 13
EQUILIBRIUM RATIOS FOR CH_4 AT 40°F.
Data of Sage & Lacey
This Work
C = 0.0
C = 0.2
C = 0.4
C = 0.655
C = 0.6
K_{CH_4}
PRESSURE - lbs / in.^{2} abs.
25.0
22.5
20.0
17.5
15.0
12.5
10.0
7.5
5.0
2.5
1.0
0
200
400
600
800
1000
1200
1400
1600
1800
2000

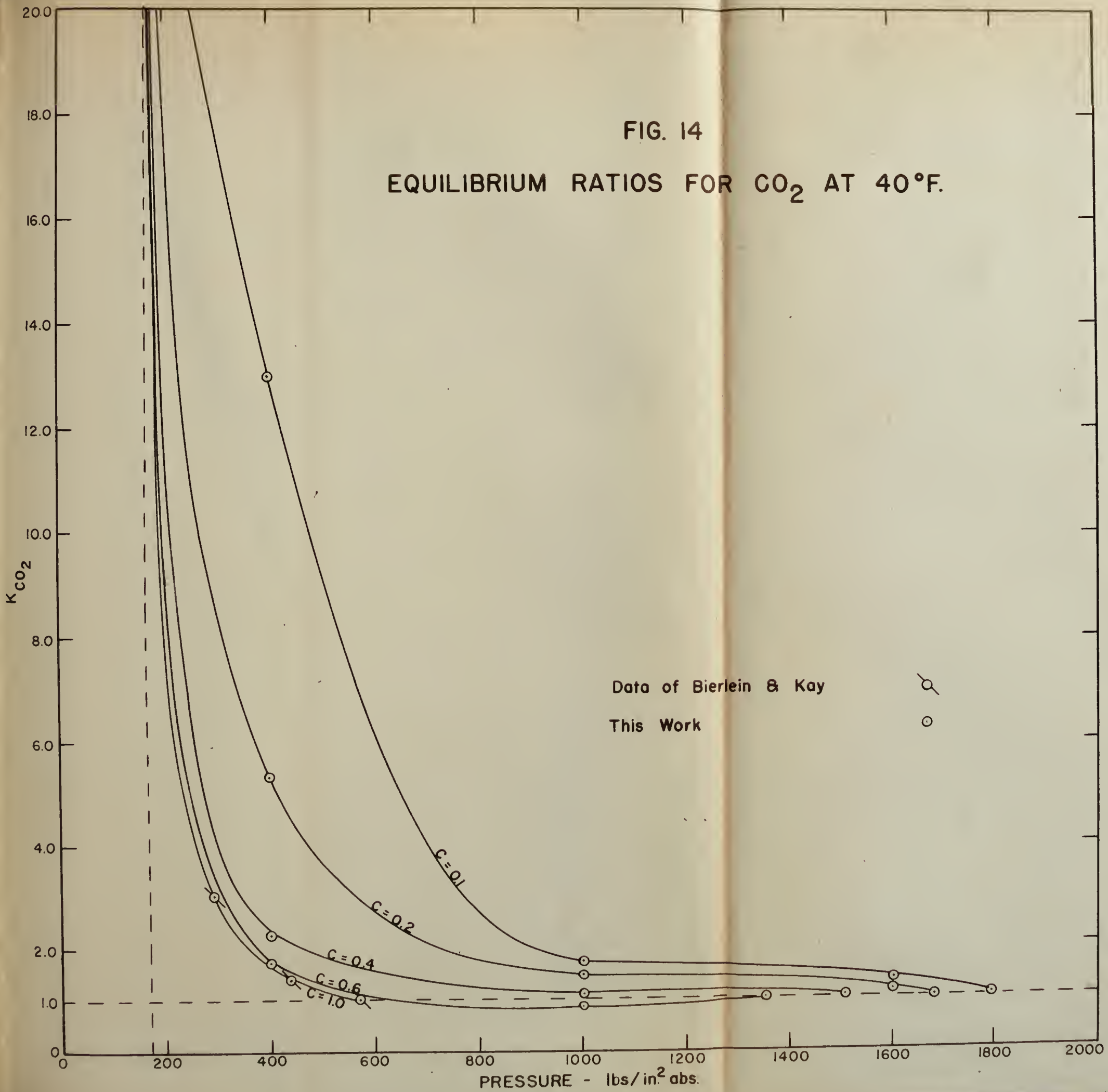
FIG. 14
EQUILIBRIUM RATIOS FOR CO_2 AT 40°F.
Data of Bierlein & Kay
This Work
C = 0.1
C = 0.2
C = 0.4
C = 0.6
C = 1.0
K_{CO_2}
PRESSURE - lbs/in.^{2} abs.
0
1.0
2.0
4.0
6.0
8.0
10.0
12.0
14.0
16.0
18.0
20.0
200
400
600
800
1000
1200
1400
1600
1800
2000

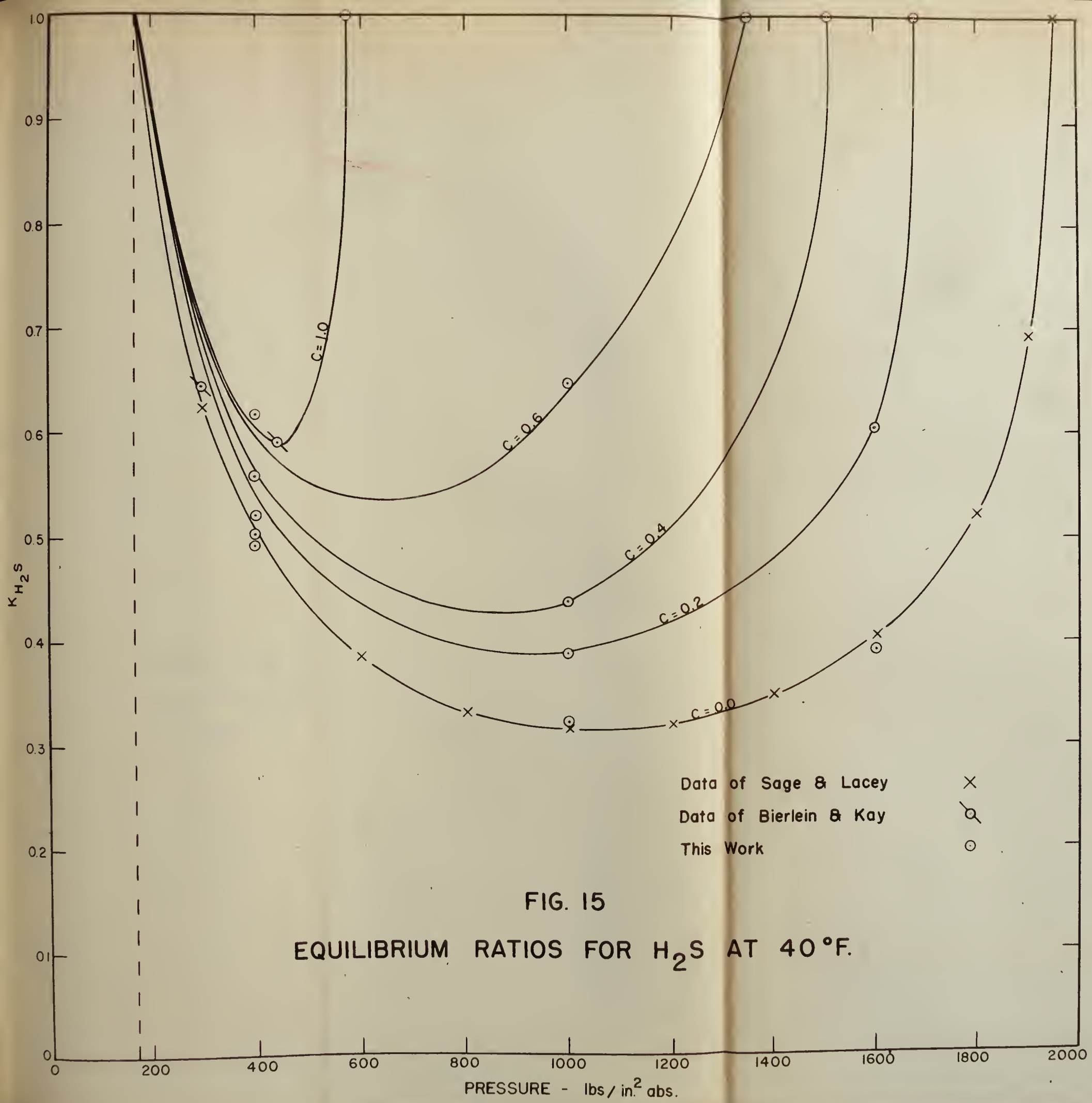

FIG. 15

EQUILIBRIUM RATIOS FOR H_2S AT 40 °F.

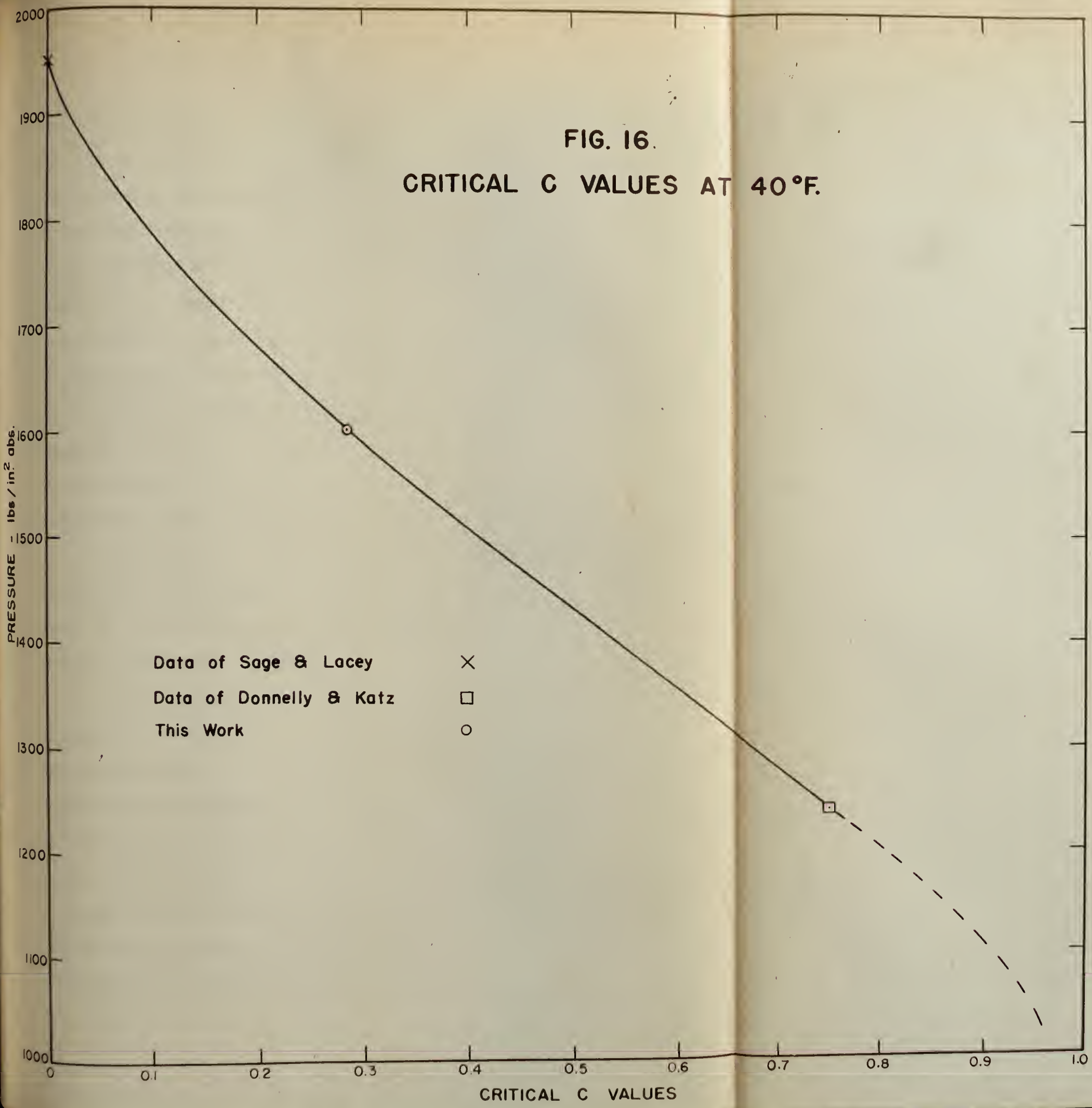
FIG. 16.
CRITICAL C VALUES AT 40°F.
PRESSURE - lbs / in.² abs.
2000
1900
1800
1700
1600
1500
1400
1300
1200
1100
1000
Data of Sage & Lacey
Data of Donnelly & Katz
This Work
0
0.1
0.2
0.3
0.4
0.5
0.6
0.7
0.8
0.9
1.0
CRITICAL C VALUES

represented by Fig. 16. The pressure for a C value of zero represents the critical pressure for the binary system methane-hydrogen sulfide. The critical C value at a pressure of 1600 lbs/in.^{2} abs. corresponds to the critical composition at that pressure, which was obtained in this study. The critical C value at a pressure of 1240 lbs/in.^{2} abs. corresponds to the critical composition for the methane-carbon dioxide system at 40 degrees F., which was estimated from a consideration of the values, at temperatures below 40 degrees F., reported in the literature. The curve indicating variation of critical C value with pressure becomes asymptotic to a C value of unity since this represents the carbon dioxide-hydrogen sulfide system for which no critical point exists at a temperature of 40 degrees F.

Fig. 13 indicates that for any particular composition the equilibrium ratio for methane decreases with increasing pressure. This is a result of the fact that more methane is forced into the liquid phase as the system pressure is increased.

Fig. 14 illustrates the variation of equilibrium ratio with pressure for carbon dioxide. As with methane, the curves are asymptotic to the vapor pressure of hydrogen sulfide at the system temperature and the value of the equilibrium ratio decreases with increasing pressure. For certain system compositions a value of the equilibrium ratio below unity is shown, which indicates that for these systems the concentration of carbon dioxide is greater in the liquid phase than in the vapor phase. The curves are terminated at equilibrium ratios of unity at pressures corresponding to the critical pressure for each particular composition.

For a corresponding system pressure and composition, the equilibrium ratio for carbon dioxide is lower than that for methane because of the fact that the vapor pressure is lower.

Fig. 15 illustrates the variation of equilibrium ratio with pressure for hydrogen sulfide. For every composition, the curve originates at an equilibrium ratio of unity at the vapor pressure of hydrogen sulfide, decreases with increasing pressure, passes through a minimum, and then increases to a value of unity at the critical pressure for that particular composition. The curve for a C value of one, which represents the carbon dioxide-hydrogen sulfide system, terminates at an equilibrium ratio of unity at the vapor pressure of carbon dioxide.

The equilibrium ratios for the phase equilibrium study at 160 degrees F. are presented in Tables 9 and 10 in the Appendix for pressures of 1000 and 1600 lbs/in.^{2} abs. respectively.

Fig. 17 illustrates the variation of equilibrium ratio with pressure for methane at 160 degrees F. Consideration of the figure indicates that the curves are very similar to those obtained for methane at 40 degrees F. All curves become asymptotic to the vapor pressure of hydrogen sulfide at 160 degrees F. and terminate at equilibrium ratios of unity at the critical pressures corresponding to the system compositions. These critical pressures were obtained from Fig. 20 which is a plot of critical C value versus pressure. The equilibrium ratio decreases with increasing pressure as more methane is forced into the liquid phase. A comparison of the equilibrium ratio versus pressure curves for the two temperatures studied indicates that

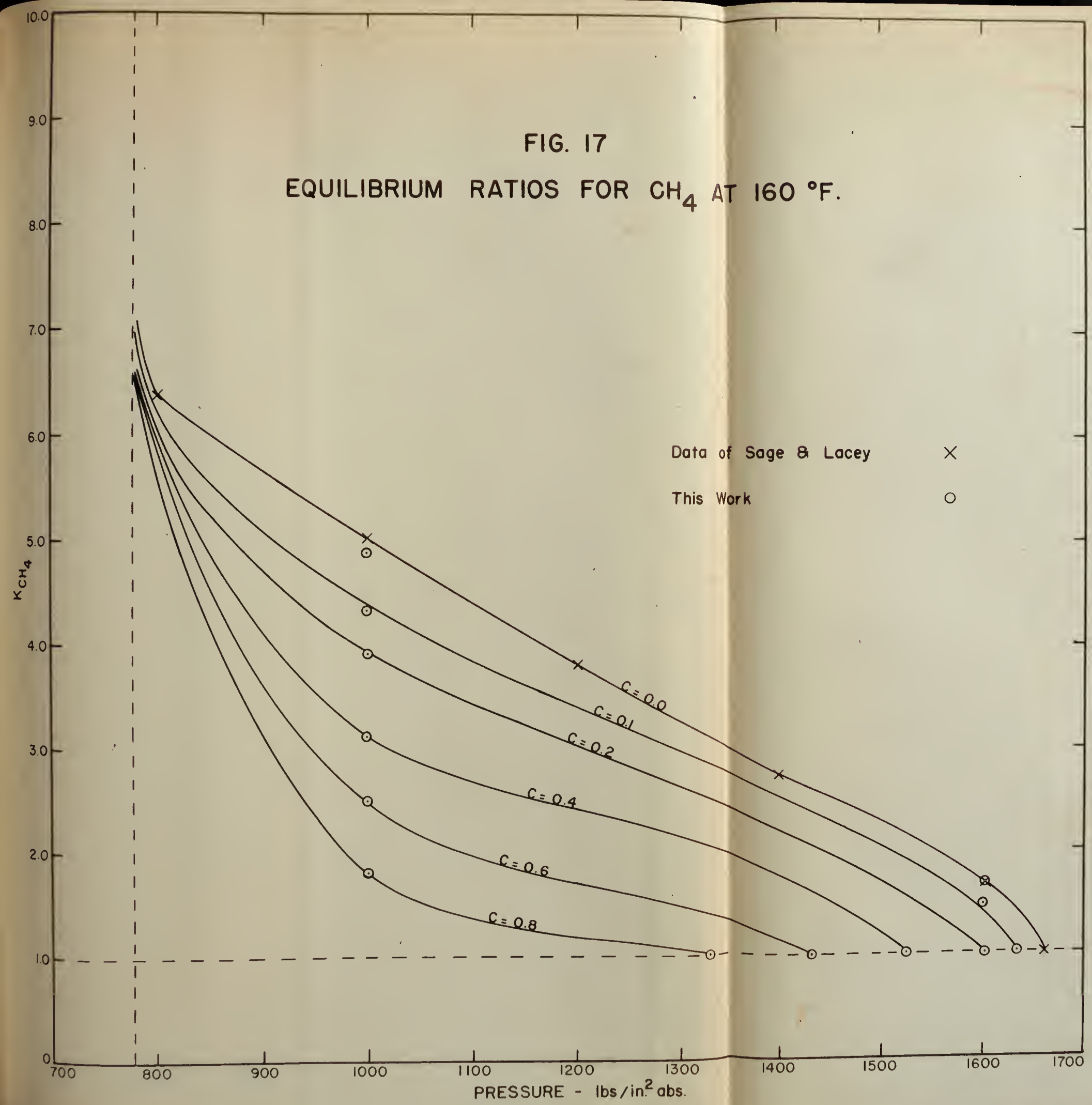
FIG. 17
EQUILIBRIUM RATIOS FOR CH_4 AT 160 °F.
Data of Sage & Lacey ×
This Work ○
C = 0.0
C = 0.1
C = 0.2
C = 0.4
C = 0.6
C = 0.8
K_{CH_4}
10.0
9.0
8.0
7.0
6.0
5.0
4.0
3.0
2.0
1.0
0
700
800
900
1000
1100
1200
1300
1400
1500
1600
1700
PRESSURE - lbs/in.^{2} abs.

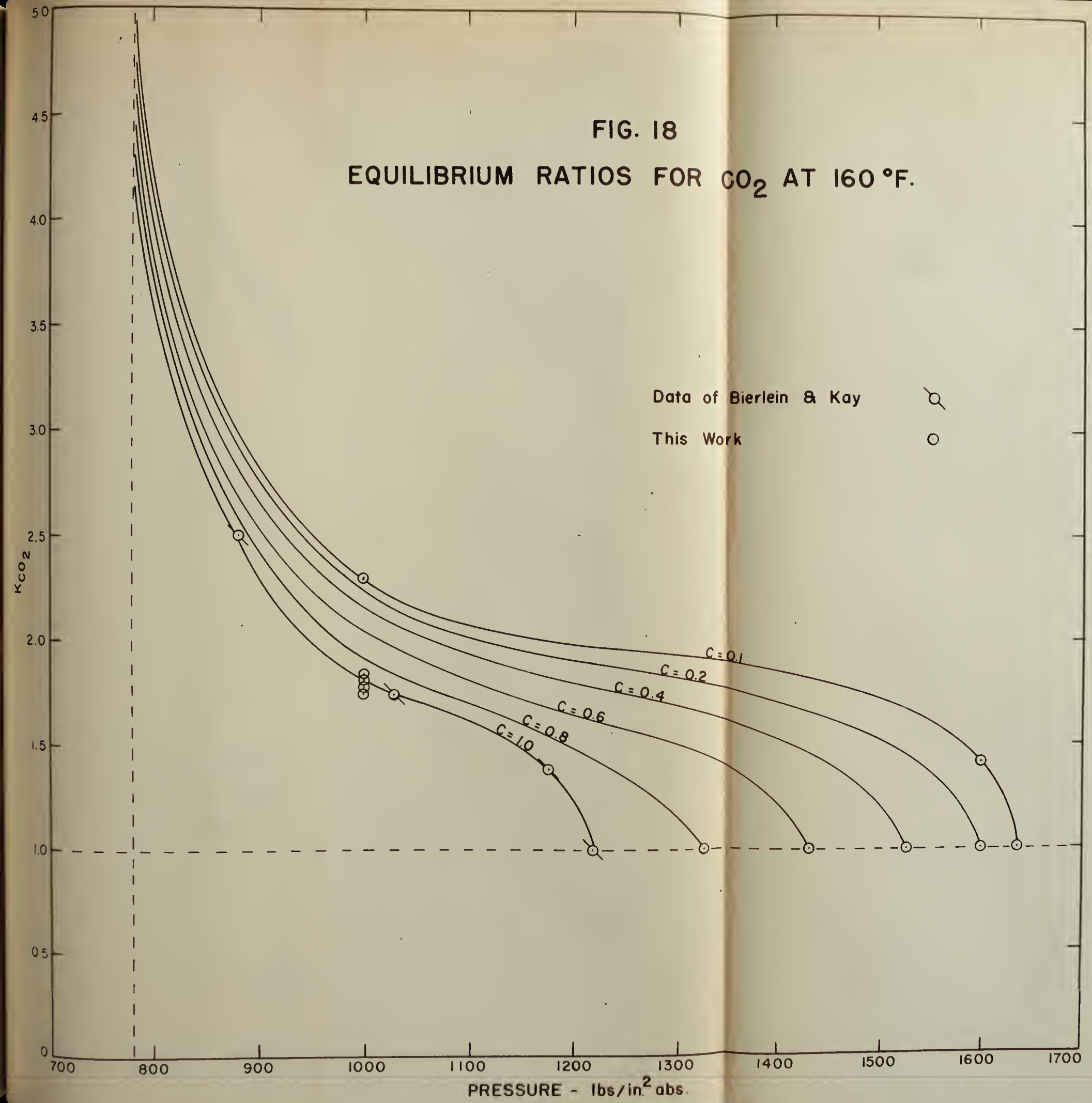
FIG. 18
EQUILIBRIUM RATIOS FOR CO_2 AT 160 °F.
Data of Bierlein & Kay
This Work
C = 0.1
C = 0.2
C = 0.4
C = 0.6
C = 0.8
C = 1.0
K_{CO_2}
5.0
4.5
4.0
3.5
3.0
2.5
2.0
1.5
1.0
0.5
0
700
800
900
1000
1100
1200
1300
1400
1500
1600
1700
PRESSURE - lbs/in.^{2} abs.

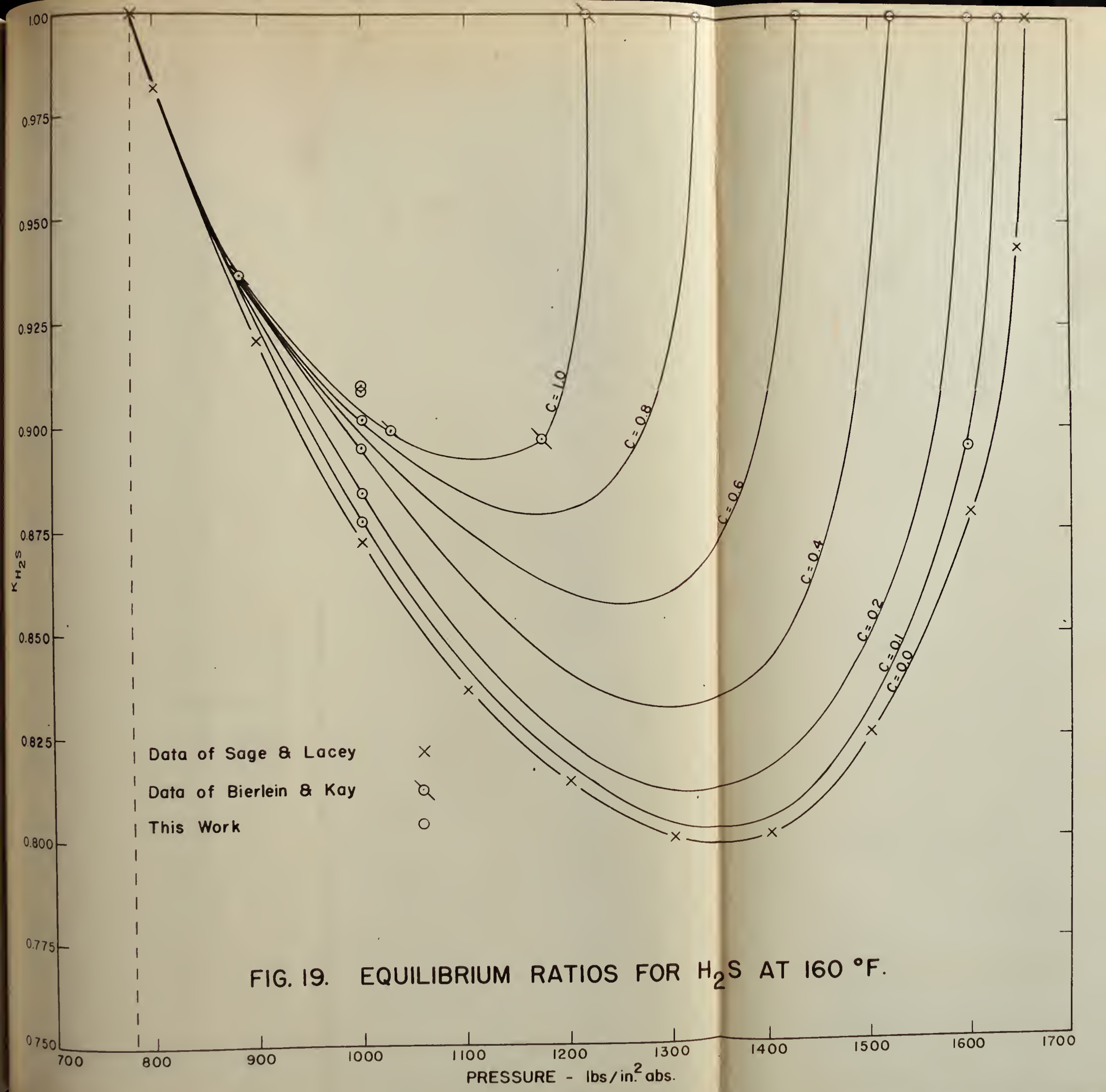

FIG. 19. EQUILIBRIUM RATIOS FOR H_2S AT 160 °F.

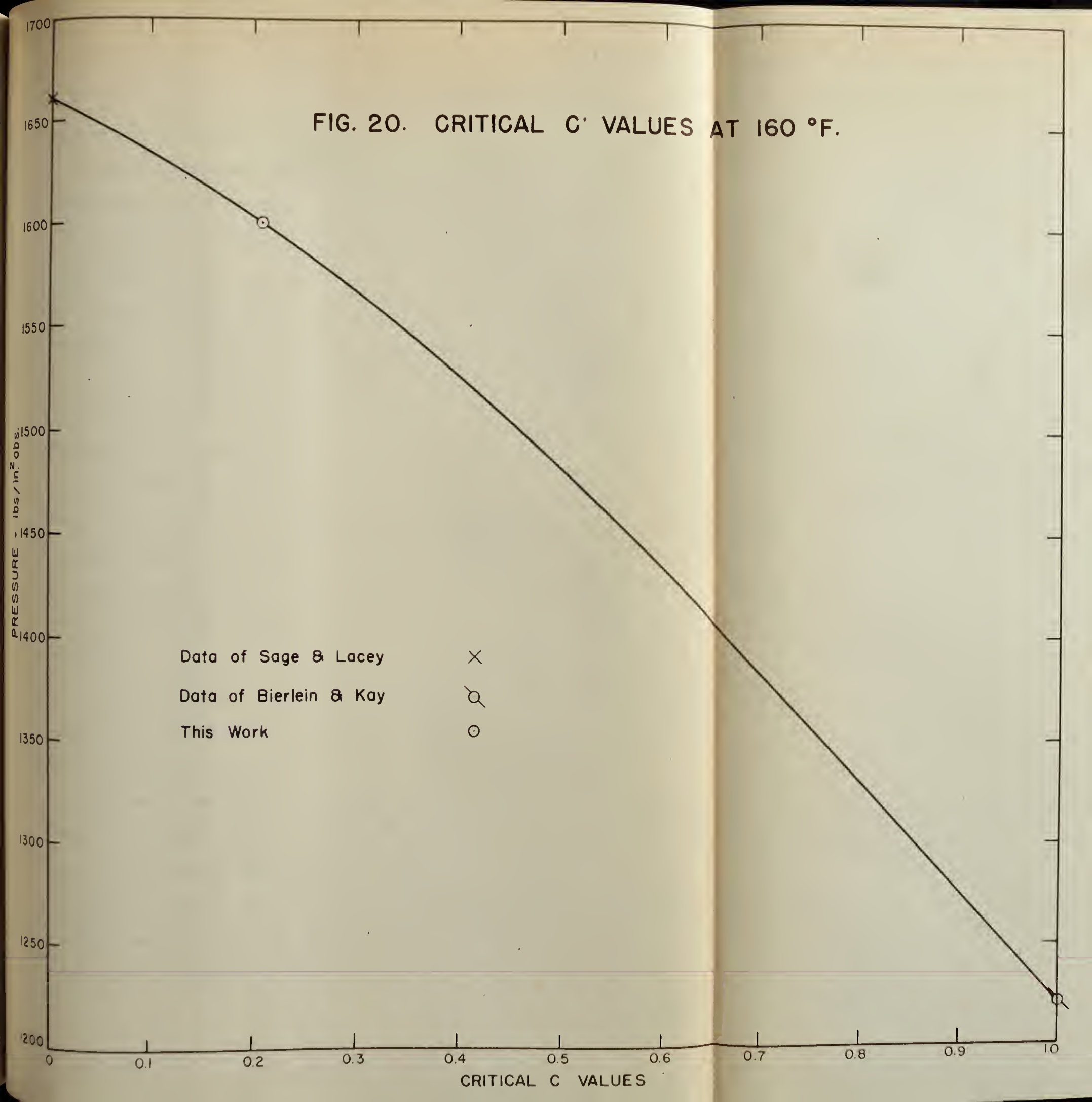
FIG. 20. CRITICAL C' VALUES AT 160 °F.
PRESSURE - lbs / in.² abs.
1700
1650
1600
1550
1500
1450
1400
1350
1300
1250
1200
Data of Sage & Lacey
Data of Bierlein & Kay
This Work
0
0.1
0.2
0.3
0.4
0.5
0.6
0.7
0.8
0.9
1.0
CRITICAL C VALUES

temperature does not have a very great effect on the equilibrium ratio for methane. For corresponding pressures and system compositions, the equilibrium ratios usually do not differ by very much at the two temperatures. No general statement as to the effect of temperature on the equilibrium ratio for methane can be made since at some combinations of pressure and composition the equilibrium ratio is greater at 40 degrees F. and at others it is greater at 160 degrees F.

Fig. 18 illustrates the variation of equilibrium ratio with pressure for carbon dioxide at 160 degrees F. A comparison of this figure with the corresponding plot at 40 degrees F. (Fig. 14) indicates that the effect of pressure is more pronounced at the lower temperature but that in both cases the equilibrium ratio decreases as increasing pressure forces more carbon dioxide into the liquid phase. For corresponding pressures and system compositions, the equilibrium ratio for carbon dioxide is always higher at 160 degrees F. than at 40 degrees F.

The variation of equilibrium ratio with pressure for hydrogen sulfide at 160 degrees F. is illustrated by Fig. 19. Comparison with the corresponding figure at 40 degrees F. (Fig. 15) indicates that an increase in temperature results in an increase in the equilibrium ratio of hydrogen sulfide. This would probably be due to the fact that with increasing temperature the vapor pressure of hydrogen sulfide approaches nearer to the system pressure and, hence, more hydrogen sulfide goes into the vapor phase and the equilibrium ratio increases. The effect of pressure is found to be similar at both temperatures,

with the value of the equilibrium ratio passing through a minimum at a particular pressure dependent upon the system composition.

(c) Activity Coefficients

The deviation of the liquid and vapor phases from ideal solution behavior was indicated by determination of an activity coefficient. Activity coefficients were calculated from smoothed experimental equilibrium ratios, taken from the plots of equilibrium ratio versus pressure, in conjunction with theoretical equilibrium ratios computed by the method previously discussed.

Activity coefficients at 40 degrees F. and at pressures of 400, 1000 and 1600 lbs/in.^{2} abs. are reported in Tables 11, 12 and 13 respectively. The activity coefficients for each component were plotted as a function of system composition at the particular pressures studied. Fig. 21 illustrates the variation of the theoretical equilibrium ratio with pressure and was used to obtain the values of the theoretical equilibrium ratio which were required in the calculation of the activity coefficients. Figures 22, 23 and 24 illustrate the activity coefficients for methane, carbon dioxide and hydrogen sulfide respectively.

Determination of the theoretical equilibrium ratio required pressure-volume data for each component as well as the vapor pressure of each component at the system temperature. A system temperature of 40 degrees F. was below the critical temperatures for carbon dioxide and hydrogen sulfide and, hence, the vapor pressures for these components were real and could be obtained from the literature. A value of 4100 lbs./in.^{2} abs. was obtained for the vapor pressure of methane at

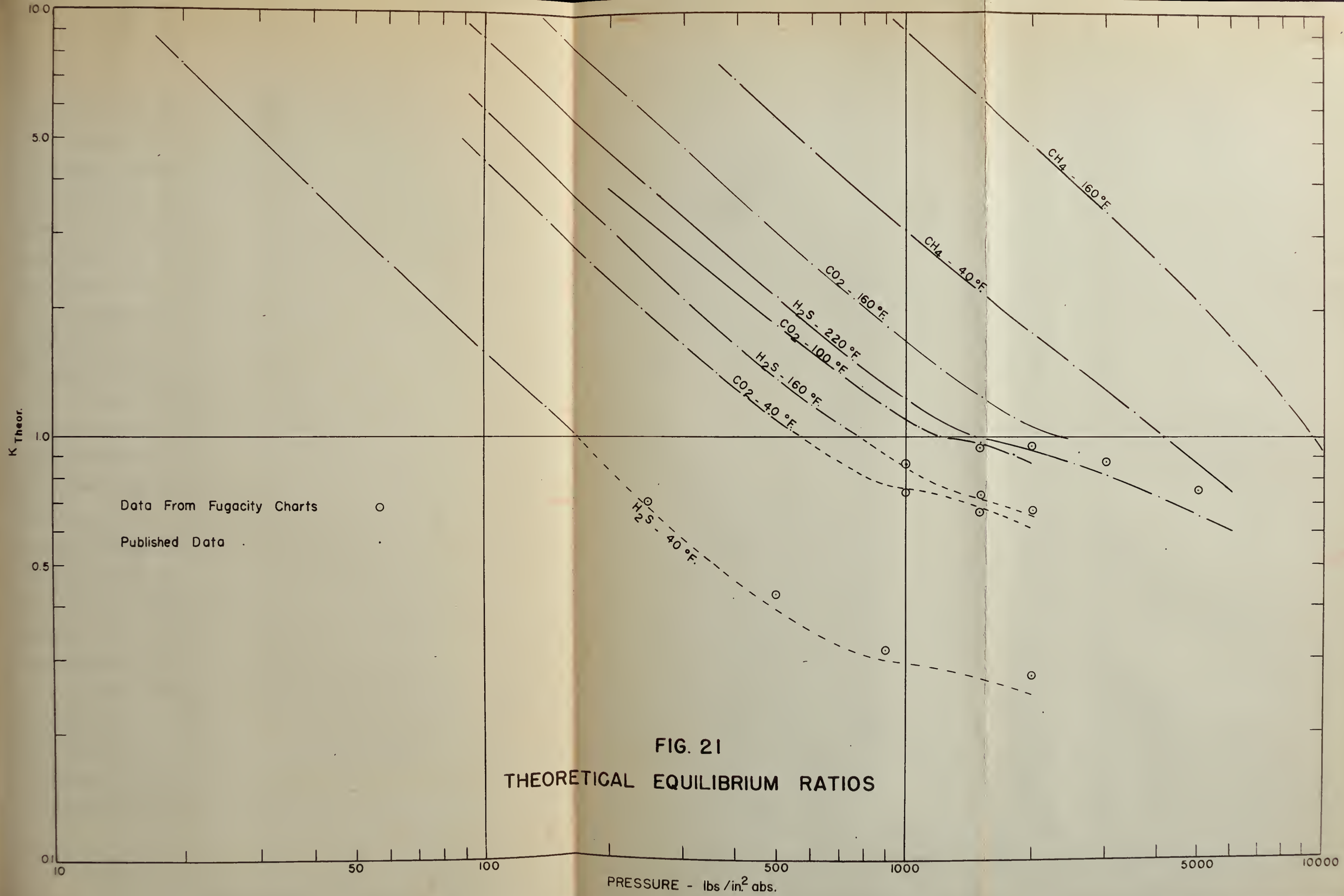

FIG. 21

THEORETICAL EQUILIBRIUM RATIOS

40 degrees F. by extrapolation of known vapor pressure data.

Pressure-volume data for methane at 40 degrees F. were not available directly. However, data were available in the literature for temperatures of 70 and 100 degrees F. (9) and for a temperature of 32 degrees F. (10). The data at 32 degrees F. were converted to pressures corresponding to those reported at 70 and 100 degrees F. and then values at 40 degrees F. were obtained by interpolation.

For carbon dioxide, pressure-volume data at pressures below that corresponding to the vapor pressure at 40 degrees F. were obtained by interpolation of data reported in the literature for 0 and 50 degrees F. (14). The plot of theoretical equilibrium ratio versus pressure was extended to pressures above the vapor pressure by using the curve for a temperature above the critical as a guide. The temperature chosen was 100 degrees F. and data were available in the literature for this temperature. (14). To facilitate the extrapolation to pressures above the vapor pressure, values for the theoretical equilibrium ratio were obtained at both 40 degrees F. and 100 degrees F. from the generalized fugacity charts in Hougen and Watson. (5). The extrapolation was performed so that the deviation from the generalized values was in the same direction at both temperatures.

Pressure-volume data for hydrogen sulfide at pressures below its vapor pressure were obtained directly from the literature. (11). The plot of theoretical equilibrium ratio versus pressure was extrapolated to pressures above the vapor pressure by using the curve at 220 degrees F. as a guide. Data at 220 degrees F., which is above the critical

temperature of hydrogen sulfide, were available directly in the same reference. As with carbon dioxide, values from the generalized fugacity charts were calculated to facilitate the extrapolation.

The numerical value of the activity coefficient is indicative of the effect of the non-ideal behavior of the liquid upon the distribution of the component between vapor and liquid phases in equilibrium. If ideal vapor-liquid behavior occurred then the theoretical and experimental equilibrium ratios would be equal and, hence, the activity coefficient would have a value of unity. Values of the activity coefficient of less than unity indicate that the component actually exists in higher concentration in the liquid phase and lower concentration in the vapor phase than the ideal coefficient predicts. Conversely, activity coefficients greater than unity indicate a concentration of the component in the vapor phase greater than the theoretical.

Fig. 22 illustrates the effect of system composition and pressure on the activity coefficients for methane at 40 degrees F. At all of the pressures studied, an increase in the value of the composition parameter-which means an increase in the relative proportion of carbon dioxide in the system - results in a decrease in the value of the activity coefficient. Thus, increasing the proportion of carbon dioxide causes the concentration of methane in the liquid phase to increase relative to that predicted by ideal solution behavior. Similarly, an increase in pressure at a fixed system composition causes a relative increase in the concentration of methane in the liquid phase.

The effect of variation of system composition and pressure is

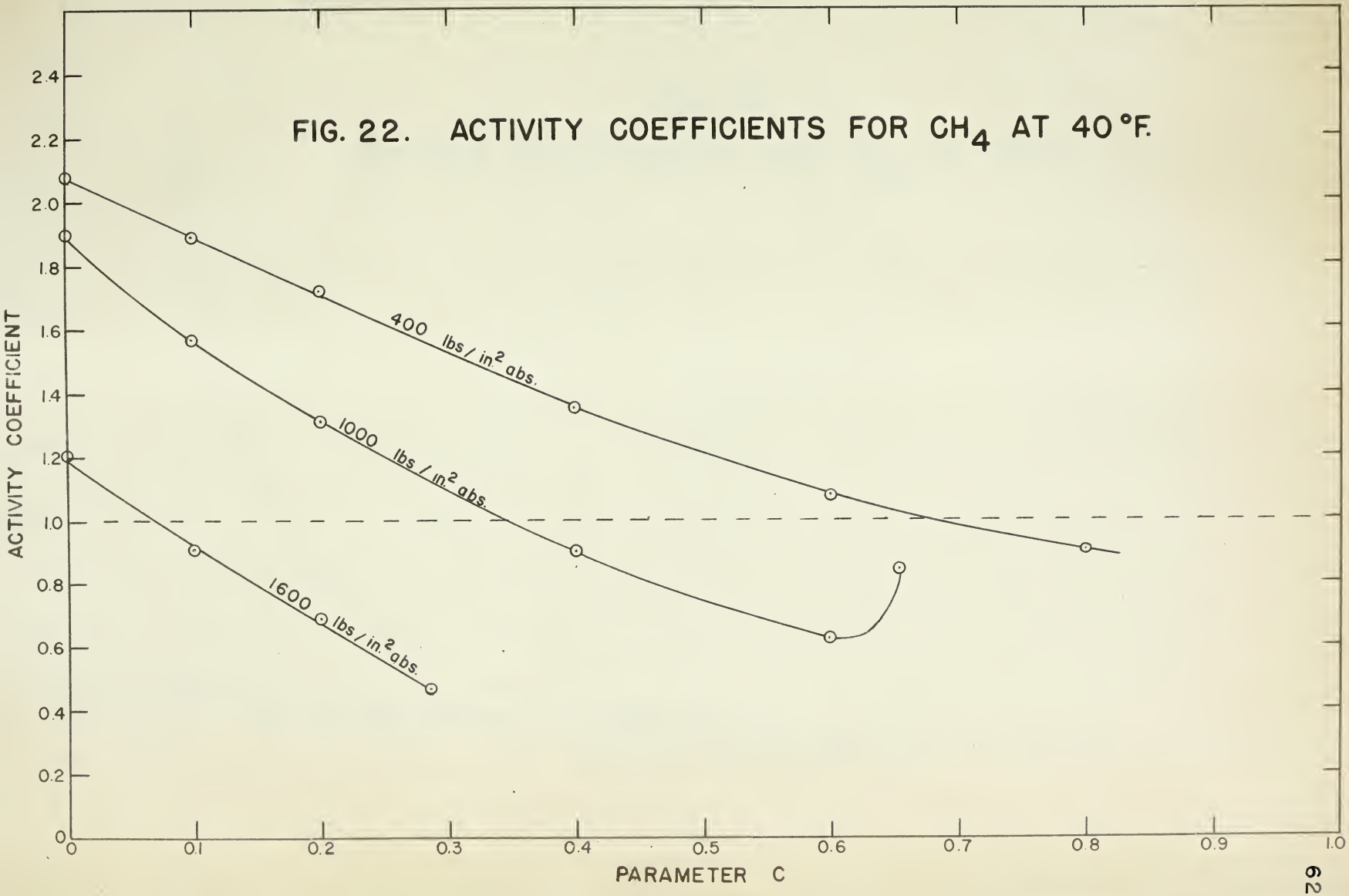

FIG. 22. ACTIVITY COEFFICIENTS FOR CH_4 AT 40°F.

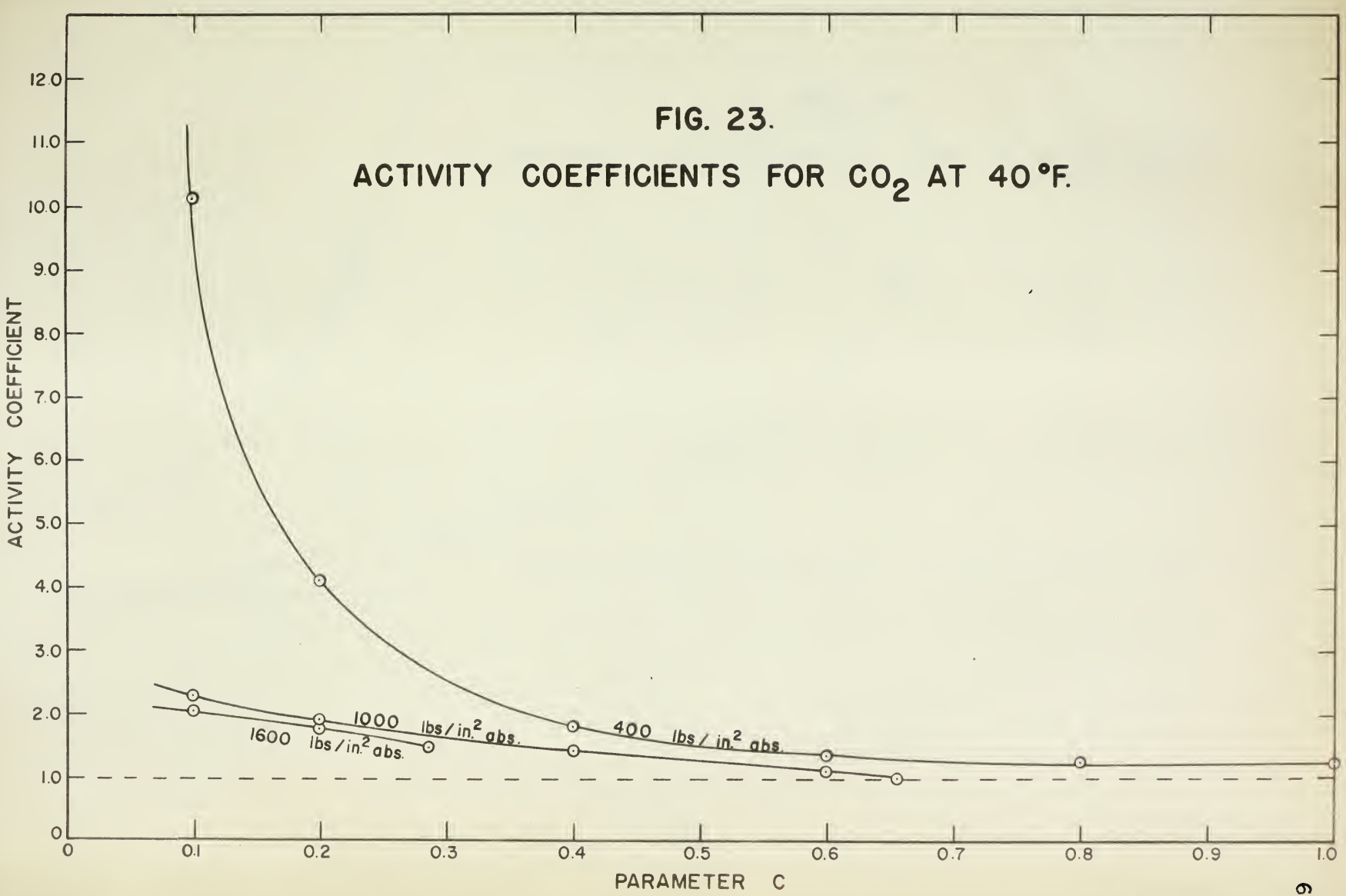
FIG. 23.
ACTIVITY COEFFICIENTS FOR CO_2 AT 40°F.
ACTIVITY COEFFICIENT
PARAMETER C
400 lbs/in.^{2} abs.
1000 lbs/in.^{2} abs.
1600 lbs/in.^{2} abs.
0
1.0
2.0
3.0
4.0
5.0
6.0
7.0
8.0
9.0
10.0
11.0
12.0
0.1
0.2
0.3
0.4
0.5
0.6
0.7
0.8
0.9
1.0

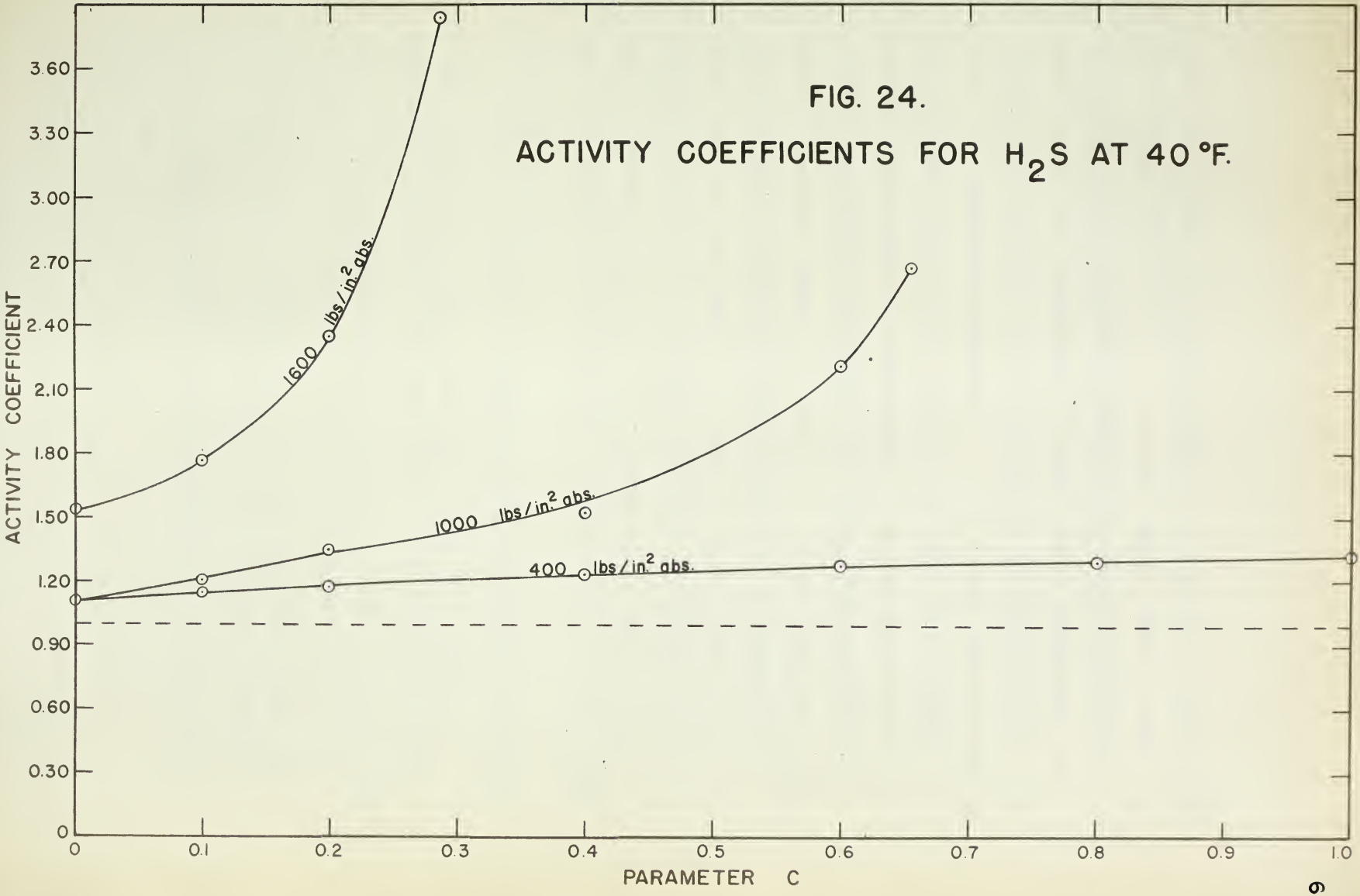
FIG. 24.
ACTIVITY COEFFICIENTS FOR H_2S AT 40 °F.
ACTIVITY COEFFICIENT
PARAMETER C
1600 lbs/in.^{2} abs.
1000 lbs/in.^{2} abs.
400 lbs/in.^{2} abs.
3.60
3.30
3.00
2.70
2.40
2.10
1.80
1.50
1.20
0.90
0.60
0.30
0
0.1
0.2
0.3
0.4
0.5
0.6
0.7
0.8
0.9
1.0

illustrated in Fig. 23 for carbon dioxide at 40 degrees F. Consideration of this figure indicates that as the system becomes richer in carbon dioxide the activity coefficient decreases and, hence, an increasing proportion of carbon dioxide must be forced into the liquid phase. This effect is most pronounced for low pressures and for systems having a low value of the composition parameter C, i.e. for systems that are relatively lean in carbon dioxide. Once a value of C of about 0.4 is reached, increase in the amount of carbon dioxide in the system has little or no effect on the activity coefficient. At a fixed system composition, an increase in pressure results in a decrease in activity coefficient since, as with methane, a relatively greater proportion of the component is forced into the liquid phase. The activity coefficients for carbon dioxide at 40 degrees F. are always above unity, regardless of the pressure or system composition; thus indicating that there is always more carbon dioxide in the vapor phase than there would be if the liquid was an ideal solution.

Fig. 24 illustrates the effect of system composition and pressure on the activity coefficients for hydrogen sulfide at 40 degrees F. Increase in the proportion of carbon dioxide in the system has little effect on the activity coefficient of hydrogen sulfide at 400 lbs/in.^{2}abs. At higher pressures, increase in carbon dioxide content results in an increase in activity coefficient for hydrogen sulfide which means that an increasing amount of hydrogen sulfide must go into the vapor phase. A similar result is produced by increasing pressure at a fixed system composition.

Activity coefficients at 160 degrees F. and at pressures of 1000 and 1600 lbs/in.^{2} abs. are reported in Tables 14 and 15 respectively. The variation of activity coefficient with system composition is indicated for methane by Fig. 25, for carbon dioxide by Fig. 26 and for hydrogen sulfide by Fig. 27.

Hydrogen sulfide has a real vapor pressure of 779 lbs/in.^{2} abs. at a temperature of 160 degrees F. However, this temperature is above the critical temperatures of methane and carbon dioxide and, hence, the vapor pressures of these components had to be obtained by extrapolation. The value obtained for methane was 9300 lbs/in.^{2} abs.; while that for carbon dioxide was 2350 lbs/in.^{2} abs. Pressure-volume data at 160 degrees F. were available directly in the literature for methane (9) and could be interpolated from published data for carbon dioxide.(14). For hydrogen sulfide, pressure-volume data at pressures below its vapor pressure could be obtained directly from the literature. (11). The plot of theoretical equilibrium ratio versus pressure for hydrogen sulfide at 160 degrees F. was extrapolated to pressures above the vapor pressure by using the curve at 220 degrees F. as a guide. (Fig. 21). To aid the extrapolation, values of the theoretical equilibrium ratio at 160 degrees F. were obtained from the generalized fugacity charts.

The effect of system composition and pressure on the activity coefficient of methane at 160 degrees F. is illustrated by Fig. 25. A comparison of this figure with the corresponding one for a temperature of 40 degrees F. (Fig. 22)shows that the effects of increase in pressure or composition parameter are similar at both temperatures. For a fixed

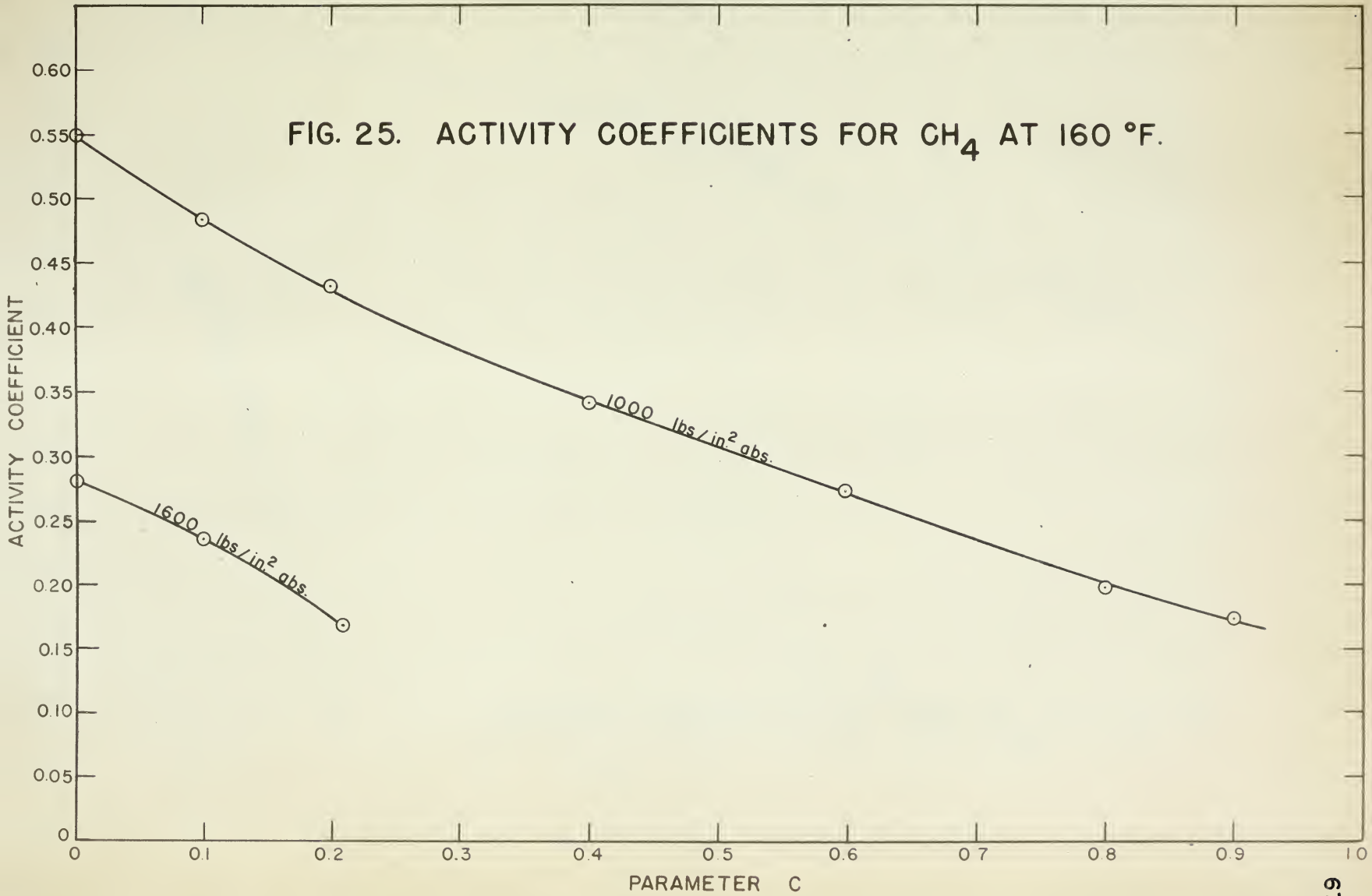

FIG. 25. ACTIVITY COEFFICIENTS FOR CH_4 AT 160 °F.

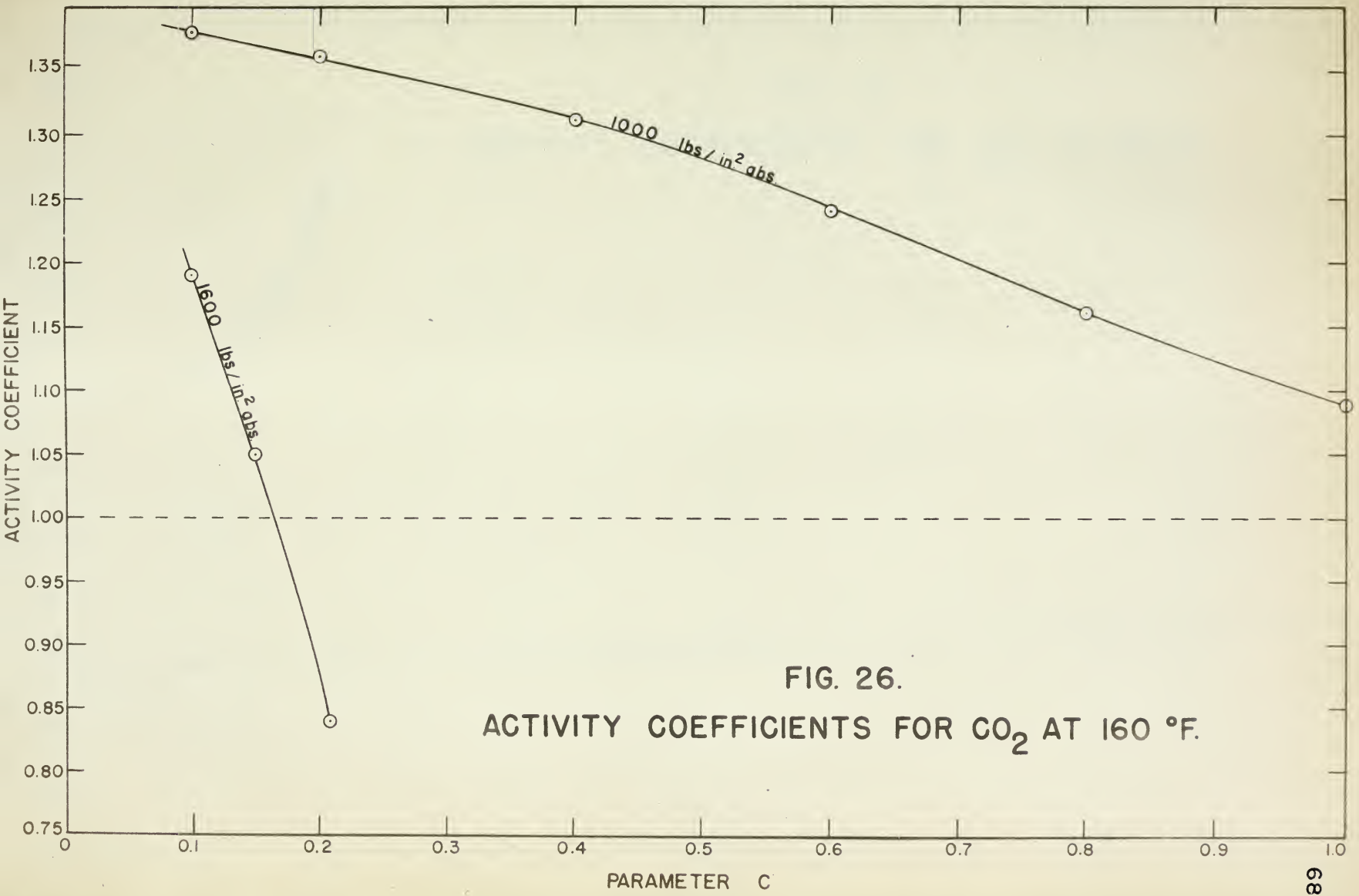

FIG. 26.

ACTIVITY COEFFICIENTS FOR CO_2 AT 160 °F.

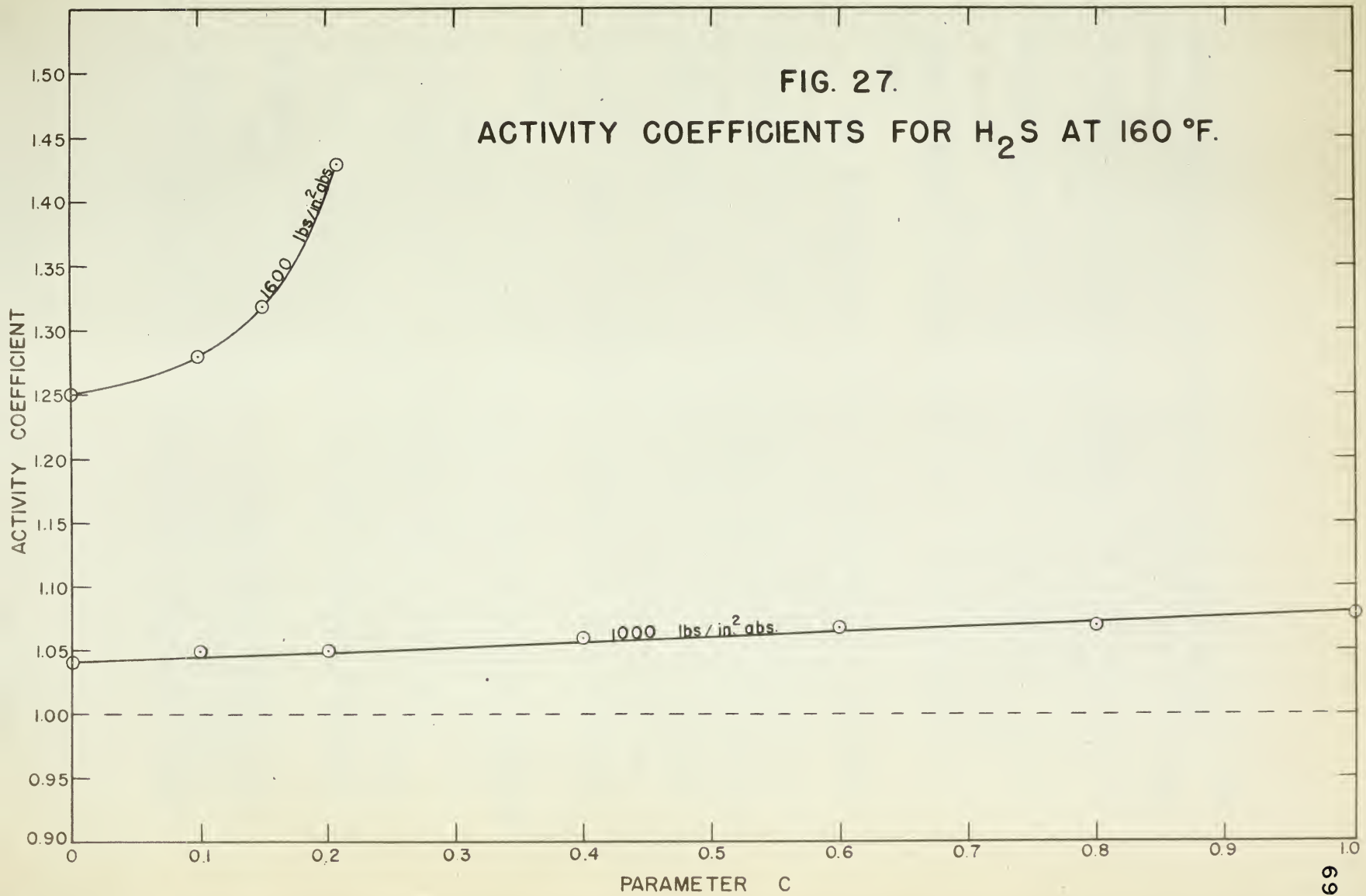
FIG. 27.
ACTIVITY COEFFICIENTS FOR H_2S AT 160 °F.
ACTIVITY COEFFICIENT
1.50
1.45
1.40
1.35
1.30
1.25
1.20
1.15
1.10
1.05
1.00
0.95
0.90
1600 lbs/in.^{2} abs.
1000 lbs/in.^{2} abs.
0
0.1
0.2
0.3
0.4
0.5
0.6
0.7
0.8
0.9
1.0
PARAMETER C

system composition and a fixed pressure, the activity coefficient is lower at the higher temperature. Thus, an increase in temperature causes an increase in the concentration of methane in the liquid phase relative to that predicted by ideal behavior. The liquid phase appears to be somewhat further from ideal solution behavior at 160 degrees F. than at 40 degrees F. This is probably a result of the fact that the higher system temperature is further removed from the critical temperature of methane.

Fig. 26 illustrates the effect of system composition and pressure on the activity coefficient of carbon dioxide at 160 degrees F. A comparison with the figure at 40 degrees F. (Fig. 23) indicates that at the lower temperature the effect of system composition is more pronounced at low pressures; while at the higher temperature it is more pronounced at high pressures. The effects of variation of pressure, temperature or system composition on the activity coefficient of carbon dioxide are analogous to those for methane.

Fig. 27 illustrates the effects of pressure and system composition on the activity coefficient for hydrogen sulfide at 160 degrees F. and it is clearly similar to the corresponding figure at 40 degrees F. (Fig. 24). The effect of increasing temperature is to cause a decrease in activity coefficient and, thus, an increase in hydrogen sulfide concentration in the liquid phase.

Considering the composition of the actual system relative to that predicted by ideal solution behavior, the general effects of changes in pressure, temperature or system composition may be summarized as follows:

(1) Upon increase in system pressure at fixed composition and fixed temperature:

(a) Methane concentration in liquid phase increases.

(b) Carbon dioxide concentration in liquid phase increases.

(c) Hydrogen sulfide concentration in liquid phase decreases.

(2) Upon increase in the value of the composition parameter at fixed pressure and fixed temperature:

(a) Methane concentration in liquid phase increases.

(b) Carbon dioxide concentration in liquid phase increases.

(c) Hydrogen sulfide concentration in liquid phase decreases.

(3) Upon increase in system temperature at fixed composition and fixed pressure:

(a) Methane concentration in liquid phase increases.

(b) Carbon dioxide concentration in liquid phase increases.

(c) Hydrogen sulfide concentration in liquid phase increases.

(d) Predicted Phase Equilibrium Data

Phase equilibrium data were calculated at pressures between those at which experimental studies were carried out. Equilibrium ratios for each component at these pressures were obtained through use of the plots of equilibrium ratio versus pressure at regular values of the composition parameter C. The equations expressing the equilibrium ratios and the expression for the parameter C were solved simultaneously to yield equations for the mole fraction of each component in the liquid phase.

The equations required were:

$$K_{CH_4} = \frac{y_{CH_4}}{x_{CH_4}} \qquad \text{--- (23)}$$

$$K_{CO_2} = \frac{y_{CO_2}}{x_{CO_2}} \qquad \text{--- (24)}$$

$$K_{H_2S} = \frac{y_{H_2S}}{x_{H_2S}} \qquad \text{--- (25)}$$

$$C = \frac{y_{CO_2}}{y_{CH_4} + y_{CO_2}} \qquad \text{--- (26)}$$

These equations combine to give expressions for the component mole fractions in terms of the known equilibrium ratios and the parameter C. The particular equations employed were:

$$x_{CO_2} = \frac{C(1 - K_{H_2S})\, K_{CH_4}}{C\, K_{CH_4}\,(K_{CO_2} - K_{H_2S}) + K_{CO_2}(K_{CH_4} - K_{H_2S})(1-C)} \qquad (27)$$

$$x_{CH_4} = \frac{(1 - C)\, K_{CO_2}\; x_{CO_2}}{C\, K_{CH_4}} \qquad \text{--- (28)}$$

$$x_{H_2S} = 1 - (x_{CO_2} + x_{CH_4}) \qquad \text{--- (29)}$$

The liquid phase mole fractions, calculated by means of the above equations, were then combined with the known equilibrium ratios to obtain the corresponding vapor phase mole fractions.

The computed data for a temperature of 40 degrees F. and pressures of 700 and 1300 lbs/in.^{2} abs. are reported in Tables 16 and 17; while the data for a temperature of 160 degrees F. and a pressure of

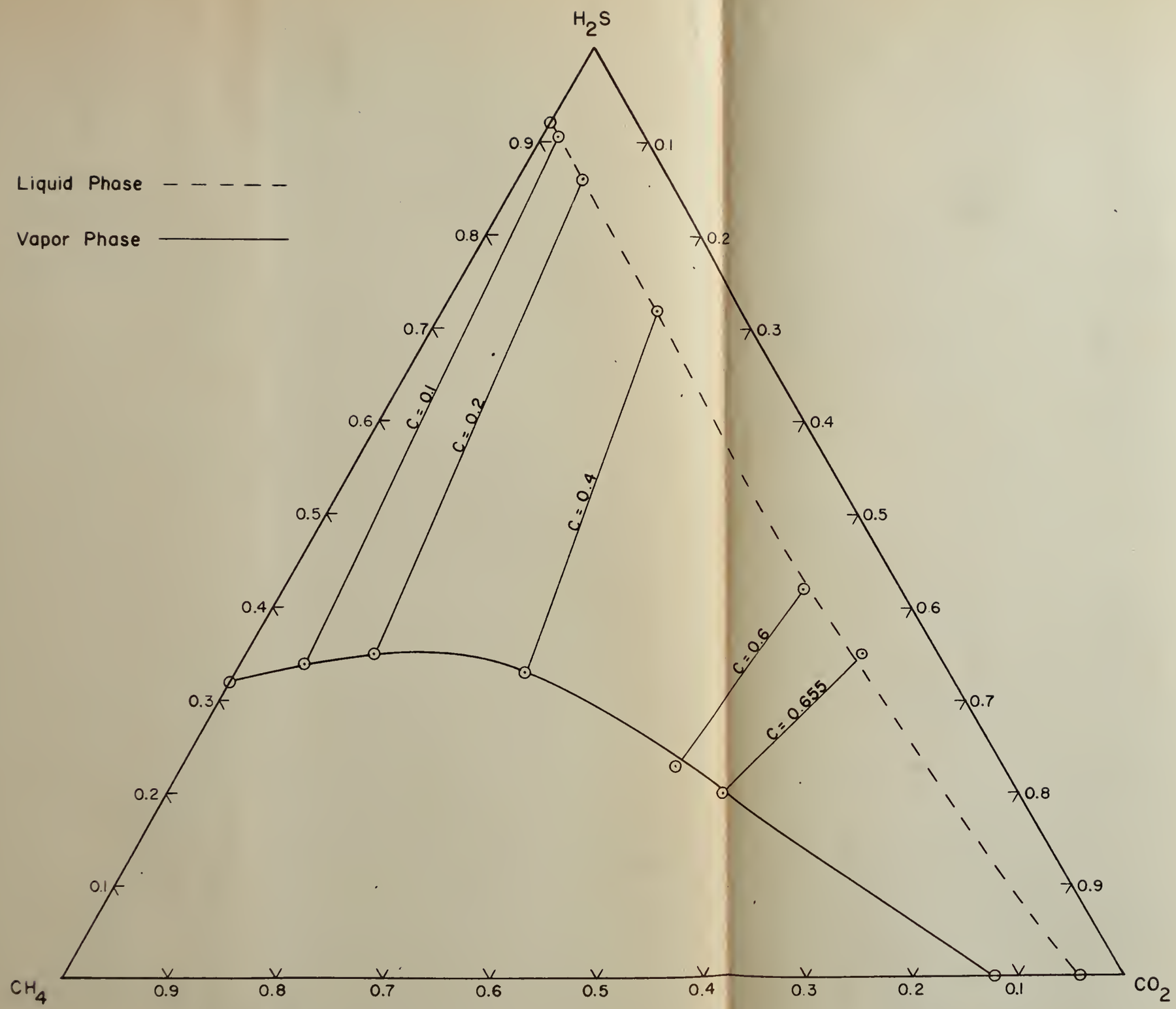

FIG. 28. PREDICTED MOLAR COMPOSITION DIAGRAM

T = 40 °F. P = 700 lbs/in.^{2} abs.

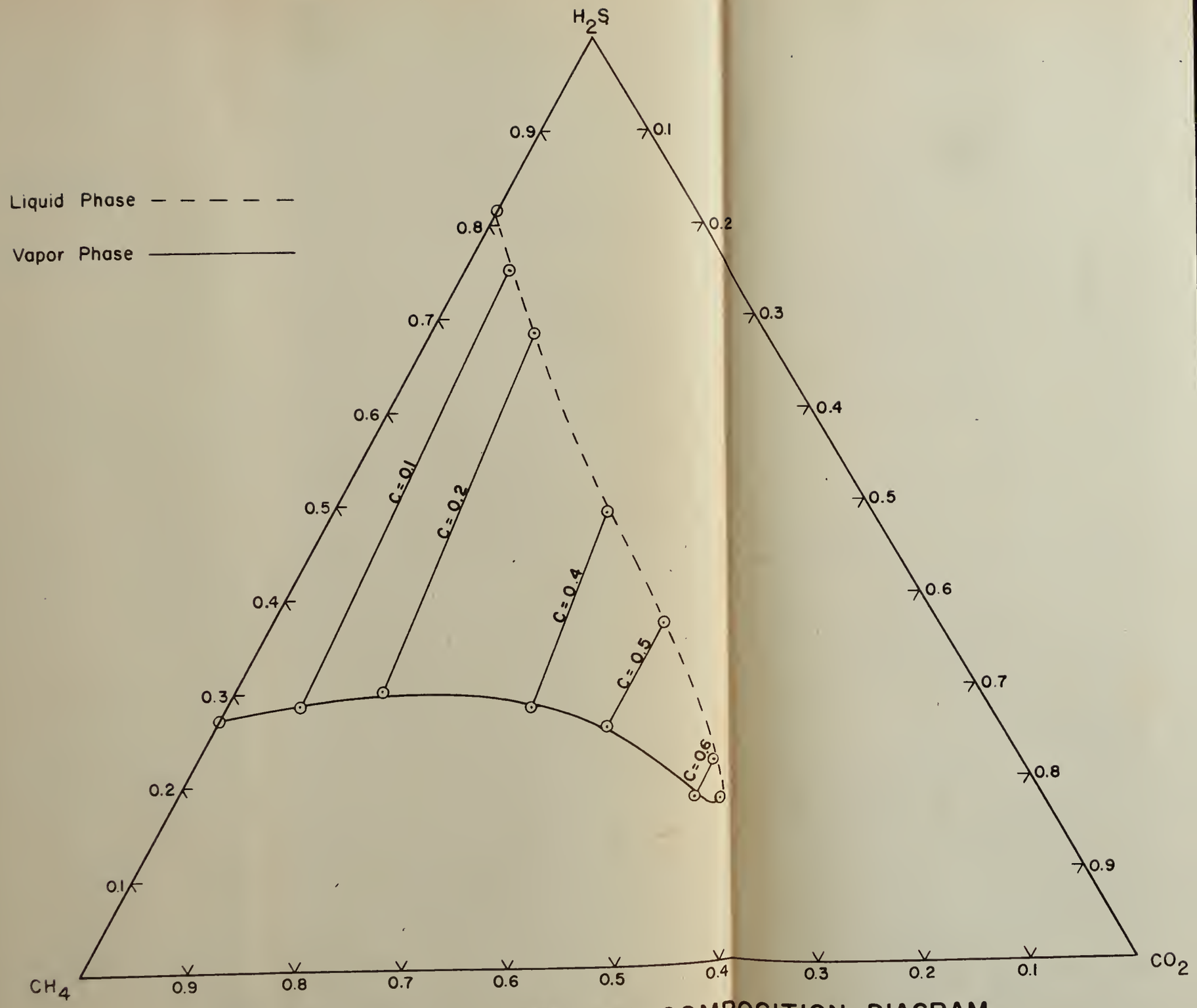

FIG. 29. PREDICTED MOLAR COMPOSITION DIAGRAM

T = 40 °F.

P = 1300 lbs / in.^{2} abs.

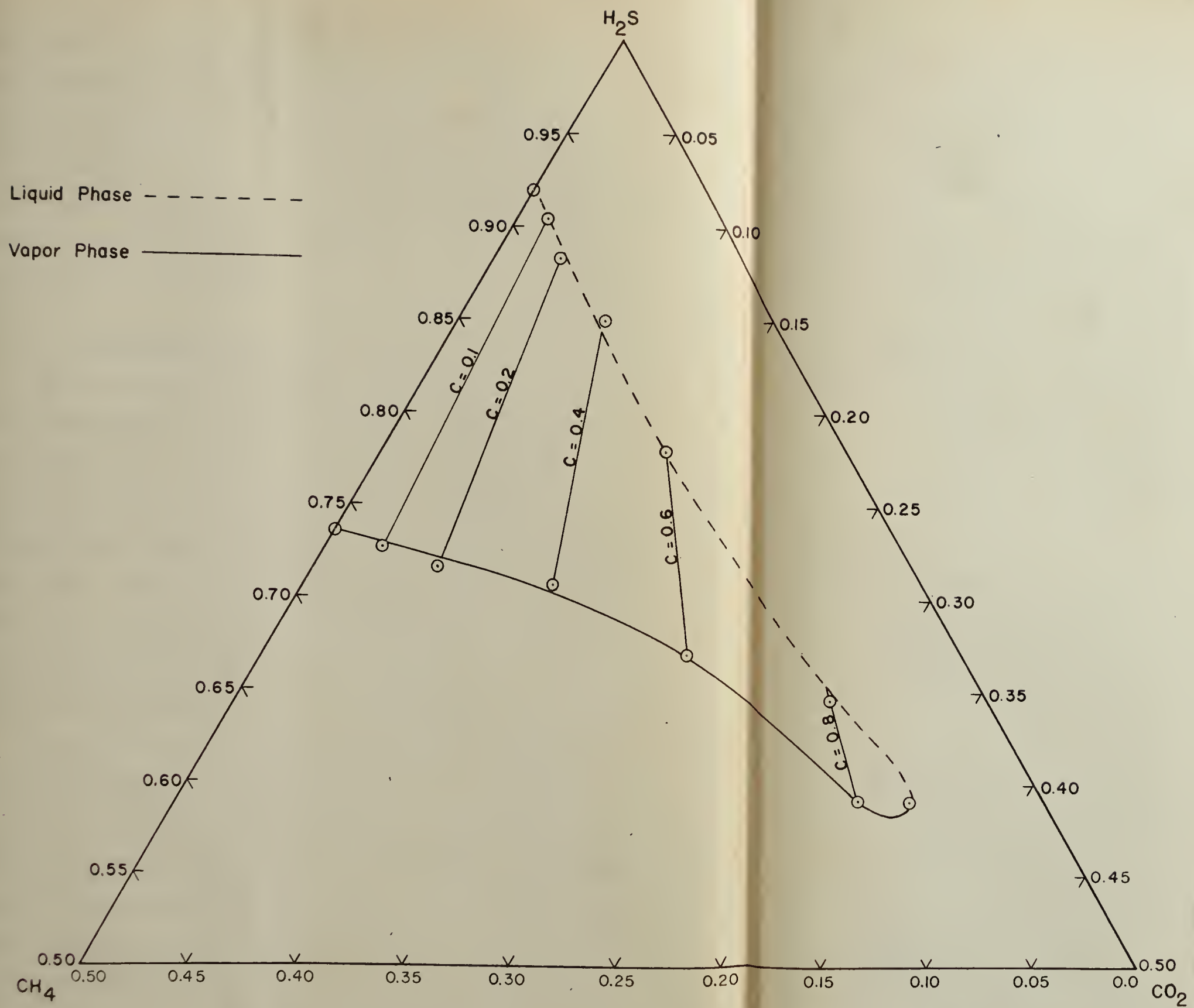

FIG. 30. PREDICTED MOLAR COMPOSITION DIAGRAM

T = 160 °F. P = 1300 lbs/in.^{2} abs.

1300 lbs/in.^{2} abs. are reported in Table 18. The ternary isobaric phase equilibrium is illustrated by Fig. 28 for a temperature of 40 degrees F. and a pressure of 700 lbs/in.^{2} abs., by Fig. 29 for a temperature of 40 degrees F. and a pressure of 1300 lbs/in.^{2} abs., and by Fig. 30, in which only the portion of the triangular diagram above the 50 per cent hydrogen sulfide boundary is shown, for a temperature of 160 degrees F. and a pressure of 1300 lbs/in.^{2} abs.

(e) General Description of Ternary System at 40 Degrees F.

Fig. 31 represents the complete three dimensional phase diagram for the three component system at 40 degrees F. The general shape of the two phase region is defined by the three pressure-composition loops of the binary systems and by the three isobaric triangular diagrams representing the ternary equilibrium at pressures of 400, 1000 and 1600 lbs/in.^{2} abs. The predicted isobaric ternary diagramsat 700 and 1300 lbs/in.^{2} abs. were omitted from the figure to lessen the confusion of intersecting lines which results when a three dimensional figure is portrayed in two dimensions.

Each of the isobaric triangular diagrams shows the tie lines at even values of the composition parameter C. The line connecting the tie lines for each pressure at a C value of 0.2 is a locus of points located on the phase boundary surfaces for systems of corresponding composition at all intermediate pressures. This line intersects the ternary critical locus at a pressure corresponding to the critical pressure for a system having a C value of 0.2. This critical pressure

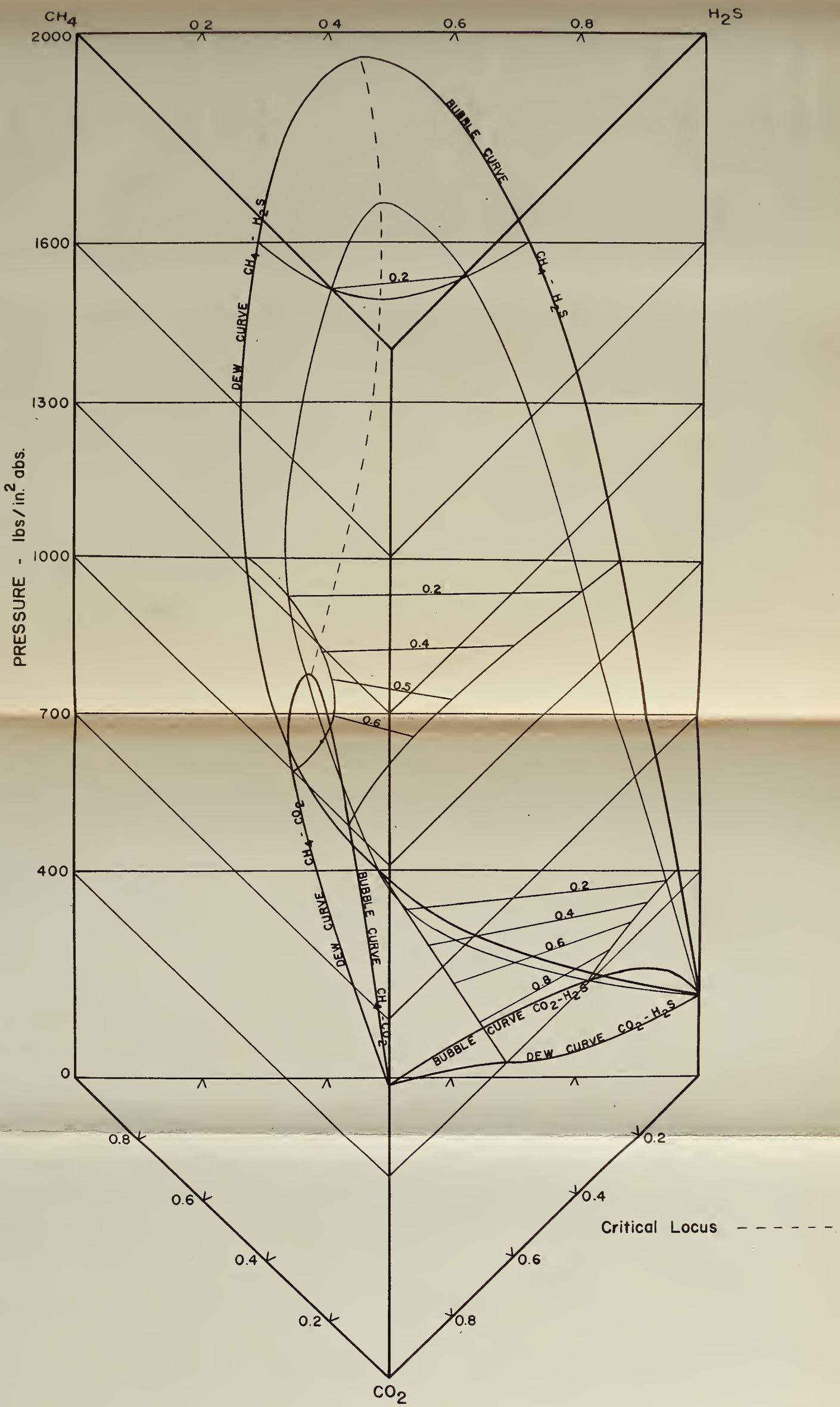

FIG. 31. PHASE DIAGRAM FOR THE TERNARY SYSTEM AT 40 °F.

is 1680 lbs/in.^{2} abs. as may be seen by reference to Fig. 16. Similar lines, originating at the hydrogen sulfide vertex at 169 lbs/in.^{2} abs. and intersecting the ternary critical locus at the appropriate critical pressures, could be shown for each value of the composition parameter C.

Consideration of Fig. 31 indicates that at pressures below 169 lbs/in.^{2} abs., which is the vapor pressure of hydrogen sulfide at 40 degrees F., no liquefaction can occur in the ternary system. At pressures slightly above 169 lbs/in.^{2} abs. the formation of two phases occurs, but only with systems that are very rich in hydrogen sulfide. As the pressure is increased, the two phase region approaches nearer to the carbon dioxide vertex; reaching it at a pressure of 570 lbs/in.^{2} abs., which is the vapor pressure of carbon dioxide at 40 degrees F. Over the pressure range from 169 to 570 lbs/in.^{2} abs., the two phase region extends from the methane-hydrogen sulfide boundary to the carbon dioxide-hydrogen sulfide boundary.

With increasing pressure above 570 lbs/in.^{2} abs., the two phase region retreats from the carbon dioxide vertex and moves towards the methane vertex. The two phase region extends from the methane-hydrogen sulfide boundary to the methane-carbon dioxide boundary over the pressure range from 570 lbs/in.^{2} abs. to 1240 lbs/in.^{2} abs., which is the critical pressure of the methane-carbon dioxide system at 40 degrees F. At 1240 lbs/in.^{2} abs. the ternary liquid and vapor phase surfaces meet at the critical point for the methane-carbon dioxide system.

With increasing pressure above 1240 lbs/in.^{2} abs., the two phase region retreats from the methane-carbon dioxide boundary towards the

methane-hydrogen sulfide boundary. It gradually diminishes in magnitude until it disappears at the methane-hydrogen sulfide critical point at 1949 lbs/in.^{2} abs. and 0.55 mole fraction methane. Over the pressure range from 1240 to 1949 lbs/in.^{2} abs., the ternary liquid and vapor phase surfaces meet at the locus of ternary critical points. The composition spread between the ternary liquid and vapor phase surfaces is greatest at about 1000 lbs/in.^{2} abs. and decreases only slightly up to about 1600 lbs/in.^{2} abs., when the surfaces begin to merge more rapidly as a result of the convergence of the dew point and bubble point curves of the methane-hydrogen sulfide system.

(f) General Description of Ternary System at 160 Degrees F.

The complete three dimensional phase diagram for the ternary system at 160 degrees F. is represented by Fig. 32. Since two phase equilibrium exists only for systems rich in hydrogen sulfide, only the portion of the three dimensional figure between the 50 per cent hydrogen sulfide boundary and the hydrogen sulfide apex is shown. The two phase region is outlined by the pressure-composition loops for the methane-hydrogen sulfide and carbon dioxide-hydrogen sulfide systems and by the isobaric triangular diagrams representing the ternary equilibrium at pressures of 1000, 1300 and 1600 lbs/in.^{2} abs.

Two phase equilibrium in the ternary system begins at the vapor pressure of hydrogen sulfide, which is 779 lbs/in.^{2} abs. at 160 degrees F. With increasing pressure the two phase region retreats slightly from the hydrogen sulfide apex, but still extends from the methane-hydrogen sulfide boundary to the carbon dioxide-hydrogen sulfide boundary up to a

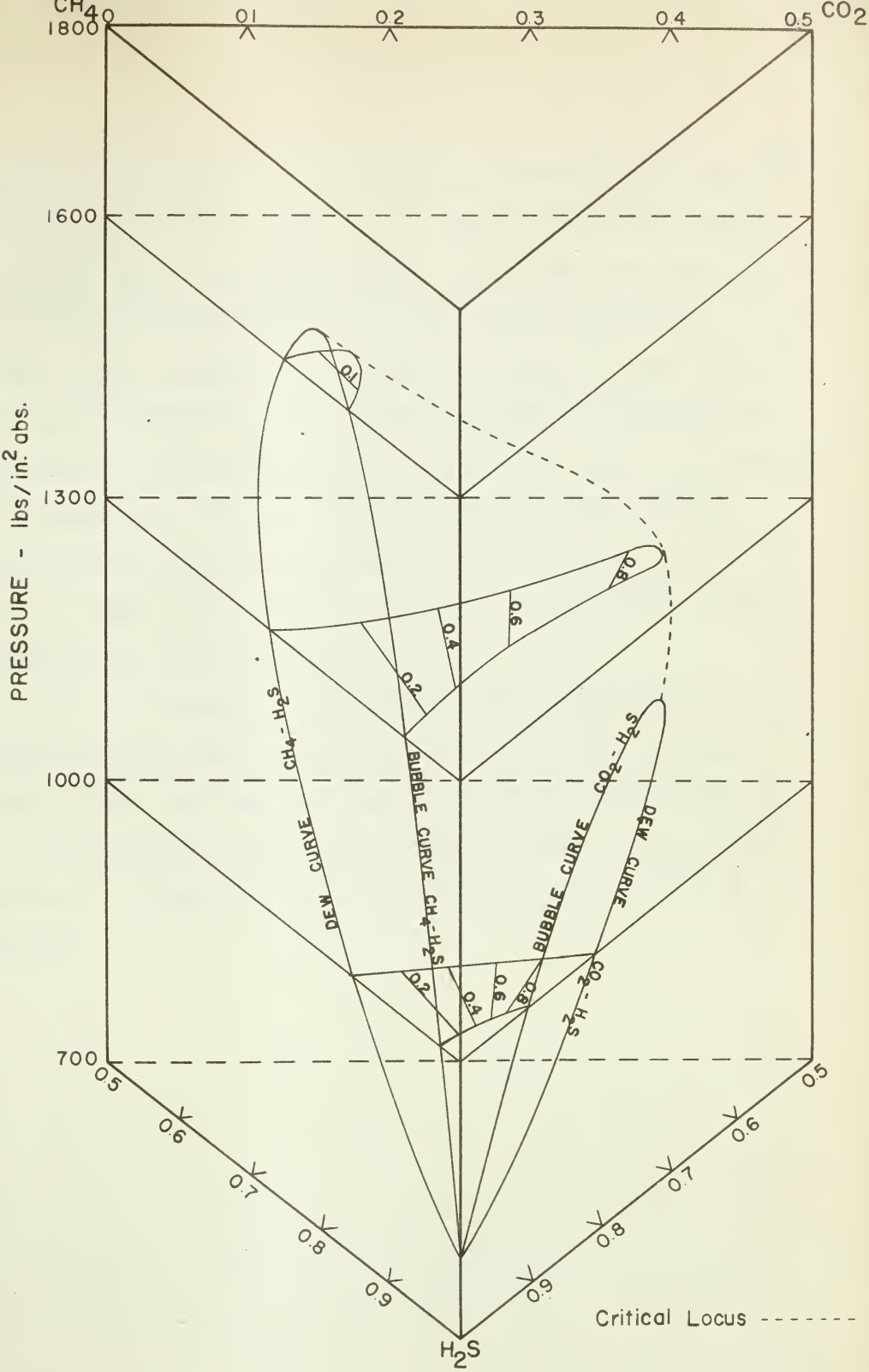

FIG. 32.

PHASE DIAGRAM FOR THE TERNARY SYSTEM AT 160 °F.

pressure of 1220 lbs/in.^{2} abs. - the critical pressure for the carbon dioxide-hydrogen sulfide system. As the pressure is increased above 1220 lbs/in.^{2} abs., the two phase region retreats from the carbon dioxide-hydrogen sulfide boundary and moves towards the methane-hydrogen sulfide boundary. At the same time, there is a shift towards the carbon dioxide apex so that a maximum proportion of carbon dioxide is reached at a pressure of about 1300 lbs/in.^{2} abs. Above this pressure, the two phase region retreats rapidly towards the methane-hydrogen sulfide boundary, diminishing in magnitude until it disappears at a pressure of 1660 lbs/in.^{2} abs. - the critical pressure for the methane-hydrogen sulfide system at 160 degrees F.

Over the pressure range from 1220 to 1660 lbs/in.^{2} abs., the ternary liquid and vapor phase surfaces meet at the locus of ternary critical points. The composition spread between the phase surfaces is quite narrow over the entire pressure range of ternary critical point formation but increases as the methane-hydrogen sulfide boundary is approached.

V. CONCLUSIONS

(1) Validity of Experimental Results

The validity of the experimental results is dependent upon three factors. These are the control and measurement of the primary variables (temperature, pressure and volume), the maintenance of equilibrium conditions during the sampling operation, and the accuracy of the analytical work.

Error in the measurement of the primary variables was relatively slight. Control and measurement of temperature to ± 0.1 degrees F. was achieved. However, since the thermocouples were embedded in the cell wall and the temperature of this point was taken as being equal to the system temperature, and since slight variation in temperature over the length of the cell always occurred, it would be more realistic to consider the error in measurement of system temperature to be somewhat greater. Temperature control in the work at 160 degrees F. was not quite as good as in that at 40 degrees F. due to the greater spread between system temperature and room temperature.

Estimated accuracy of the pressure measurement is ± 1 pound up to a pressure of 1000 lbs/in.^{2} abs. and ± 3 pounds above 1000 lbs/in.^{2} abs. Thus, the maximum error in a particular pressure measurement would usually be less than one half of one per cent. Volumetric measurements, obtained by use of the cathetometer in conjunction with volumetric calibration curves, are estimated to be accurate to within 0.1 c.c. Since component volumes were almost always 20 c.c. or greater, the

maximum error would be ± 0.5%.

The error arising from loss of equilibrium during the sampling operation is much more difficult to estimate. Generally speaking, pressures were maintained within ± 3 pounds of the desired value throughout the sampling operation. However, greater deviations sometimes occurred as the sampling operation was very difficult to control. These pressure fluctuations were always only of brief duration as the desired pressure could be quickly re-established and, hence, it is felt that errors arising from loss of equilibrium were small.

The analytical procedure is considered to have had accuracy comparable to that attained in measurement of the variables or in collection of representative phase samples. Volumes could be determined with the Orsat equipment to ± 0.1 c.c. with a resulting accuracy of about ± 0.4% in determining the percentage methane. The Tutweiler analysis was less accurate; but, by taking duplicate samples and averaging, the error was kept to less than ± 1.0%.

A further source of error was present in the fact that overall system compositions were probably incorrect in some cases by about 1%. A fraction of the gaseous component would be trapped in the mercury lines during transfer from the measuring cell to the equilibrium cell; and, hence, the overall composition, as calculated from the component quantities present in the measuring cell, would not represent the actual overall composition in the equilibrium cell. This error did not affect the location of the dew point or bubble point loci as these were drawn as best fit curves through the compositions determined by the analytical

work. However, this error did affect the location of the tie lines, which were drawn as best fit straight lines through the vapor phase, liquid phase and overall compositions; and, hence, it affected the equilibrium ratios.

It may be concluded that the accuracy of the experimental work was sufficient to correctly describe the ternary phase equilibrium at fixed pressure and temperature and, hence, to give a good outline of the overall phase behavior of the system. The work was not sufficiently accurate to give exact values of the equilibrium ratio as a very small error in vapor or liquid composition can give a very large error in equilibrium ratio, particularly if there is only a very small amount of the component present in the system.

(2) Discussion of Experimental Data

The present study, when combined with the work done by Bailey, gives a fairly complete representation of the phase behavior of the methane-carbon dioxide-hydrogen sulfide system over a wide temperature range.

The general nature of the phase equilibrium in the system may be summarized as follows:

(1) At 40 degrees F., the system forms co-existing vapor and liquid phases over a pressure range from 169 lbs/in.^{2} abs. to 1949 lbs/in.^{2} abs. The overall system must be rich in hydrogen sulfide at both extremes of the pressure range; but, a wide range of system compositions will form two phases at the intermediate pressures.

At 160 degrees F., two phase equilibrium occurs over a pressure range from 779 lbs/in.^{2} abs. to 1660 lbs/in.^{2} abs.; but only for systems that contain 60 per cent or more hydrogen sulfide.

(2) The ternary isobaric phase equilibrium deviates considerably from that predicted by the ideal solution law. The deviation from ideal behavior becomes much more pronounced at the higher pressures but is greater for the vapor phase than for the liquid phase, even at the lower pressures.

(3) The existence of the type of intermolecular forces which lead to azeotrope formation is indicated by the tendency of the dew point locus to approach the bubble point locus in the middle region of the pressure range over which two phase equilibrium exists. This effect occurs at both temperatures studied. However, no ternary azeotrope actually forms and it is evident that such formation could not occur in this system since there is no azeotrope formation in any of the binary systems over the temperature ranges reported in the literature.

(4) A locus of ternary critical points occurs at 40 degrees F. over a pressure range from 1240 to 1949 lbs/in.^{2} abs. and at 160 degrees F. over a pressure range from 1220 to 1660 lbs/in.^{2} abs. In neither case is there any indication of the formation of a "maximum pressure" ternary critical point existing at a pressure higher than the critical pressure of the methane-hydrogen sulfide system.

(5) In this system, equilibrium ratios are functions of pressure, temperature and composition. At a fixed temperature, the effect of pressure on equilibrium ratio is relatively greater at the lower pressures

for all three components. The effect of an increase in carbon dioxide content is to force more methane and carbon dioxide into the liquid phase, thus decreasing their equilibrium ratios; but to force more hydrogen sulfide into the vapor phase, thus increasing its equilibrium ratio. Temperature does not affect the equilibrium ratios to as great an extent as pressure does. Increasing temperature at fixed pressure causes an increase in equilibrium ratio for carbon dioxide and hydrogen sulfide but has a varying effect on that of methane depending upon system composition.

(6) The activity coefficients indicate that deviation of the liquid and vapor phases from ideal solution behavior is also a function of pressure, temperature and system composition. All three factors appear to affect the activity coefficient to a comparable extent. Real solutions which approach or attain ideal solution behavior, with respect to one of the components, occur at certain combinations of pressure, temperature and system composition.

Two phase equilibrium in the methane-carbon dioxide-hydrogen sulfide system can exist up to a maximum temperature of +212.7 degrees F. However, investigations at temperatures above 160 degrees F. would add little to the information now obtained since the two phase region would exist only over a very limited composition range, i.e. only for systems that are very high in hydrogen sulfide. Investigations at temperatures below 40 degrees F. could be carried out provided that a sufficiently effective refrigerating system was devised. An extension of the study to lower temperatureswould be very helpful in obtaining an overall picture of the phase equilibrium in this system.

LIST OF REFERENCES

1. Bailey, J. B., M.Sc. Thesis, University of Alberta, (1957).

2. Bierlein and Kay, Ind. Eng. Chem., 45, 618, (1953).

3. Billman, Sage and Lacey, A.I.M.M.E. Trans., 142, 70, (1943).

4. Donnelly and Katz, Ind. Eng. Chem., 46, 511, (1954).

5. Hougen and Watson, "Chemical Process Principles - Part Two," John Wiley and Sons Inc., New York (1947).

6. Keyes and Burks, J. Am. Chem. Soc., 49, 1403, (1927).

7. Kurata and Kohn, Pet. Processing, VII, N12, 57, (1956).

8. Kvalnes and Gaddy, J. Am. Chem. Soc., 53, 394, (1931).

9. Olds, Reamer, Sage and Lacey, Ind. Eng. Chem., 35, 922, (1943).

10. Perry, J. H., "Chemical Engineers' Handbook," McGraw-Hill Book Co., Inc., New York, (1950).

11. Reamer, Sage and Lacey, Ind. Eng. Chem., 42, 140, (1950).

12. Reamer, Sage and Lacey, Ind. Eng. Chem., 43, 976, (1951).

13. Riesenfeld and Orbach, Petroleum Engr., 25, C 32, (1953).

14. Sweigert, Weber and Allen, Ind. Eng. Chem., 38, 185, (1946).

A P P E N D I X

(1) Tabulated Data

(2) Sample Calculations

TABLE I

PHASE COMPOSITION DATA FOR SERIES A TESTS

T=40 Degrees Fahrenheit P=400 lbs/in^{2}abs.

Test Number	Total System Composition			Vapor Phase Composition			Liquid Phase Composition		
	CH_4	CO_2	H_2S	CH_4	CO_2	H_2S	CH_4	CO_2	H_2S
	0.323	0.0	0.677	0.511	0.0	0.489	0.023	0.0	0.977
A - 7	0.194	0.081	0.725	0.392	0.131	0.477	0.033	0.027	0.940
A - 2	0.198	0.142	0.660	0.354	0.192	0.454	0.041	0.070	0.889
A - 3	0.167	0.197	0.636	0.318	0.253	0.429	0.039	0.129	0.832
A - 4	0.121	0.259	0.620	0.225	0.352	0.423	0.033	0.148	0.819
A - 5	0.087	0.339	0.574	0.146	0.450	0.404	0.018	0.280	0.702
A - 6	0.056	0.426	0.518	0.081	0.503	0.416	0.015	0.350	0.635
	0.0	0.549	0.451	0.0	0.635	0.365	0.0	0.403	0.597

TABLE II

PHASE COMPOSITION DATA FOR SERIES B TESTS

T=40 Degrees Fahrenheit P=1000 lbs/in^2 abs.

Test Number	Total System Composition			Vapor Phase Composition			Liquid Phase Composition		
	CH_4	CO_2	H_2S	CH_4	CO_2	H_2S	CH_4	CO_2	H_2S
	0.406	0.0	0.594	0.716	0.0	0.284	0.122	0.0	0.878
B - 1	0.324	0.125	0.551	0.570	0.139	0.291	0.154	0.090	0.756
B - 2	0.275	0.252	0.473	0.475	0.266	0.259	0.154	0.221	0.625
B - 4	0.288	0.392	0.320	0.418	0.353	0.229	0.174	0.414	0.412
B - 5	0.259	0.523	0.218	0.350	0.471	0.179	0.179	0.537	0.284
B - 6	0.256	0.627	0.117	0.329	0.567	0.104	0.176	0.680	0.144
	0.256	0.744	0.0	0.345	0.655	0.0	0.133	0.867	0.0

TABLE III

PHASE COMPOSITION DATA FOR SERIES C TESTS

T=40 Degrees Fahrenheit P=1600 lbs/in^2 abs.

Test Number	Total System Composition			Vapor Phase Composition			Liquid Phase Composition		
	CH_4	CO_2	H_2S	CH_4	CO_2	H_2S	CH_4	CO_2	H_2S
	0.474	0.0	0.526	0.708	0.0	0.292	0.256	0.0	0.744
C - 2	0.467	0.089	0.444	0.602	0.087	0.311	0.294	0.063	0.643
C - 3	0.408	0.155	0.437	0.518	0.142	0.340	0.377	0.135	0.488
C - 4	0.437	0.175	0.388	Critical Composition For 1600 lbs/in^2 abs.					

TABLE IV

PHASE COMPOSITION DATA FOR SERIES D TESTS

T=160 Degrees Fahrenheit P=1000 lbs/in^2 abs.

Test Number	Total System Composition			Vapor Phase Composition			Liquid Phase Composition		
	CH_4	CO_2	H_2S	CH_4	CO_2	H_2S	CH_4	CO_2	H_2S
D - 1	0.092	0.0	0.908	0.156	0.0	0.844	0.032	0.0	0.968
D - 4	0.070	0.054	0.876	0.103	0.061	0.836	0.033	0.031	0.936
D - 5	0.046	0.093	0.861	0.060	0.118	0.822	0.026	0.063	0.911
D - 2	0.0	0.149	0.851	0.0	0.189	0.811	0.0	0.109	0.891

TABLE V

PHASE COMPOSITION DATA FOR SERIES E TESTS

T=160 Degrees Fahrenheit P=1600 lbs/in^2 abs.

Test Number	Total System Composition			Vapor Phase Composition			Liquid Phase Composition		
	CH_4	CO_2	H_2S	CH_4	CO_2	H_2S	CH_4	CO_2	H_2S
E - 1	0.216	0.0	0.784	0.265	0.0	0.735	0.159	0.0	0.841
E - 3	0.203	0.028	0.769	0.236	0.027	0.737	0.164	0.018	0.818
E - 2	0.194	0.051	0.755	Critical Composition For 1600 lbs/in^2 abs.					

TABLE VI

EQUILIBRIUM RATIOS AT REGULAR VALUES OF THE PARAMETER C

T=40 Degrees Fahrenheit P=400 lbs/in^2 abs.

Value of C	Vapor Phase Composition			Liquid Phase Composition			Equilibrium Ratios		
	CH_4	CO_2	H_2S	CH_4	CO_2	H_2S	CH_4	CO_2	H_2S
0.0	0.507	0.0	0.493	0.022	0.0	0.978	23.0	.....	0.505
0.1	0.466	0.052	0.482	0.023	0.004	0.973	20.3	13.0	0.495
0.2	0.423	0.106	0.471	0.030	0.020	0.950	14.1	5.30	0.496
0.3	0.377	0.161	0.462	0.036	0.049	0.915	10.5	3.28	0.504
0.4	0.330	0.220	0.450	0.039	0.098	0.863	8.46	2.25	0.521
0.5	0.280	0.280	0.440	0.038	0.150	0.812	7.37	1.86	0.542
0.6	0.230	0.344	0.426	0.033	0.204	0.763	6.97	1.69	0.558
0.7	0.175	0.408	0.417	0.027	0.255	0.718	6.48	1.60	0.580
0.8	0.120	0.478	0.402	0.018	0.307	0.675	6.67	1.56	0.596
0.9	0.061	0.550	0.389	0.010	0.349	0.641	6.10	1.58	0.607
1.0	0.0	0.628	0.372	0.0	0.399	0.601	.....	1.57	0.619

TABLE VII

EQUILIBRIUM RATIOS AT REGULAR VALUES OF THE PARAMETER C

T=40 Degrees Fahrenheit P=1000 lbs/in^2 abs.

Value of C	Vapor Phase Composition			Liquid Phase Composition			Equilibrium Ratios		
	CH_4	CO_2	H_2S	CH_4	CO_2	H_2S	CH_4	CO_2	H_2S
0.0	0.716	0.0	0.284	0.122	0.0	0.878	5.87	...	0.324
0.1	0.639	0.071	0.290	0.138	0.041	0.821	4.63	1.73	0.353
0.2	0.566	0.142	0.292	0.150	0.098	0.752	3.77	1.45	0.388
0.3	0.505	0.216	0.279	0.158	0.165	0.677	3.20	1.31	0.412
0.4	0.450	0.301	0.249	0.163	0.270	0.567	2.76	1.12	0.439
0.5	0.395	0.395	0.210	0.174	0.458	0.368	2.27	0.862	0.571
0.6	0.340	0.510	0.150	0.179	0.590	0.231	1.90	0.864	0.649
0.62	0.333	0.543	0.124	0.177	0.641	0.182	1.88	0.848	0.681
0.64	0.331	0.589	0.080	0.169	0.724	0.107	1.96	0.814	0.748
0.65	0.334	0.620	0.046	0.159	0.784	0.057	2.10	0.788	0.807
0.655	0.345	0.655	0.0	0.133	0.867	0.0	2.59	0.755	.....

TABLE VIII

EQUILIBRIUM RATIOS AT REGULAR VALUES OF THE PARAMETER C

T=40 Degrees Fahrenheit P=1600 lbs/in^2 abs.

Value of C	Vapor Phase Composition			Liquid Phase Composition			Equilibrium Ratios		
	CH_4	CO_2	H_2S	CH_4	CO_2	H_2S	CH_4	CO_2	H_2S
0.0	0.708	0.0	0.292	0.256	0.0	0.744	2.77	...	0.393
0.1	0.626	0.069	0.305	0.286	0.051	0.663	2.19	1.35	0.460
0.2	0.535	0.134	0.331	0.339	0.114	0.547	1.58	1.18	0.605
0.286	0.437	0.175	0.388	0.437	0.175	0.388	1.00	1.00	1.00

TABLE IX

EQUILIBRIUM RATIOS AT REGULAR VALUES OF THE PARAMETER C

T=160 Degrees Fahrenheit P=1000 lbs/in^2 abs.

Value of C	Vapor Phase Composition			Liquid Phase Composition			Equilibrium Ratios		
	CH_4	CO_2	H_2S	CH_4	CO_2	H_2S	CH_4	CO_2	H_2S
0.0	0.156	0.0	0.844	0.032	0.0	0.968	4.87	...	0.872
0.1	0.143	0.016	0.841	0.033	0.007	0.960	4.33	2.29	0.877
0.2	0.129	0.032	0.839	0.033	0.018	0.949	3.91	1.78	0.884
0.3	0.114	0.049	0.837	0.033	0.028	0.939	3.45	1.75	0.892
0.4	0.100	0.067	0.833	0.032	0.037	0.931	3.12	1.81	0.895
0.5	0.085	0.085	0.830	0.030	0.047	0.923	2.83	1.81	0.899
0.6	0.070	0.105	0.825	0.028	0.057	0.915	2.50	1.84	0.902
0.7	0.053	0.124	0.823	0.025	0.067	0.908	2.12	1.85	0.907
0.8	0.036	0.145	0.819	0.020	0.080	0.900	1.80	1.81	0.909
0.9	0.019	0.166	0.815	0.012	0.095	0.893	1.58	1.75	0.912
1.0	0.0	0.189	0.811	0.0	0.109	0.891	....	1.73	0.910

TABLE X

EQUILIBRIUM RATIOS AT REGULAR VALUES OF THE PARAMETER C

T=160 Degrees Fahrenheit P=1600 lbs/in^{2}abs.

Value of C	Vapor Phase Composition			Liquid Phase Composition			Equilibrium Ratios		
	CH_4	CO_2	H_2S	CH_4	CO_2	H_2S	CH_4	CO_2	H_2S
0.0	0.265	0.0	0.735	0.159	0.0	0.841	1.67	...	0.873
0.1	0.238	0.027	0.735	0.160	0.019	0.821	1.49	1.42	0.895
0.208	0.194	0.051	0.755	0.194	0.051	0.755	1.00	1.00	1.00

TABLE XI

ACTIVITY COEFFICIENTS AT REGULAR VALUES OF THE PARAMETER C

T=40 Degrees Fahrenheit P=400 lbs/in^2 abs.

Value of C	Smoothed Experimental Equilibrium Ratios			Theoretical Equilibrium Ratios			Activity Coefficients		
	CH_4	CO_2	H_2S	CH_4	CO_2	H_2S	CH_4	CO_2	H_2S
0.0	14.5	...	0.51	6.98	...	0.46	2.08	...	1.11
0.1	13.2	13.0	0.53	6.98	1.29	0.46	1.89	10.1	1.15
0.2	12.0	5.30	0.54	6.98	1.29	0.46	1.72	4.11	1.18
0.4	9.45	2.35	0.57	6.98	1.29	0.46	1.35	1.82	1.24
0.6	7.45	1.75	0.59	6.98	1.29	0.46	1.07	1.36	1.28
0.8	6.30	1.65	0.60	6.98	1.29	0.46	0.903	1.28	1.30
1.0	....	1.60	0.61	....	1.29	0.46	....	1.24	1.33

TABLE XII

ACTIVITY COEFFICIENTS AT REGULAR VALUES OF THE PARAMETER C

T=40 Degrees Fahrenheit P=1000 lbs/in^2 abs.

Value of C	Smoothed Experimental Equilibrium Ratios			Theoretical Equilibrium Ratios			Activity Coefficients		
	CH_4	CO_2	H_2S	CH_4	CO_2	H_2S	CH_4	CO_2	H_2S
0.0	5.80	...	0.32	3.05	...	0.29	1.90	...	1.10
0.1	4.80	1.75	0.35	3.05	0.76	0.29	1.57	2.30	1.21
0.2	4.00	1.45	0.39	3.05	0.76	0.29	1.31	1.91	1.35
0.4	2.75	1.10	0.44	3.05	0.76	0.29	0.902	1.45	1.52
0.6	1.90	0.86	0.64	3.05	0.76	0.29	0.623	1.13	2.21
0.655	2.59	0.76	....	3.05	0.76	....	0.849	1.00	....

TABLE XIII

ACTIVITY COEFFICIENTS AT REGULAR VALUES OF THE PARAMETER C

T=40 Degrees Fahrenheit P=1600 lbs/in^2 abs.

Value of C	Smoothed Experimental Equilibrium Ratios			Theoretical Equilibrium Ratios			Activity Coefficients		
	CH_4	CO_2	H_2S	CH_4	CO_2	H_2S	CH_4	CO_2	H_2S
0.0	2.55	...	0.40	2.10	...	0.26	1.21	...	1.54
0.1	1.90	1.35	0.46	2.10	0.67	0.26	0.905	2.02	1.77
0.2	1.45	1.20	0.61	2.10	0.67	0.26	0.690	1.79	2.35
0.286	1.00	1.00	1.00	2.10	0.67	0.26	0.476	1.49	3.84

TABLE XIV

ACTIVITY COEFFICIENTS AT REGULAR VALUES OF THE PARAMETER C

T=160 Degrees Fahrenheit P=1000 lbs/in^{2}abs.

Value of C	Smoothed Experimental Equilibrium Ratios			Theoretical Equilibrium Ratios			Activity Coefficients		
	CH_4	CO_2	H_2S	CH_4	CO_2	H_2S	CH_4	CO_2	H_2S
0.0	5.03	...	0.872	9.15	...	0.840	0.550	...	1.04
0.1	4.41	2.29	0.877	9.15	1.65	0.840	0.482	1.38	1.05
0.2	3.94	2.25	0.884	9.15	1.65	0.840	0.431	1.36	1.05
0.4	3.12	2.17	0.895	9.15	1.65	0.840	0.341	1.31	1.06
0.6	2.50	2.05	0.898	9.15	1.65	0.840	0.273	1.24	1.07
0.8	1.80	1.92	0.902	9.15	1.65	0.840	0.197	1.16	1.07
1.0	....	1.79	0.904	....	1.65	0.840	.....	1.09	1.08

TABLE XV

ACTIVITY COEFFICIENTS AT REGULAR VALUES OF THE PARAMETER C

T=160 Degrees Fahrenheit P=1600 lbs/in^2 abs.

Value of C	Smoothed Experimental Equilibrium Ratios			Theoretical Equilibrium Ratios			Activity Coefficients		
	CH_4	CO_2	H_2S	CH_4	CO_2	H_2S	CH_4	CO_2	H_2S
0.0	1.67	...	0.878	5.95	...	0.700	0.281	...	1.25
0.1	1.40	1.42	0.898	5.95	1.19	0.700	0.235	1.19	1.28
0.15	1.20	1.25	0.925	5.95	1.19	0.700	0.202	1.05	1.32
0.208	1.00	1.00	1.00	5.95	1.19	0.700	0.168	0.840	1.43

TABLE XVI

PREDICTED PHASE COMPOSITION DATA

T=40 Degrees Fahrenheit P=700 lbs/in^2 abs.

Value of C	Interpolated Experimental Equilibrium Ratios			Liquid Phase Composition			Vapor Phase Composition		
	CH_4	CO_2	H_2S	CH_4	CO_2	H_2S	CH_4	CO_2	H_2S
0.0	8.6	...	0.35	0.08	0.0	0.92	0.68	0.0	0.32
0.1	7.6	4.0	0.38	0.08	0.015	0.905	0.60	0.06	0.34
0.2	6.7	2.1	0.41	0.08	0.06	0.86	0.53	0.12	0.35
0.4	5.0	1.35	0.45	0.08	0.20	0.72	0.40	0.27	0.33
0.6	3.5	0.94	0.535	0.09	0.49	0.42	0.31	0.46	0.23
0.655	3.95	0.90	0.57	0.07	0.58	0.35	0.28	0.52	0.20
0.88	3.0	0.92	....	0.04	0.96	0.0	0.12	0.88	0.0

TABLE XVII

PREDICTED PHASE COMPOSITION DATA

T=40 Degrees Fahrenheit P=1300 lbs/in^2 abs.

Value of C	Interpolated Experimental Equilibrium Ratios			Liquid Phase Composition			Vapor Phase Composition		
	CH_4	CO_2	H_2S	CH_4	CO_2	H_2S	CH_4	CO_2	H_2S
0.0	3.95	...	0.33	0.185	0.0	0.815	0.73	0.0	0.27
0.1	3.15	1.62	0.38	0.205	0.045	0.75	0.645	0.07	0.285
0.2	2.55	1.40	0.45	0.22	0.10	0.68	0.56	0.14	0.30
0.4	1.75	1.11	0.57	0.25	0.26	0.49	0.43	0.29	0.28
0.5	1.40	1.00	0.72	0.26	0.37	0.37	0.37	0.37	0.26
0.6	1.10	0.97	0.90	0.29	0.49	0.22	0.33	0.49	0.18

TABLE XVIII

PREDICTED PHASE COMPOSITION DATA

T=160 Degrees Fahrenheit P=1300 lbs/in^2 abs.

Value of C	Interpolated Experimental Equilibrium Ratios			Liquid Phase Composition			Vapor Phase Composition		
	CH_4	CO_2	H_2S	CH_4	CO_2	H_2S	CH_4	CO_2	H_2S
0.0	3.25	...	0.800	0.081	...	0.919	0.265	...	0.735
0.1	2.97	1.94	0.804	0.083	0.014	0.903	0.247	0.027	0.726
0.2	2.62	1.83	0.812	0.087	0.031	0.882	0.227	0.057	0.716
0.4	2.16	1.70	0.832	0.081	0.069	0.850	0.176	0.117	0.707
0.6	1.48	1.50	0.860	0.089	0.132	0.779	0.132	0.198	0.670
0.8	1.14	1.15	0.920	0.075	0.280	0.645	0.086	0.322	0.592

TEST DATA FOR RUN 4 - SERIES B

T=40 Degrees Fahrenheit P=1000 lbs/in^{2}abs.

PART I. PHASE CONDITIONS FOR COMPONENTS ADDED TO EQUILIBRIUM CELL

(a) Component Pressures						(b) Component Temperatures						(c) Component Volumes			
Comp.	Gauge Press. (lbs/in^2)	Gauge Corr. (lbs/in^2)	Atm. Press. (lbs/in^2)	Hg. Head (lbs/in^2)	Absol. Press. (lbs/in^2)	Thermocouple 1 MV	Thermocouple 1 Deg.F.	Thermocouple 2 MV	Thermocouple 2 Deg.F.	Thermocouple B MV	Thermocouple B Deg.F.	Datum Elev. (cm)	Hg. Level (cm)	ΔH. (cm)	Vol. (cm^3)
H_2S	113	-0.8	13.7	23.1	149	0.168	39.8	0.168	39.8	...	....	86.67	57.41	-29.26	71.6
CH_4	170	-1.2	13.7	17.2	200	...	...	...	...	0.860	71.2	87.27	88.40	+1.13	56.7
CO_2	190	-1.3	13.7	17.8	220	...	...	...	...	0.864	71.4	87.27	86.09	-1.18	65.3

PART II. EQUILIBRIUM CONDITIONS

964	+6.5	13.7	15.8	1000	0.172	40.0	0.172	40.0	...	...	86.65	95.36	+8.71	...

PART III. SAMPLE ANALYSIS

(a) Tutweiler Analysis

Phase	Pipette	I_2 Used (cc)	I_2 for 100% H_2S (cc)	% H_2S
Gas	No. 1	1.65	7.10	23.2
	No. 2	1.55	6.85	22.6
Liquid	No. 1	2.90	7.10	40.8
	No. 2	2.85	6.85	41.6

(b) Orsat Analysis

Initial Gas Vol. (cc)	Initial Vol + Air (cc)	Vol of Air (cc)	Vol After KoH (cc)	% CH_4
50.05	93.65	43.60	64.55	41.8
45.95	88.65	42.70	50.70	17.4

Sample Calculations - Series B - Run 4

Equilibrium Conditions: T=40 Degrees Fahrenheit; P=1000 lbs/in^{2}abs.

The desired total composition in the two phase region was:

H_2S = 0.32 mole fraction.

CH_4 = 0.30 mole fraction.

CO_2 = 0.38 mole fraction.

(1) Addition of H_2S to equilibrium cell.

P = 149 lbs/in^2 abs.

T = 40 Degrees Fahrenheit = 500 Degrees R.

V = 71.6 c.c.

Z = 0.88

R = 670 $\dfrac{\text{lb c.c.}}{\text{in.}^2\ {}^{\circ}\text{R gm.mole}}$

$$n = \frac{P\,V}{Z\,R\,T} = \frac{149 \times 71.6}{0.88 \times 670 \times 499.8} = 0.0363 \text{ gm.moles.}$$

(2) Addition of CH_4 to measuring cell.

(a) Moles of CH_4 required:

$$n = \frac{30}{32} \times 0.0363 = 0.0340 \text{ gm. moles.}$$

CH_4 was to be added to the measuring cell at a pressure of 200 lbs/in^{2}abs. and at a cell temperature of 72 Degrees Fahrenheit. At these conditions the compressibility factor was 0.975. The volume required in the measuring cell was:

$$V = \frac{n\ Z\ R\ T}{P} = \frac{0.0340 \times 0.975 \times 670 \times 532}{200}$$

$$= 59.1 \text{ c.c.}$$

(b) Actual quantity of CH_4 added:

$$P = 200 \text{ lbs/in}^2\text{abs.}$$

$$T = 71 \text{ Degrees Fahrenheit} = 531 \text{ Degrees R.}$$

$$V = 56.7 \text{ c.c.}$$

$$n = \frac{P\ V}{Z\ R\ T} = \frac{200 \times 56.7}{0.975 \times 670 \times 531} = 0.0327 \text{ gm. moles.}$$

(3) Addition of CO_2 to measuring cell.

(a) Moles of CO_2 required:

$$\frac{n}{n + 0.0363 + 0.0327} = 0.38$$

$$n = 0.0423 \text{ gm. moles.}$$

CO_2 was to be added to the measuring cell at a pressure of 220 lbs/in^{2}abs. and at a cell temperature of 72 Degrees Fahrenheit. At these conditions the compressibility factor was 0.909. The volume required in the measuring cell was:

$$V = \frac{n\ Z\ R\ T}{P} = \frac{0.0423 \times 0.909 \times 670 \times 532}{220}$$

$$= 62.3 \text{ c.c.}$$

(b) Actual quantity of CO_2 added:

P = 200 lbs/in^{2}abs.

T = 71.4 Degrees Fahrenheit = 531.4 Degrees R.

V = 65.3 c.c.

$$n = \frac{P\ V}{Z\ R\ T} = \frac{220 \times 65.3}{0.909 \times 670 \times 531.4} = 0.0444 \text{ gm. moles}$$

(4) Total System Composition.

	Moles	Mole Fraction
H_2S	0.0363	0.320
CH_4	0.0327	0.288
CO_2	0.0444	0.392

(5) Compositions of Phases at Equilibrium as Determined by Analysis.

	Gas Phase	Liquid Phase
H_2S	0.229	0.412
CH_4	0.418	0.174
CO_2	0.353	0.414

B29777